# On the preparation of a prototype VCN source

E. Lychagin

CREMLIN PLUS
Connecting Russian and European Measures for Large-scale Research Infrastructures

Second meeting of the Subcommittee on Fundamental Physics of WP3
08 July 2021 On-line

Schema of the measurement:

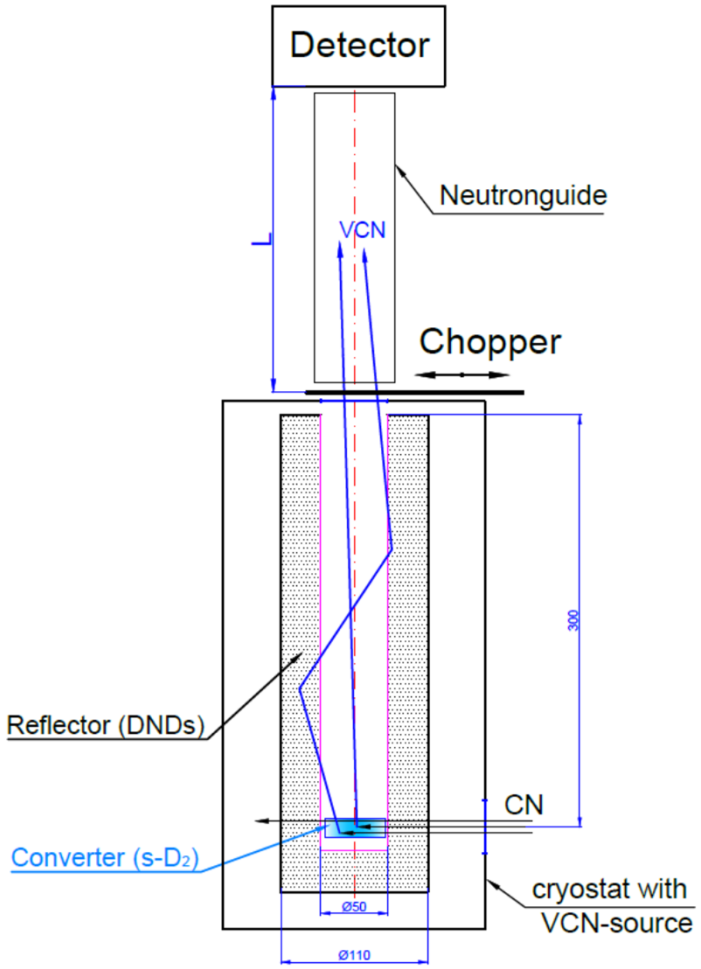


The prototype should demonstrate the properties and characteristics of both the converter and the reflector.

The main characteristic of the converter is the dependence of VCN production rate on the energy of the VCN.

The main characteristic of the reflector is the gain in the VCN flux in limited solid angle along the axe and its depending on the VCN energy.

The experiment parameters:

| | |
|---|---|
| **Neutron beam** | **PF1b, ILL** |
| **VCN converter** | **o-$SD_2$, 5K, ~4 $cm^3$** |
| **Estimated production rate $\Phi_{VCN}$** | **$1.6 \cdot 10^6$ n/s (v<100 m/s); $2 \cdot 10^5$ n/s (v<50 m/s).** |
| **Estimated detection rate without reflector $\Phi_{det}$** | **16 n/s (v<100 m/s); 8 n/s (v<50 m/s).** |
| **Estimated gain factor** | **3÷6 (v<100 m/s); 4÷15 (v<50 m/s).** |

## Main elements of the experimental set-up:

- Beam collimation system (standard equipment PF1b);
- Cryostat for VCN converter and reflector (under developing in JINR);
- Ortho-para converter for $D_2$ (under developing in JINR);
- Powder for reflector is producing by PTI and UCA
  (will be in reports A.Vul' and M.Dubois today)
- VCN chopper (was developed in JINR and located in ILL);
- VCN detector (standard equipment of ILL).

# Schema of cryostats for VCN converter and optho-para converter

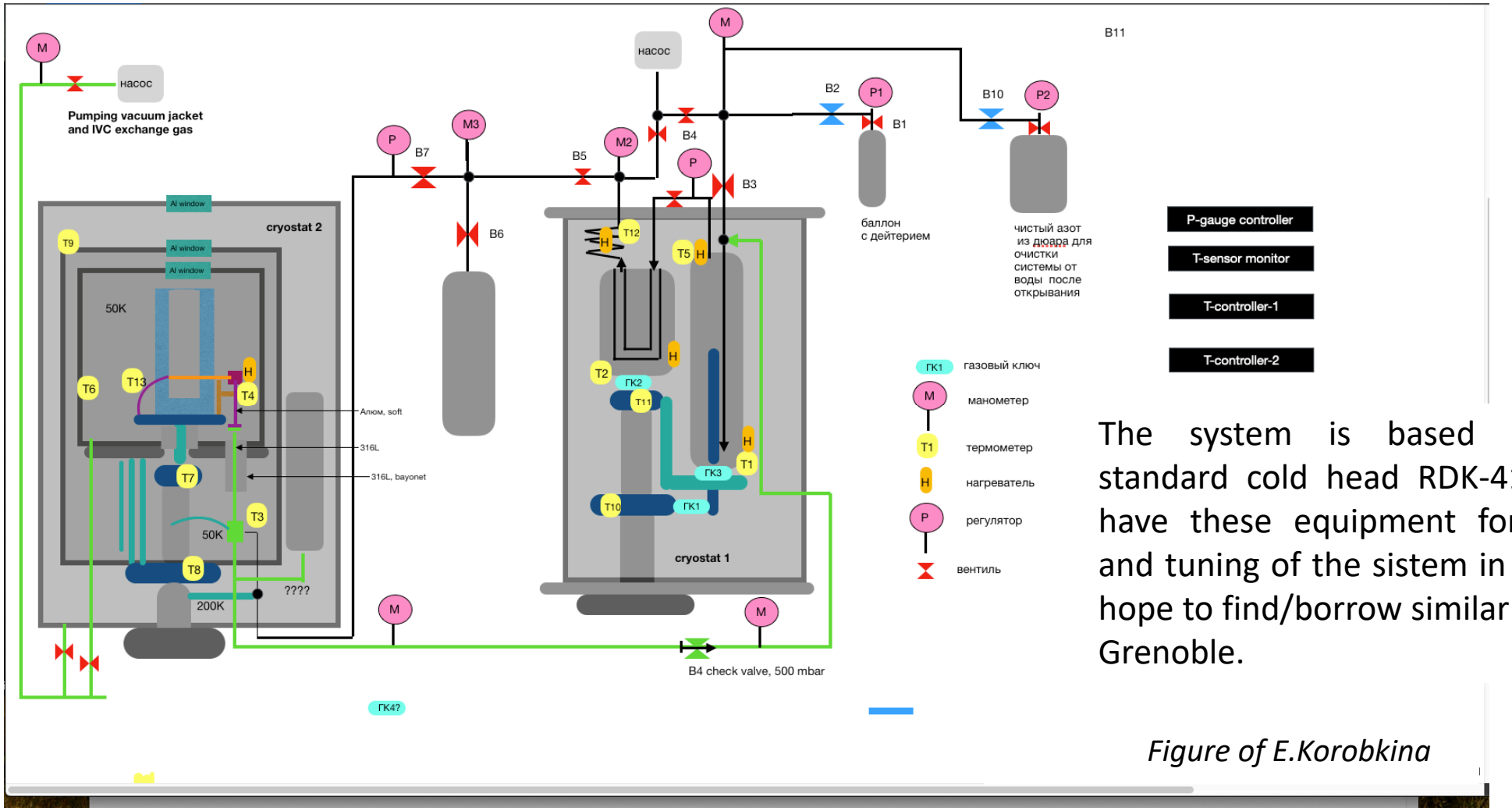


The system is based on two standard cold head RDK-415D. We have these equipment for testing and tuning of the sistem in JINR but hope to find/borrow similar heads in Grenoble.

*Figure of E.Korobkina*

# Design works

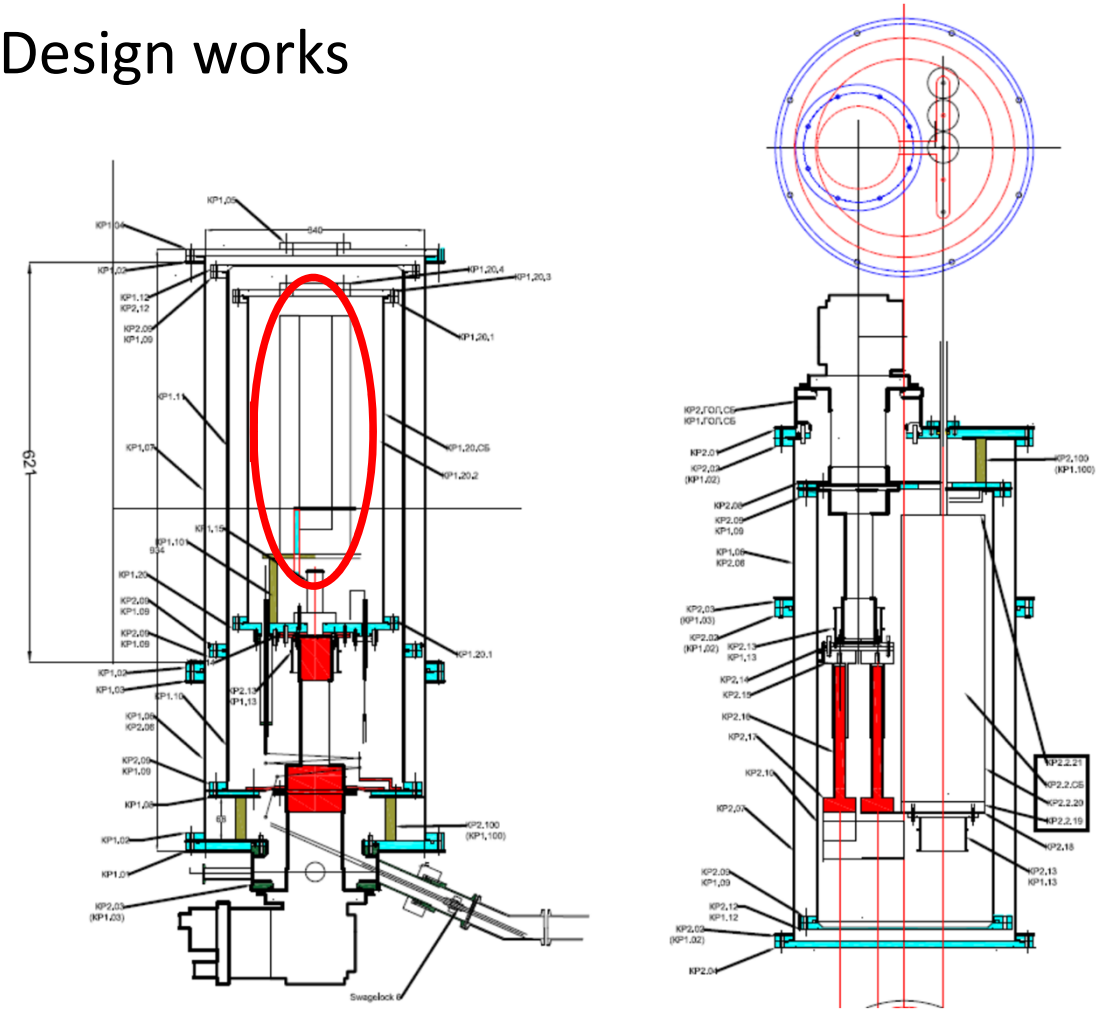

The design work was started but temporarily stopped till a final decision have been done concerning the design of the central part where the converter and reflector are located.

# Central part

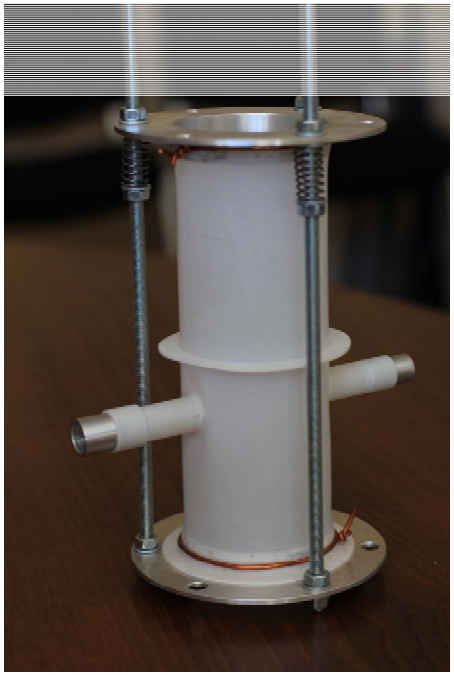

The teflon tube with 1 cm internal diameter and wall thickness 1 mm was chosen as deuterium container. This tube will have cold aluminum end to freeze the gas.

Internal wall of volume for powder reflector will produsedby teflon with 200 mu thickness.

| Loss factor | | $P_{loss}$ ($V_{VCN}$ = 100 m/s) | $P_{loss}$ ($V_{VCN}$ = 50 m/s) |
|---|---|---|---|
| Teflon: | $P_{loss}(CF_2)$ | $3 \cdot 10^{-3}$ | $6 \cdot 10^{-3}$ |
| $SD_2$: | $P_{loss}(D_2)$ | $1.4 \cdot 10^{-3}$ | $2.8 \cdot 10^{-3}$ |
| Holes: | $P_{loss}$(holes) | $1.9 \cdot 10^{-2}$ | $1.9 \cdot 10^{-2}$ |
| Powder of diamond: | $P_{loss}$(DNDs) | ~0.15 | $\sim 4 \cdot 10^{-2}$ |
| TOTAL: | $P_{loss}$ | ~0.17 | $\sim 6.8 \cdot 10^{-2}$ |

| Material | density, g/sm$^3$ | M | $\sigma_a$, barn (2200 m/s) | molecular density n *10$^{23}$, 1/cm$^3$ | n*$\sigma_a$ (50 m/s), 1/cm | thickness to suppress flux (50 m/s) at 10%, cm | Wall thickness at 50 reflections, um |
|---|---|---|---|---|---|---|---|
| Teflon | 2,200 | 50,0 | 0,023 | 0,265 | 0,026 | 3,98 | 265,4965775 |
| Mg | 1,738 | 24,3 | 0,063 | 0,431 | 0,119 | 0,88 | 58,85094118 |
| Be | 1,848 | 9,0 | 0,008 | 1,236 | 0,041 | 2,55 | 169,9277907 |

# Raman measurements

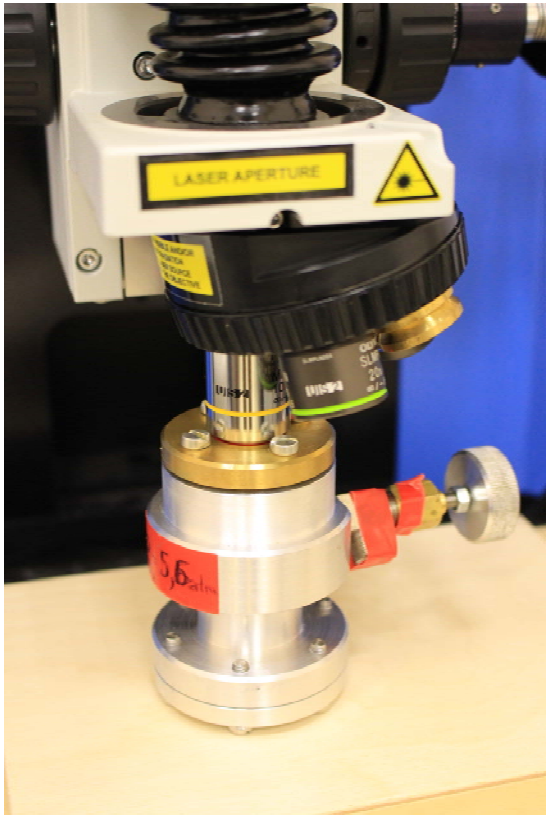


We made a gas test cell and started the game with measuring ща Raman spectra to determine ortho to para state the ratio in the  deuterium.

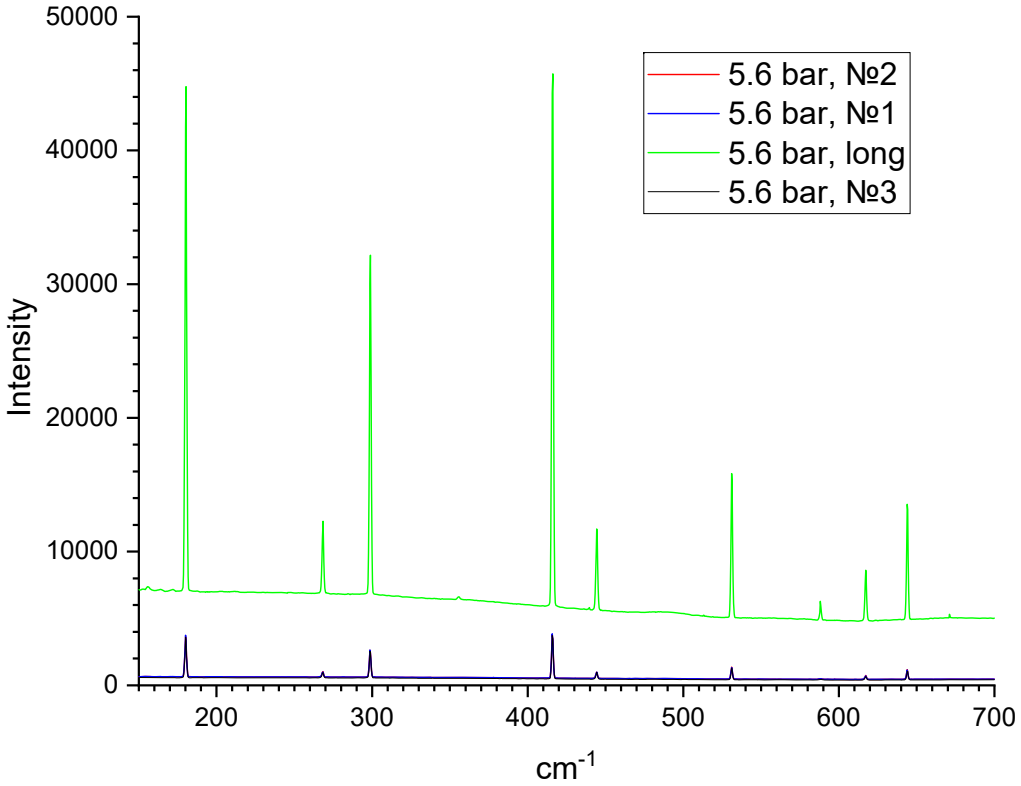

# Nearest plans (for next 6 month):

- Development of working drawings of the central part.
- Test of ortho-para conversion at 20K (et test refrigerator).
- Adjustment of the complete installation scheme and finalized list of needed equipment.
- Completion of the development of working drawings for cryostats, supports, neutron shielding.
- Start manufacturing of the set-up elements.

# On the development of a solid-deuterium VCN convertor

***Ekaterina Korobkina***

***North Carolina State University,  Raleigh, USA***

# Nuclear spins orientation: Ortho-deuterium

- D2 molecules exist in two isomeric states para-D2 (spin J=1) and ortho-D2 (spin J=0)
- During condensation the rate of conversion to the equilibrium state is extremely slow
- Neutrons can introduce such conversion
- As result, VCN/UCN gain energy of several meVs and are lost
- Therefore we need to use pre-converted ortho-deuterium to growing sD2 crystals

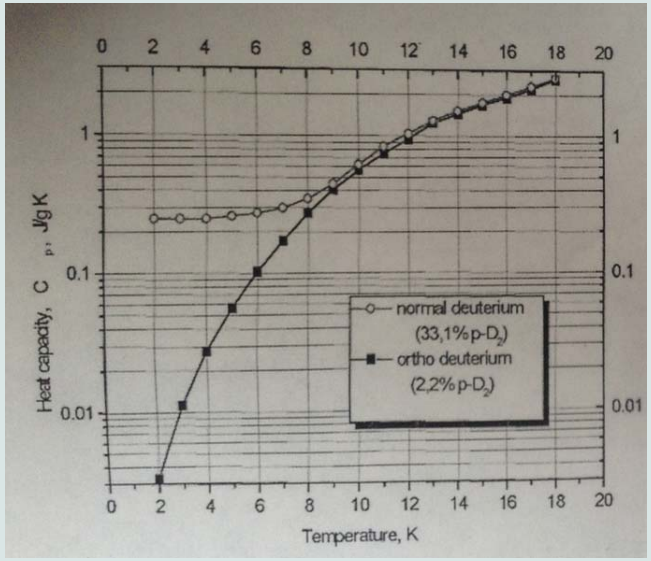


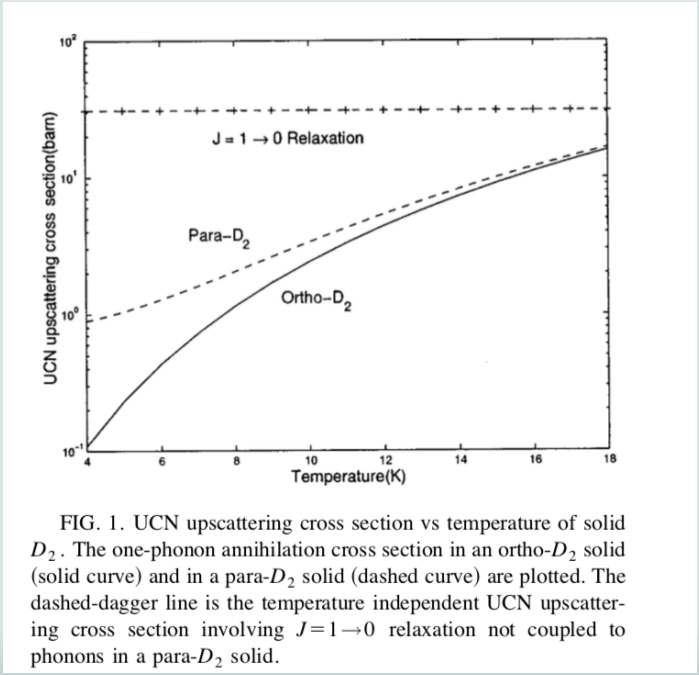


FIG. 1. UCN upscattering cross section vs temperature of solid $D_2$. The one-phonon annihilation cross section in an ortho-$D_2$ solid (solid curve) and in a para-$D_2$ solid (dashed curve) are plotted. The dashed-dagger line is the temperature independent UCN upscattering cross section involving $J=1\rightarrow0$ relaxation not coupled to phonons in a para-$D_2$ solid.

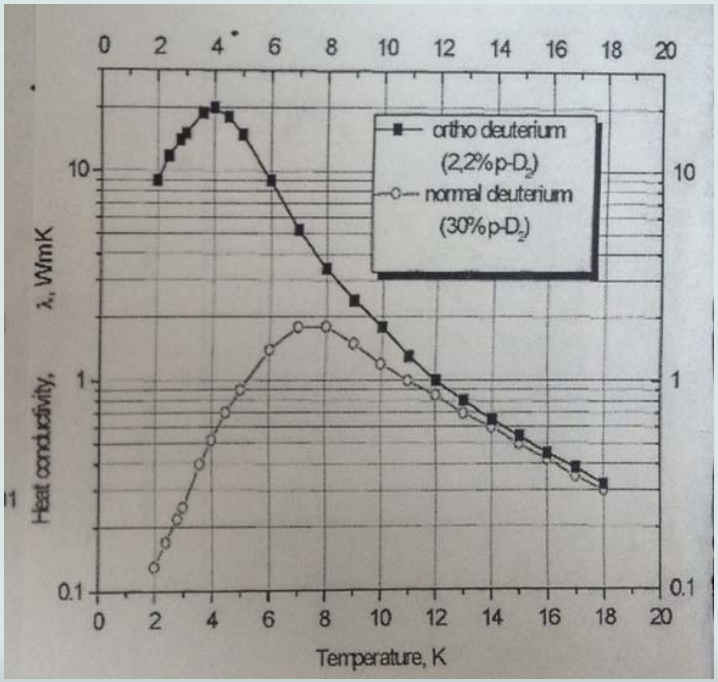

# Solid deuterium grows modes

- Freezing from the liquid phase (LANL, PSI)
- Sublimation from the vapor phase at $T_s$:
  - at the operational temperature: $T_s = T_{op}$ (Mainz Uni)
  - above operational temperature: $T_s > T_{op}$

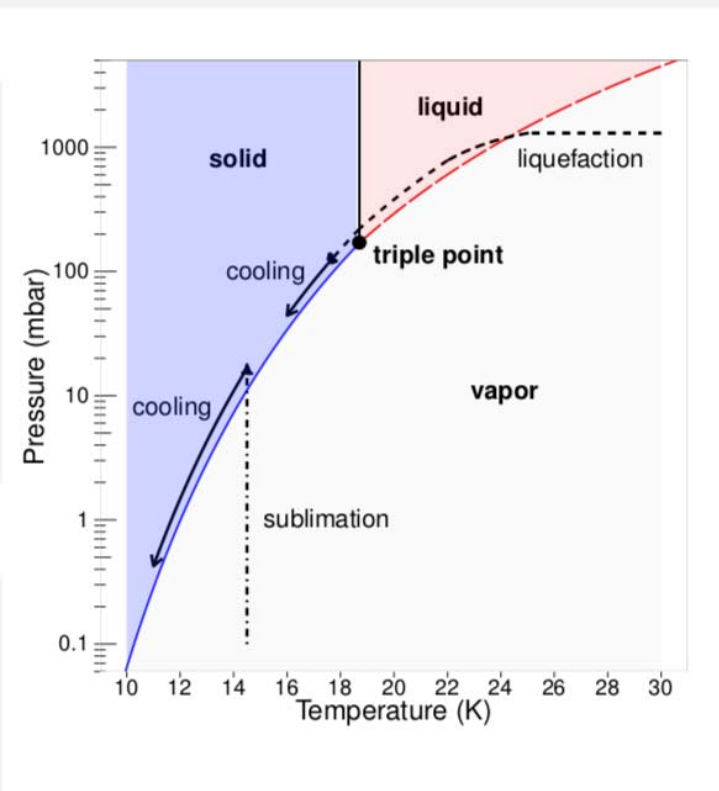


- for UCN/VCN source $T_{op}$ =5K

# Solid deuterium properties

- The SD2 crystal is a quantum crystal with a large zero T energy
- It demonstrates thermally activated diffusion above 8K ( $D(D2)=7x10^{-4}e^{-290/T}$ ) as well as surface diffusion
- It demonstrates significant shrinkage from 18.3K to 12K
- Crystals grown from vapor can be a mixture of hcp and fcc lattices

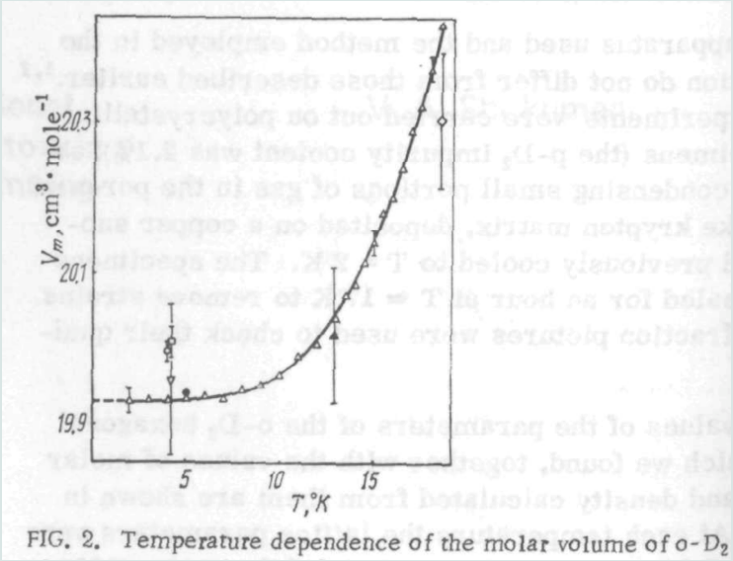

FIG. 2. Temperature dependence of the molar volume of o-$D_2$

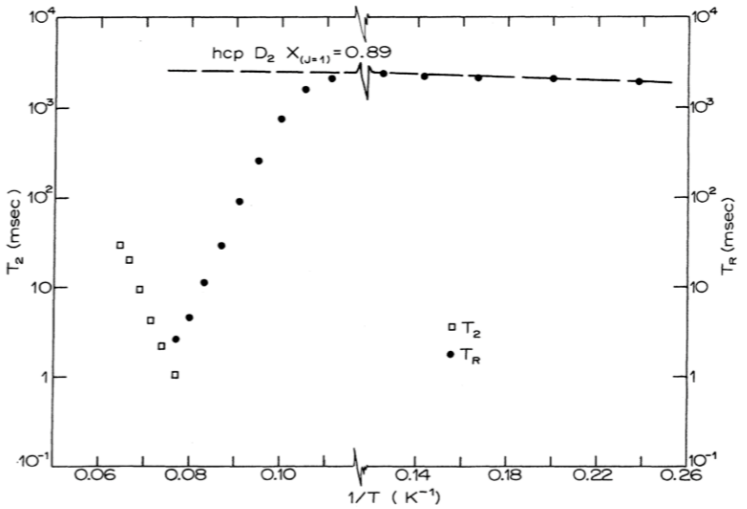

FIG. 4. Representative set of relaxation data for a sample of $D_2$ with $X = 0.89$. Left vertical scale: transverse relaxation time $T_2$; right scale: longitudinal relaxation time $T_R$ in the rotating frame. The dashed curve is the extrapolation from the nondiffusion region.

# Solid deuterium properties

- SD2 exhibits so called “triple point wetting ” (or Stranski–Krastanov film growth), i.e. it wets surface completely above the triple point, while below only films of several monolayers can be grown and the rest grows as crystallite islands

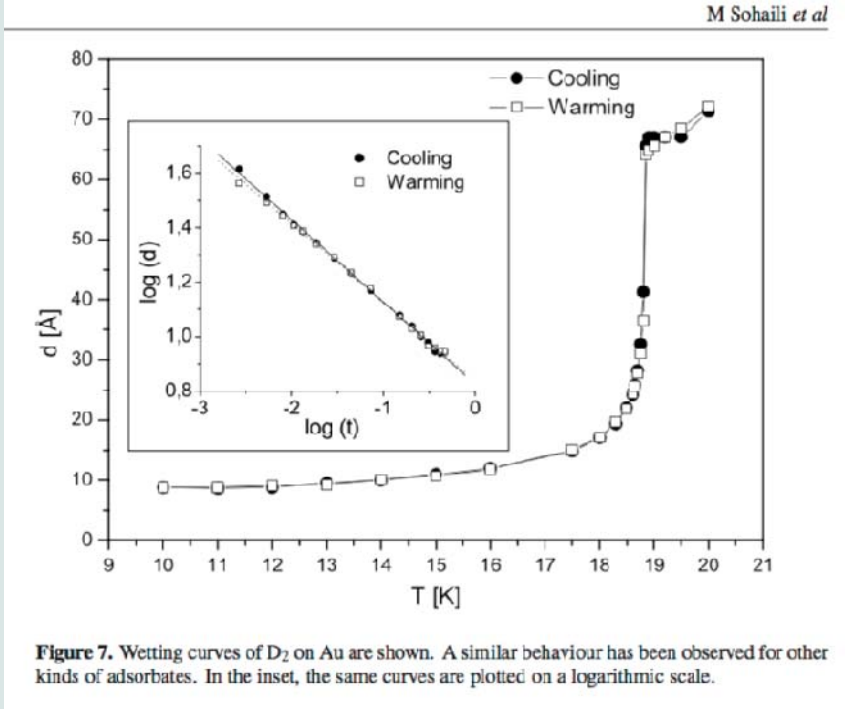


**Figure 7.** Wetting curves of $D_2$ on Au are shown. A similar behaviour has been observed for other kinds of adsorbates. In the inset, the same curves are plotted on a logarithmic scale.

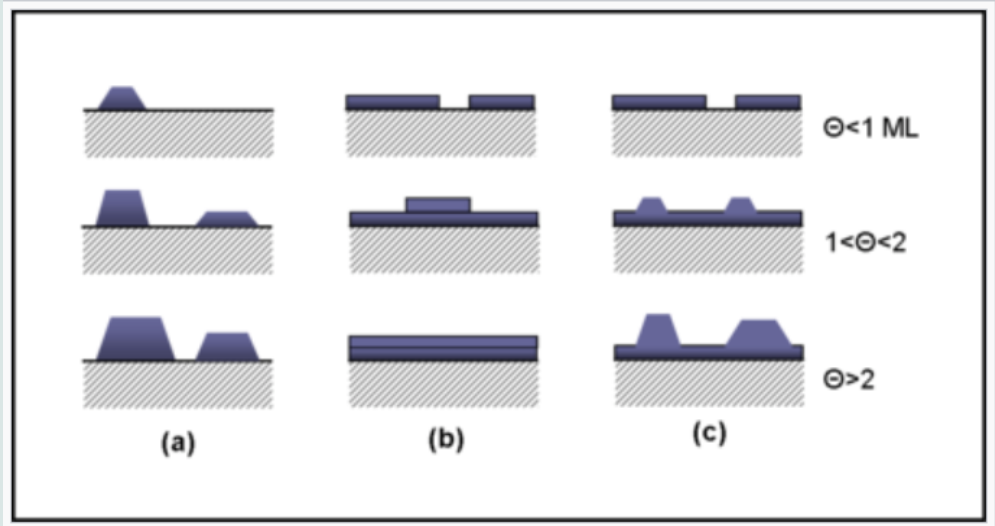


**Figure 1**. Cross-section views of the three primary modes of thin-film growth including (a) Volmer–Weber (VW: island formation), (b) Frank–van der Merwe (FM: layer-by-layer), and (c) Stranski–Krastanov (SK: layer-plus-island). Each mode is shown for several different amounts of surface coverage, Θ.

# Solid deuterium geometry for the VCN prototype

- The SD2 crystal has to be grown horizontally
- dimensions I.D.1cm x 5 cm long

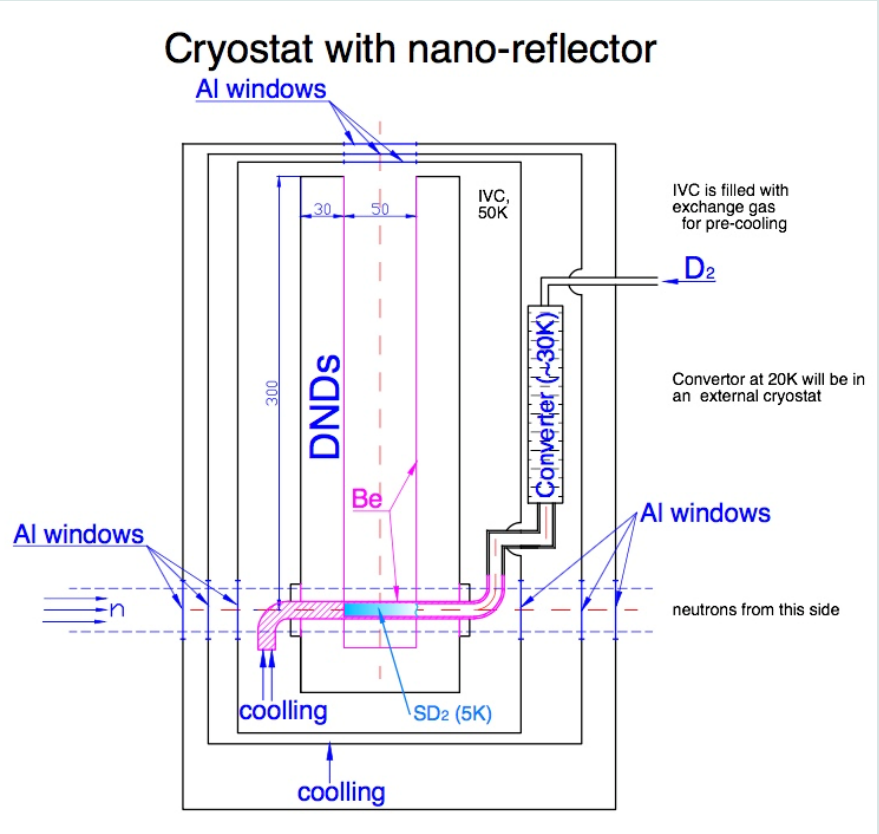

# NCSU study of growing SD2 crystals

- Visual observation
- Temperature sensors inside and outside the cryo-container which allowed us to reconstruct temperature profile of the walls

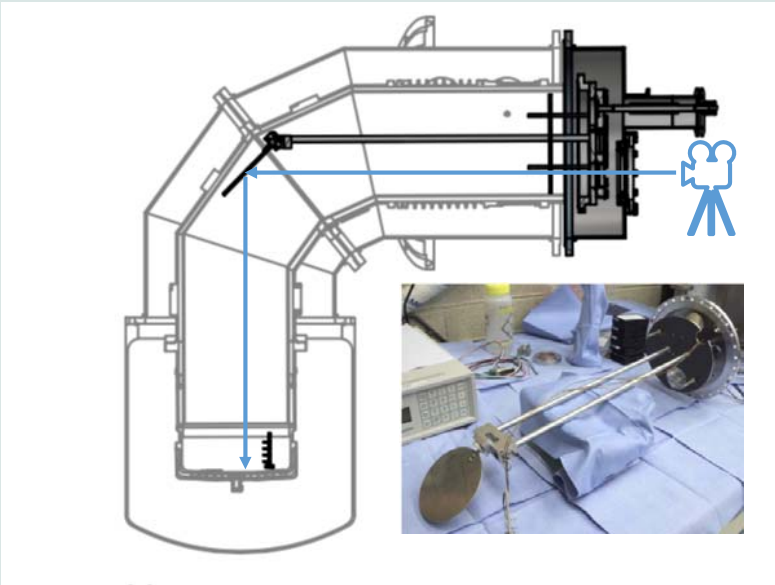

Heater wrapped
at the top of container

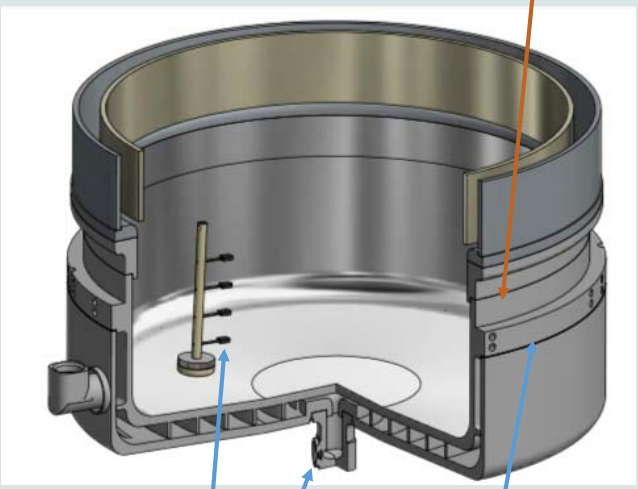

T-sensor locations
at the cry-container
plus a sensor
on the He return line

# Growing SD2 from vapor at UCN source operational temperature

# Simulation of Mainz UCN source

- this run was to simulated Mainz UCN source condensation of SD2 with cold (6K) bottom of container and slow D2 flow rate
- **5.4K(He inlet)/ 8.2K(Top)/ 7.2K(He outlet)**:
  - Small flow (0.3 l/m) produced dense multicrystall, optically opaque
  - Higher D2 flow >1 l/m produced snow-flake-like mass
- when T of container was increased (**5.4K/ 11.2K/ 8.3K** ) and crystal annealed, D2 flow =>0.8 l/m results in visibly shiny surface

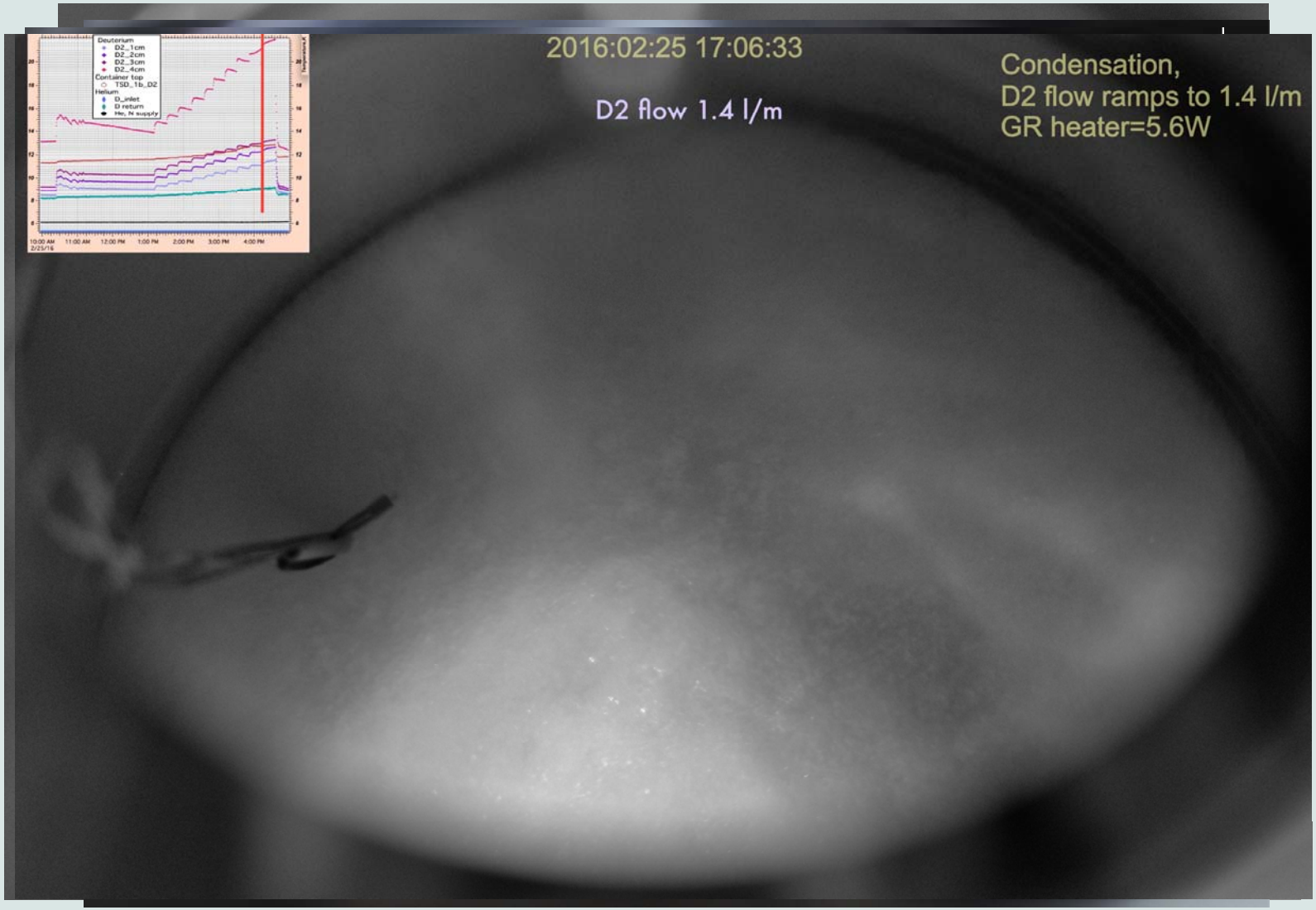

# After two days of annealing at 12K

# 2018, melting-refreezing, resulting in grainy crystal

- this melting-refreezing was done faster than 2016 run and the crystal was cooled down to 9.5K for annealing

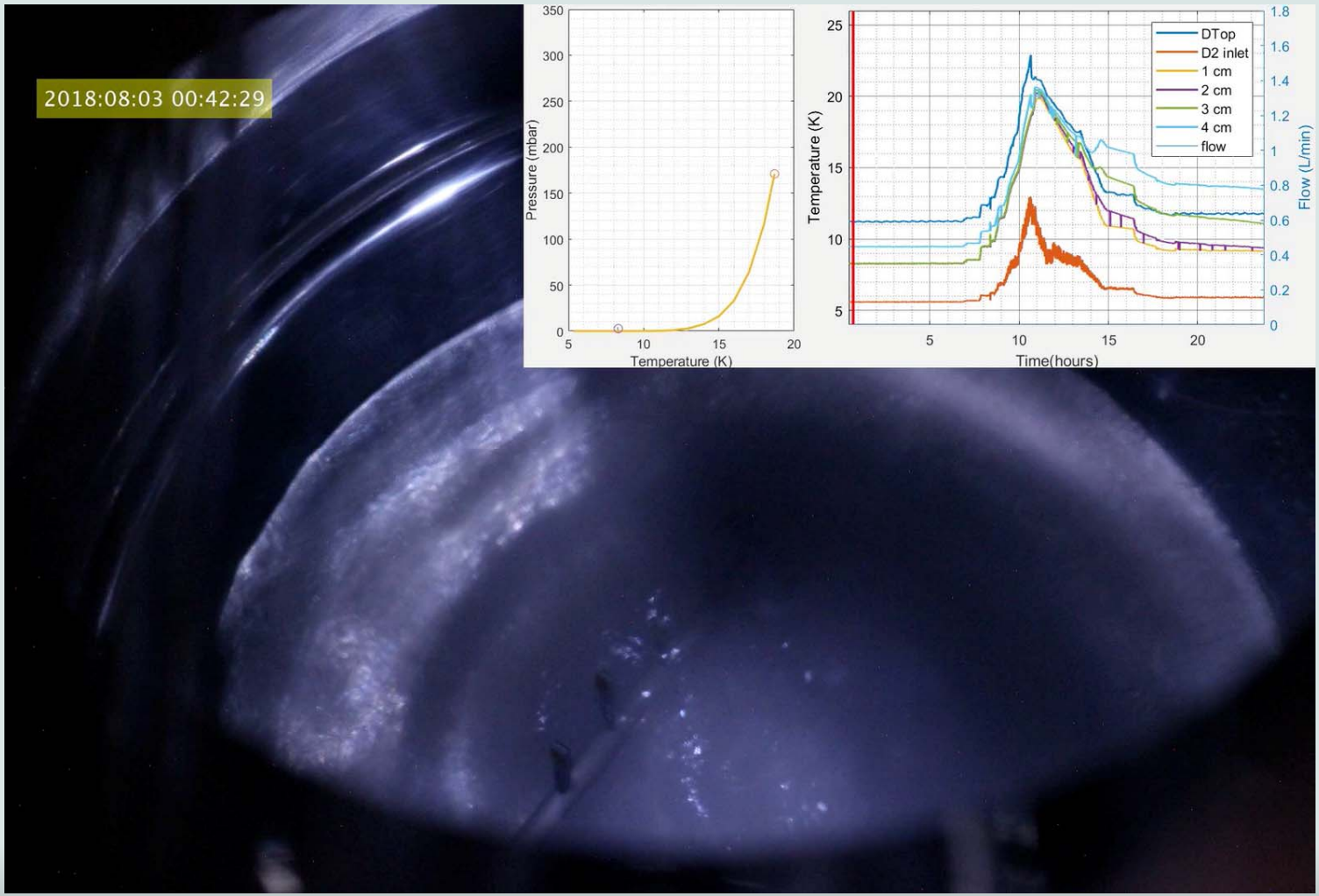

# Growing from vapor above the UCN source operational temperature: case 1

# Condensation at T close to $T_{triple}$ and annealing at 11.5K

- Mar 15 condensation, **no heaters**, small cooling power, **9/ 17.5/ 17.5, D2 flow 0.8 l/m:**
  - ideal transparent crystal
- Mar 15-16-18, evolution to a blob at 11.5K:
  - amazing mobility and tendency for avoiding warmer surfaces


- Mar 16 condensation, with heaters on, **8.5/ 18/ 15K**, 1 l/m

- **Conclusions:**
  - optically clear crystal
  - high mobility and tendency to pull off the foreign objects

# Mar 22- Mar 25 - condensation/conditioning

- Mar 22 -25 condensation, with heaters, **7.75/ 17/ 18.5-19, flow 1 l/m**
  - transparent crystal
  - all probe sensors covered, about 1050 cc total

- **Conclusions**:
  - it is possible to grow optically good crystal from vapor at warmer temperatures and flow 0.8-1 l/m
  - need to be concerned about crystal shape evolution with time

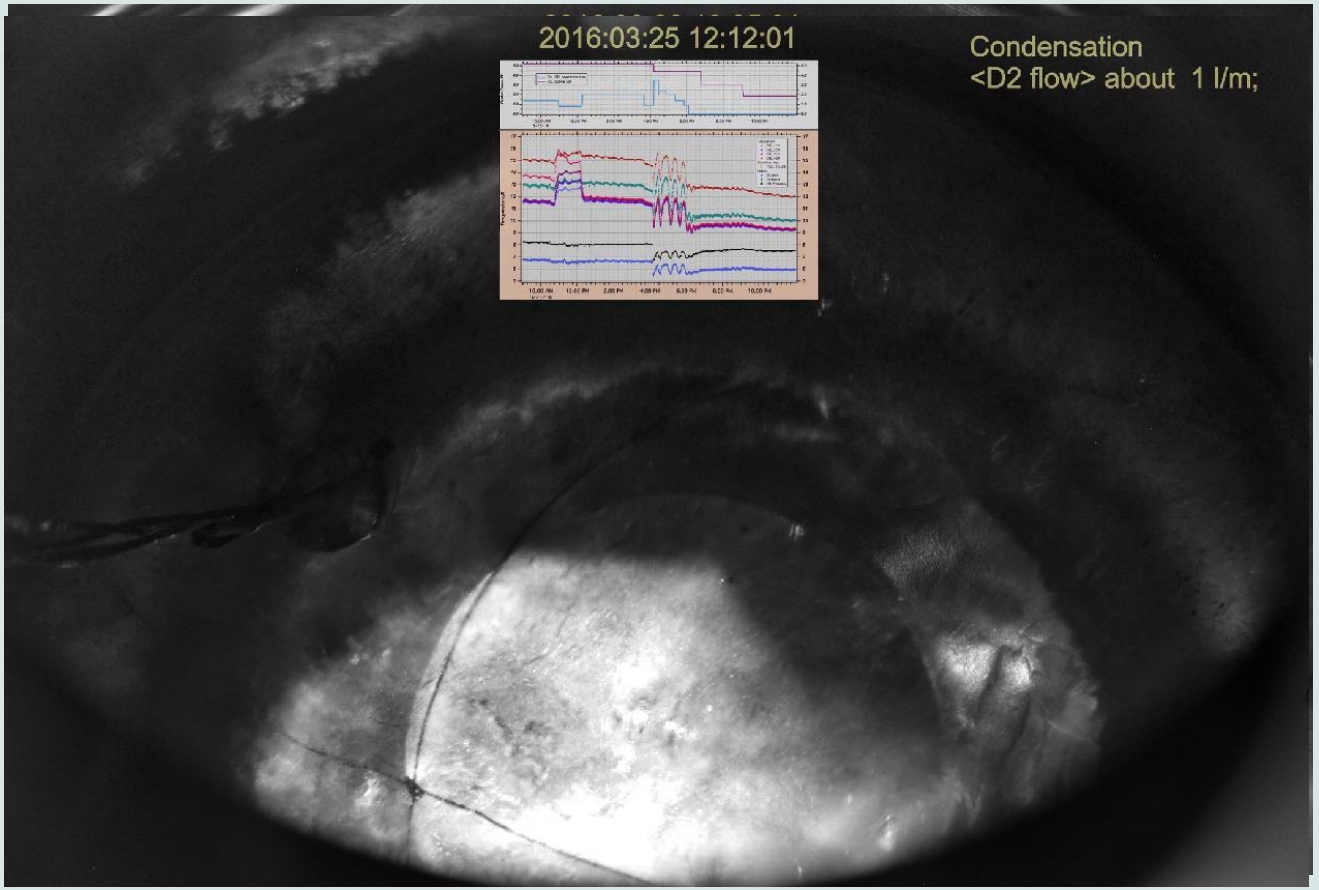

# Conclusion from first two condensation


- at T close to $T_{triple}$ , :
  - crystal is clear
  - SD2 move and re-shaping itself at 12K due to high diffusion
  - need to be concerned about crystal shape evolution with time

- at T<6K SD2 does not move
- but the growth is very inhomogeneous due to “triple-point-wetting”
- annealing at 12K improved crystal bulk

# Growing from vapor above the UCN source operational temperature: case 2

# Growing from vapor above operational T: SD2 shapes and quality vs Temperature profile of the cryo-container

# Growing from a vapor at intermediate T

- April 11-13 condensation, **8.3/ 16.2/ 13, 0.8 l/m**
- attempt to reproduce Mar 15 condensation (**9/ 17.5/ 17.5**)
- it was unsuccessful, because D-return T was nor taken into account and the container was too cold
- very interesting run for discussion of crystal properties vs T and crystal shapes

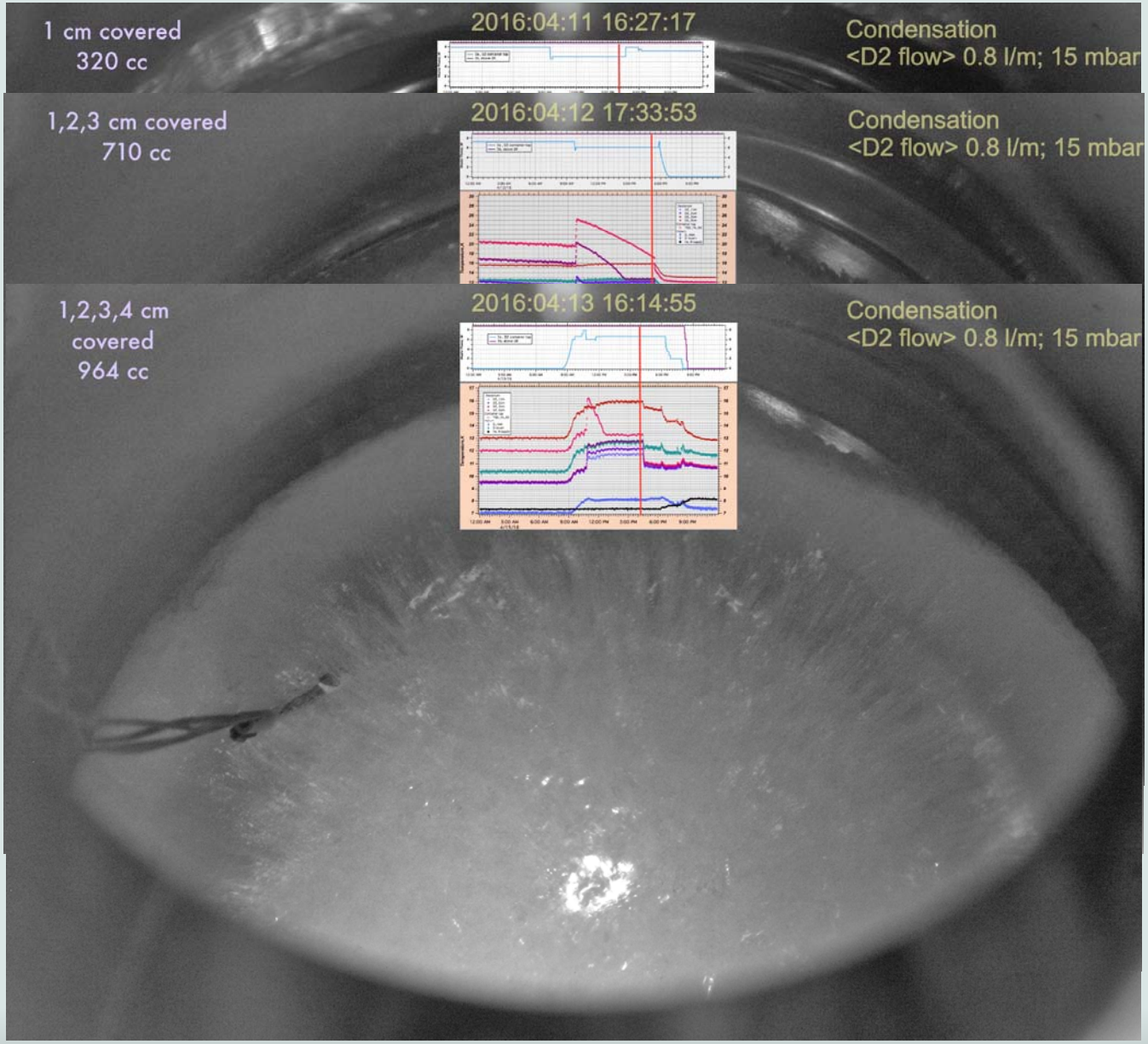

# How we can extract crystal shape from our data

- Position of the T- probe

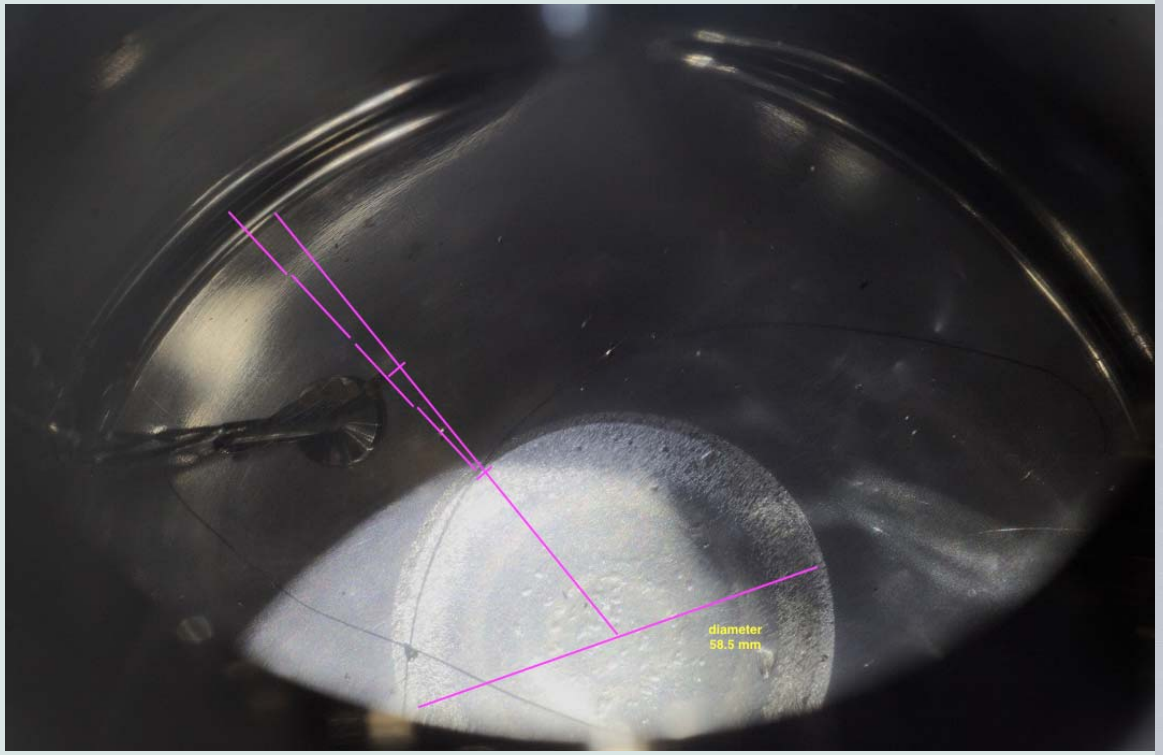


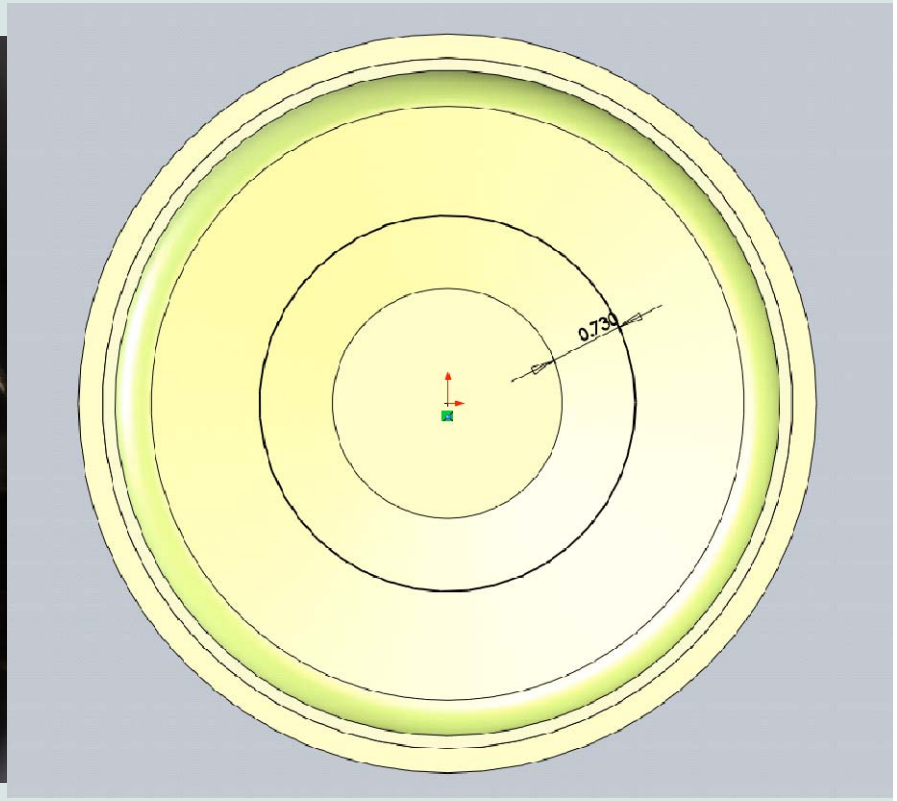

# How we can extract crystal shape from our data

- Hight at probe: coverage of probe sensors

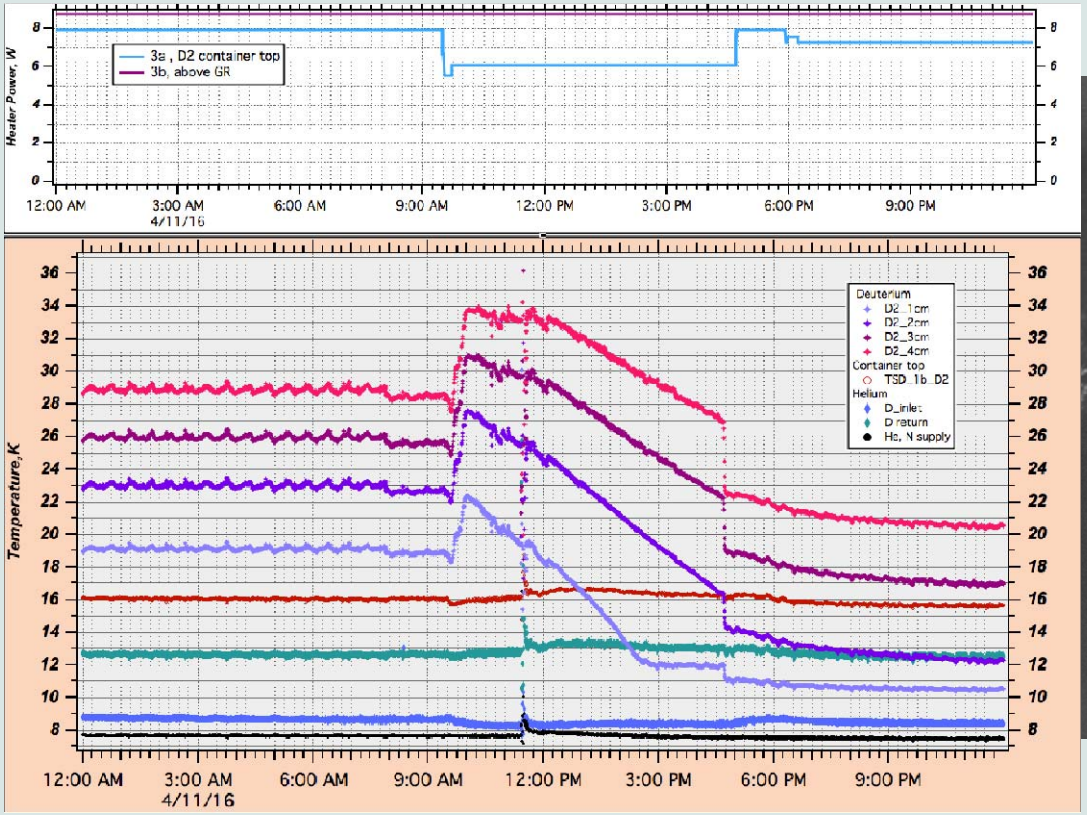


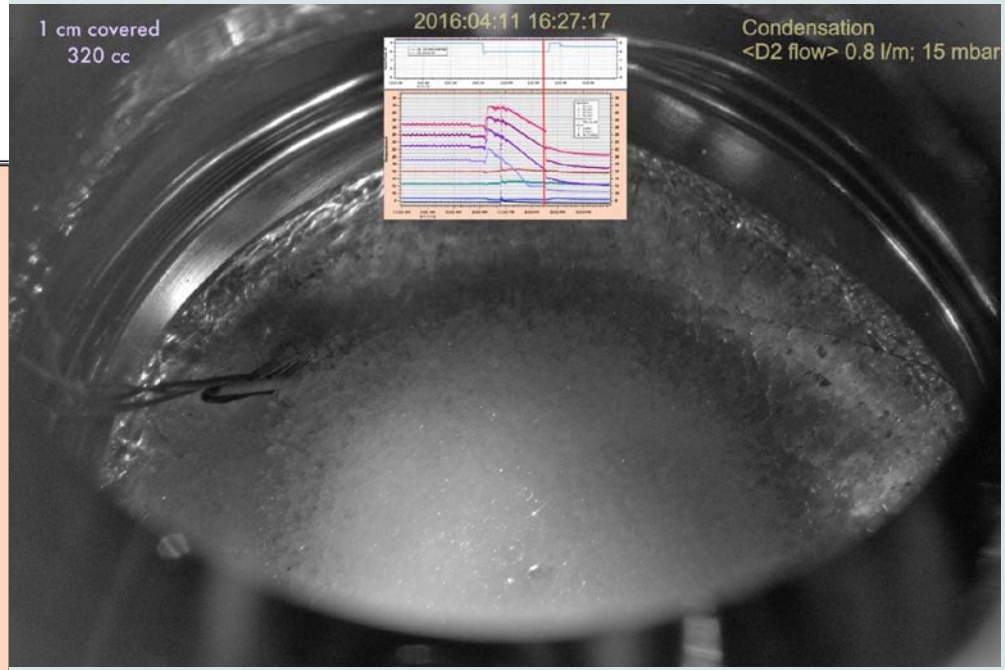

# How we can extract crystal shape from our data

- We know total Volume
- We can estimate outer diameter of the crystal

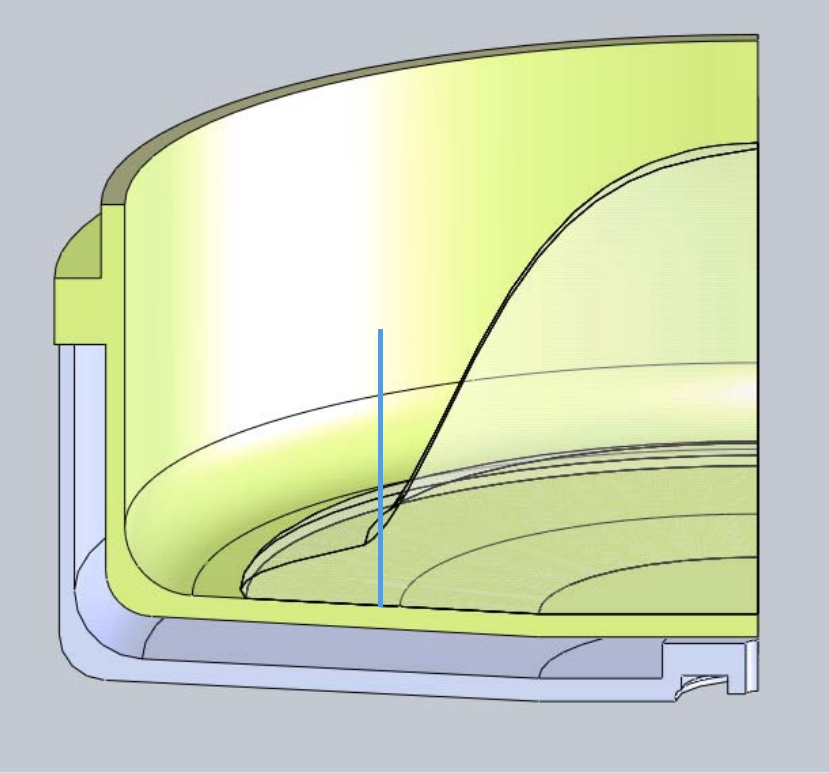

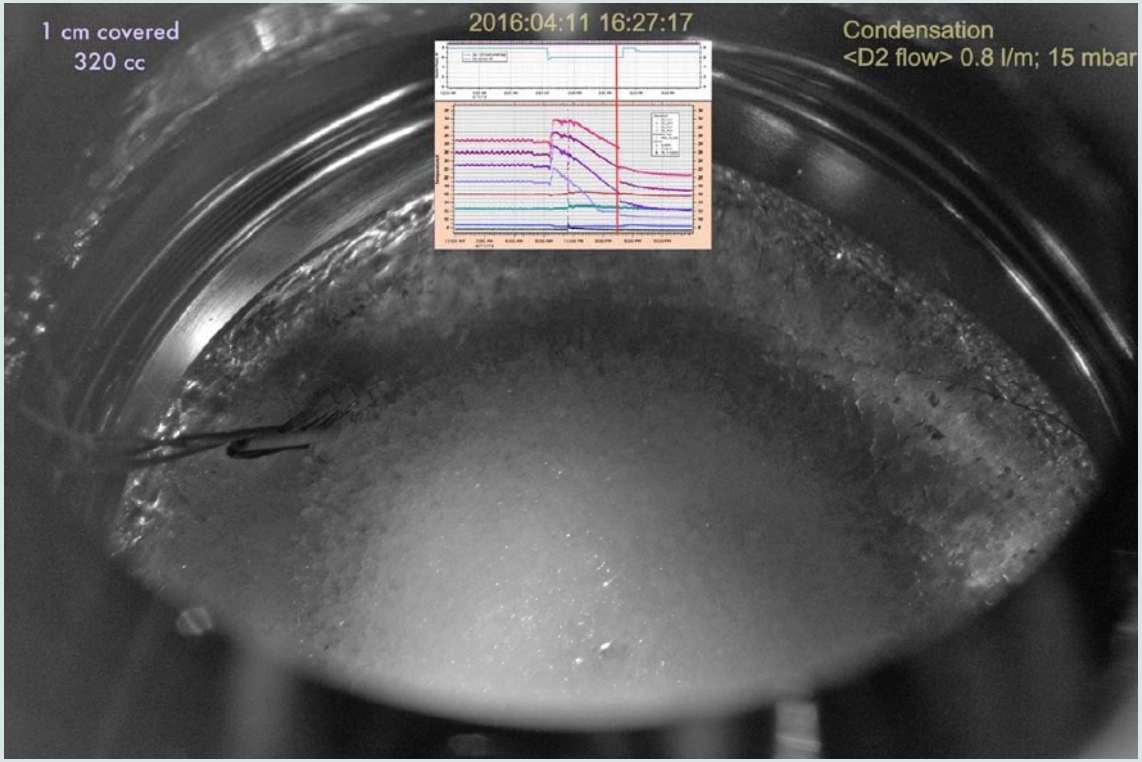

# Shape reconstruction

## Mar 15, Annealed overnight at 12K. High mobility

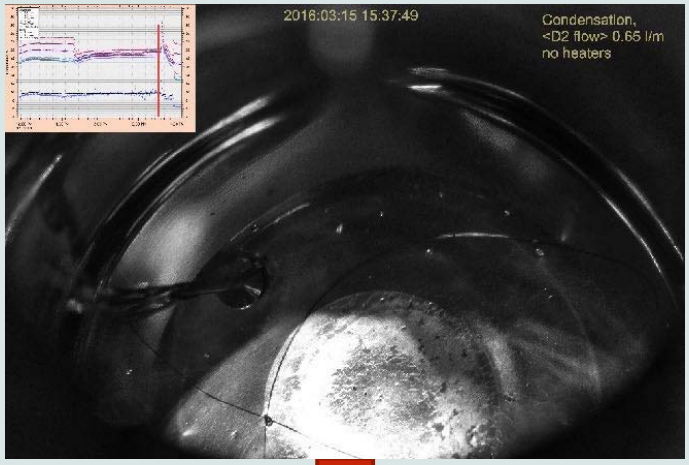



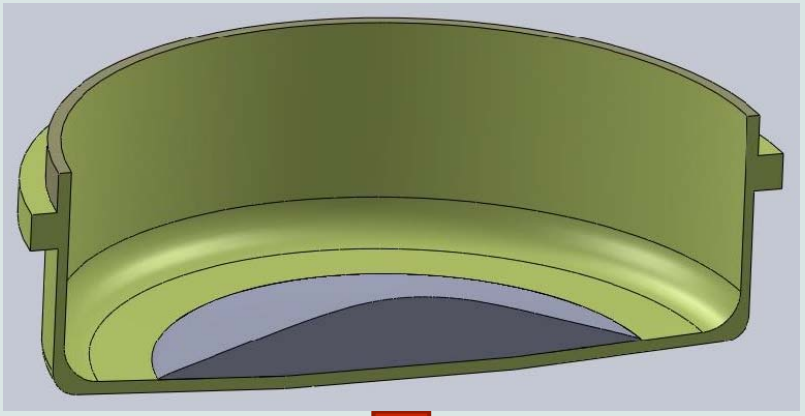

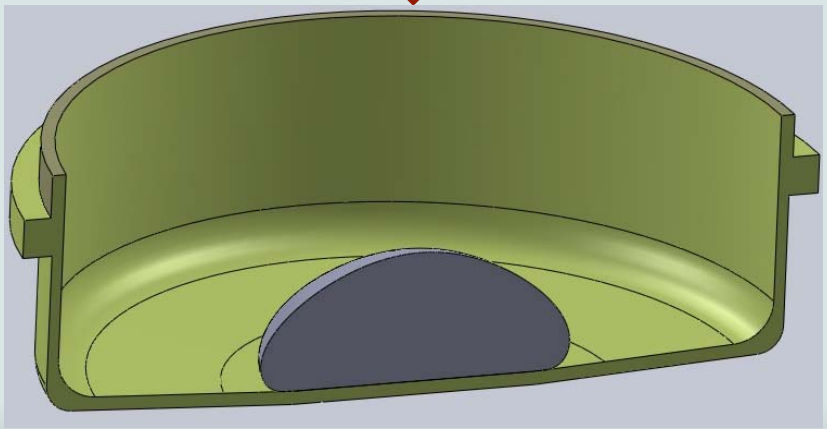

# Shape reconstruction (about 350cc)

March 22

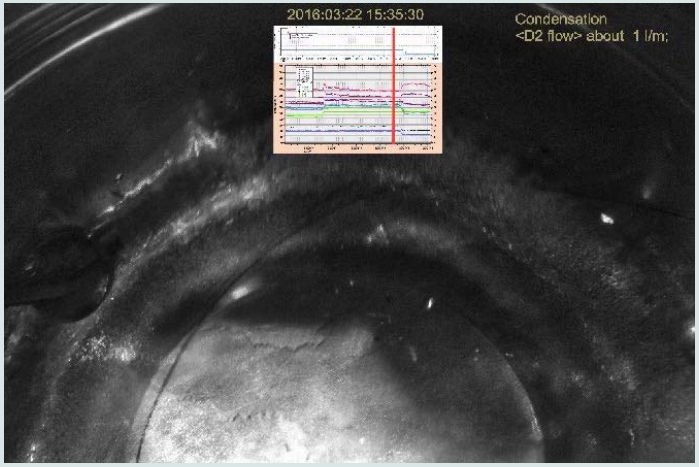


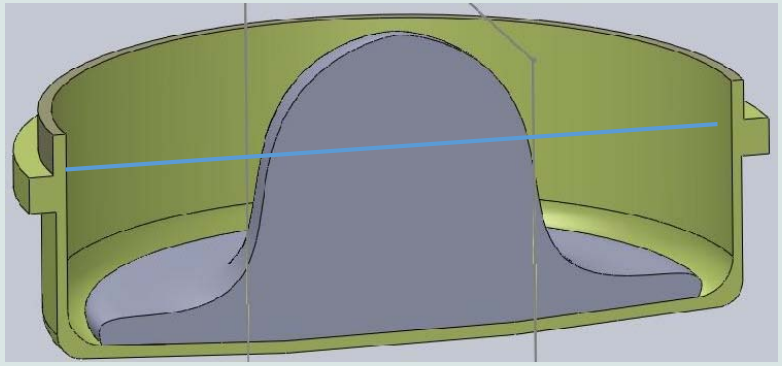

5 cm

Apr 11

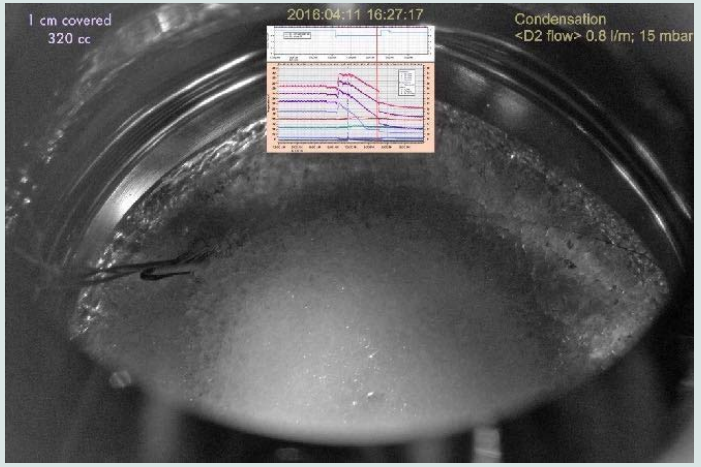


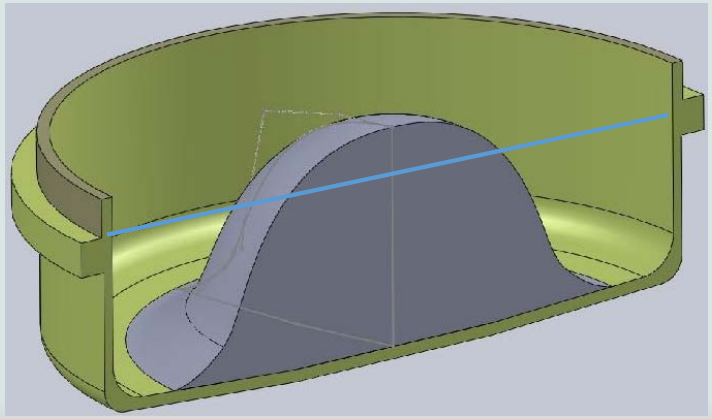

# Shape reconstruction (1050cc vs 964cc)

March 25

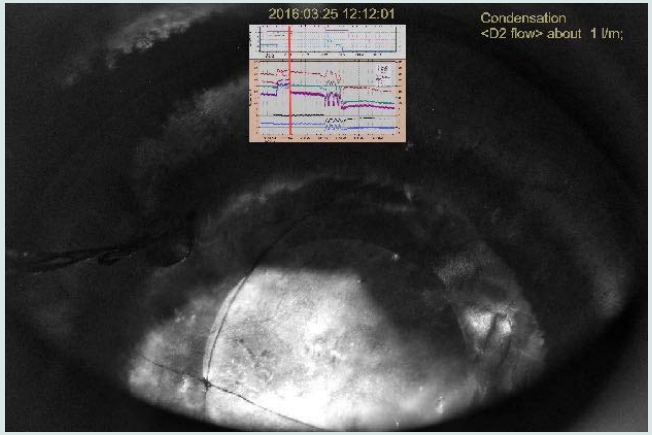


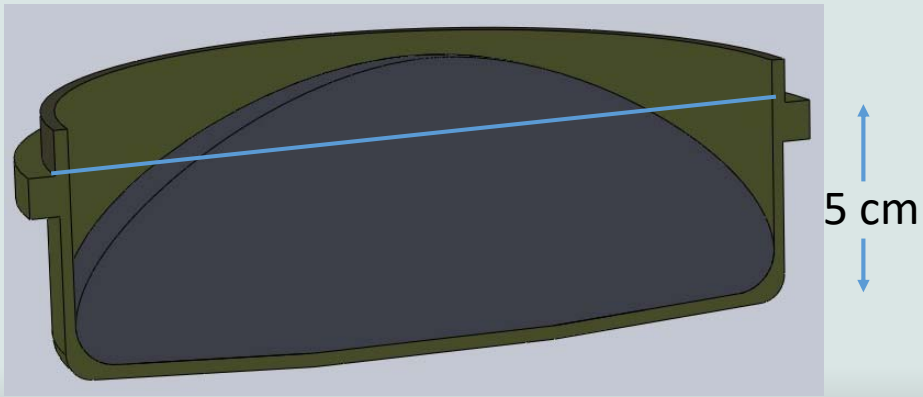


April 13

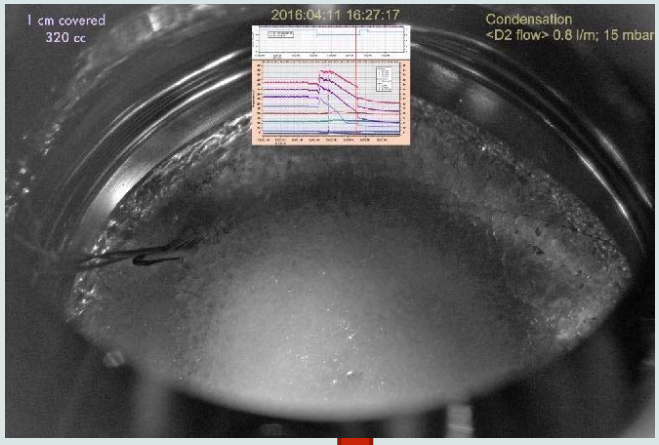


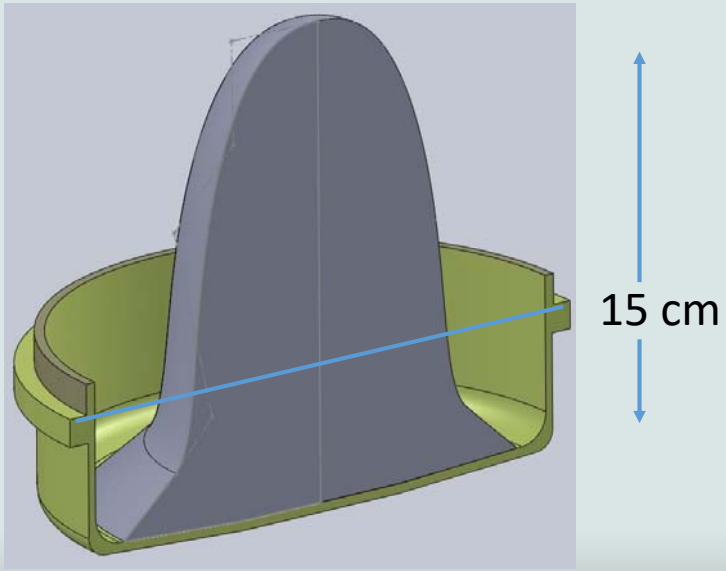

# Conclusion from SD2 shape reconstruction

The only difference between March and Apr 11 runs was temperature distribution of the container bottom

Crystal shapes and transparency are extremely temperature dependent!

# How to simulate T-distribution of container walls

- T-top and T -inlet are fixed on surfaces shown on the left
- Then temperature of the bottom circle is raised above D-inlet until 1 cm reading matches experimental value

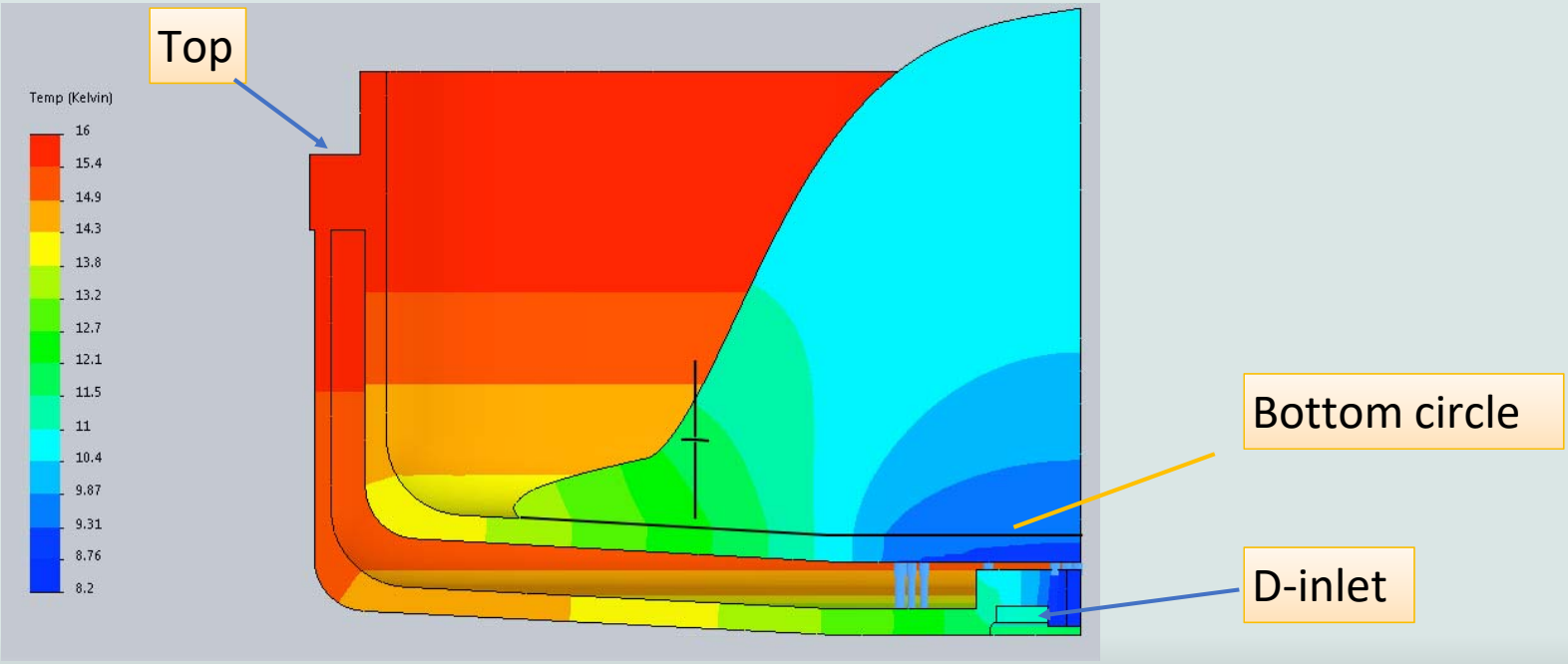

# Mar 22 condensation, 1cm=16K; 7.75/ 17/ 18.5-19K; from simulations bottom centre =14K;

- 1cm temperature can be reproduced only when assuming that bottom circle is at least 14K

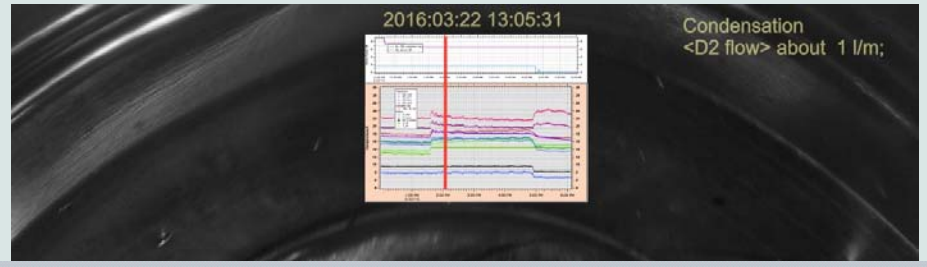


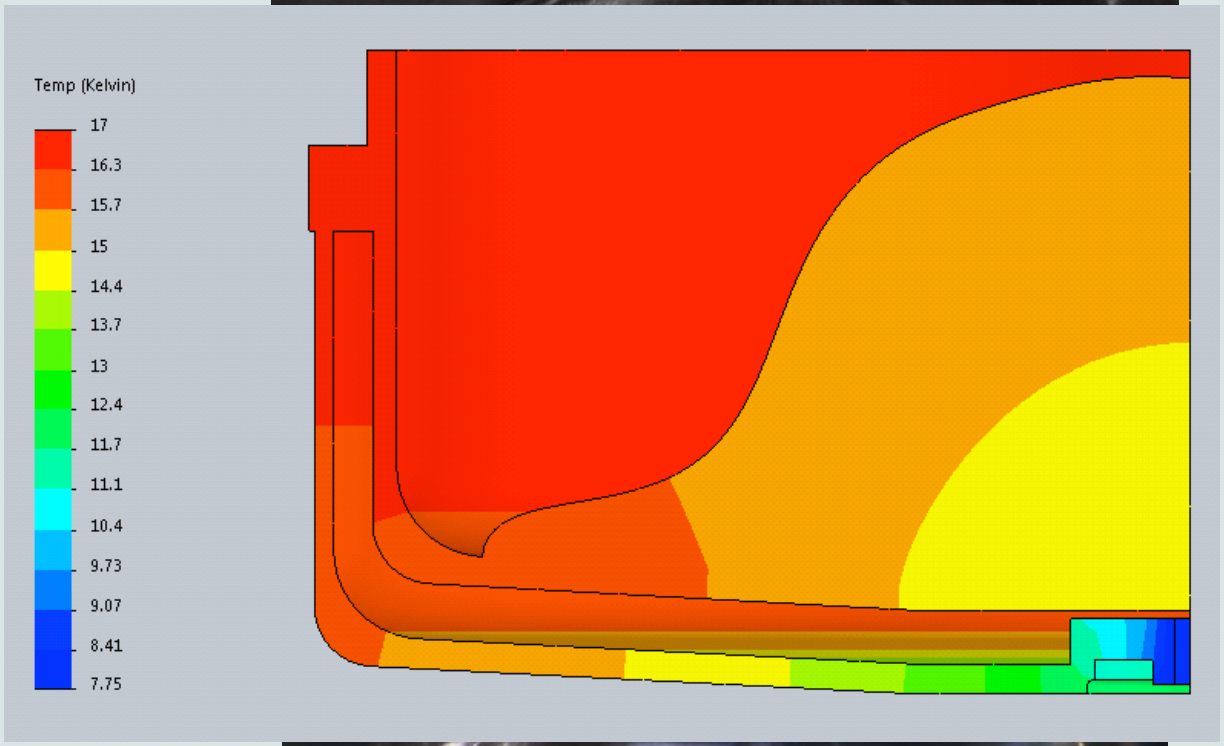


# April 11 simulation, D2 flow on and off

- 1cm temperature can be reproduced only when assuming that bottom circle is at 9.3K
- Transparent region start from above 12K
- after D2 flow was off, 1 cm dropped to 11K, while the T of container has not changed, it consistent with Bottom circle at the same T as D-inlet

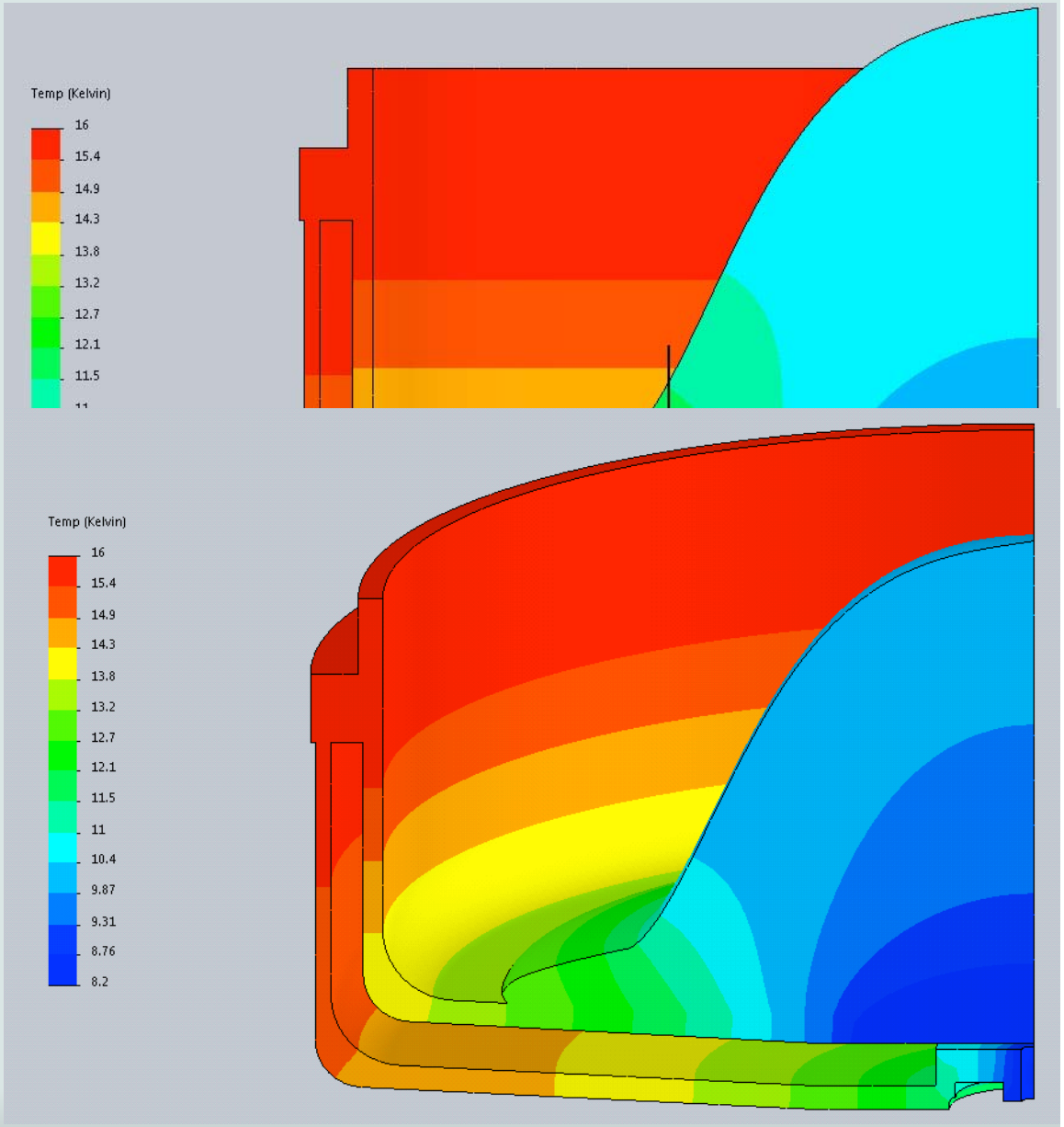

# April 25

- **9.5/ 18/ 16.2**,1cm=14.5K, about 340cc total
- 1cm temperature can be reproduced only when assuming that bottom circle is at 12K
- **Conclusion:** to grow transparent crystal, cryostat walls needs to be above 12K

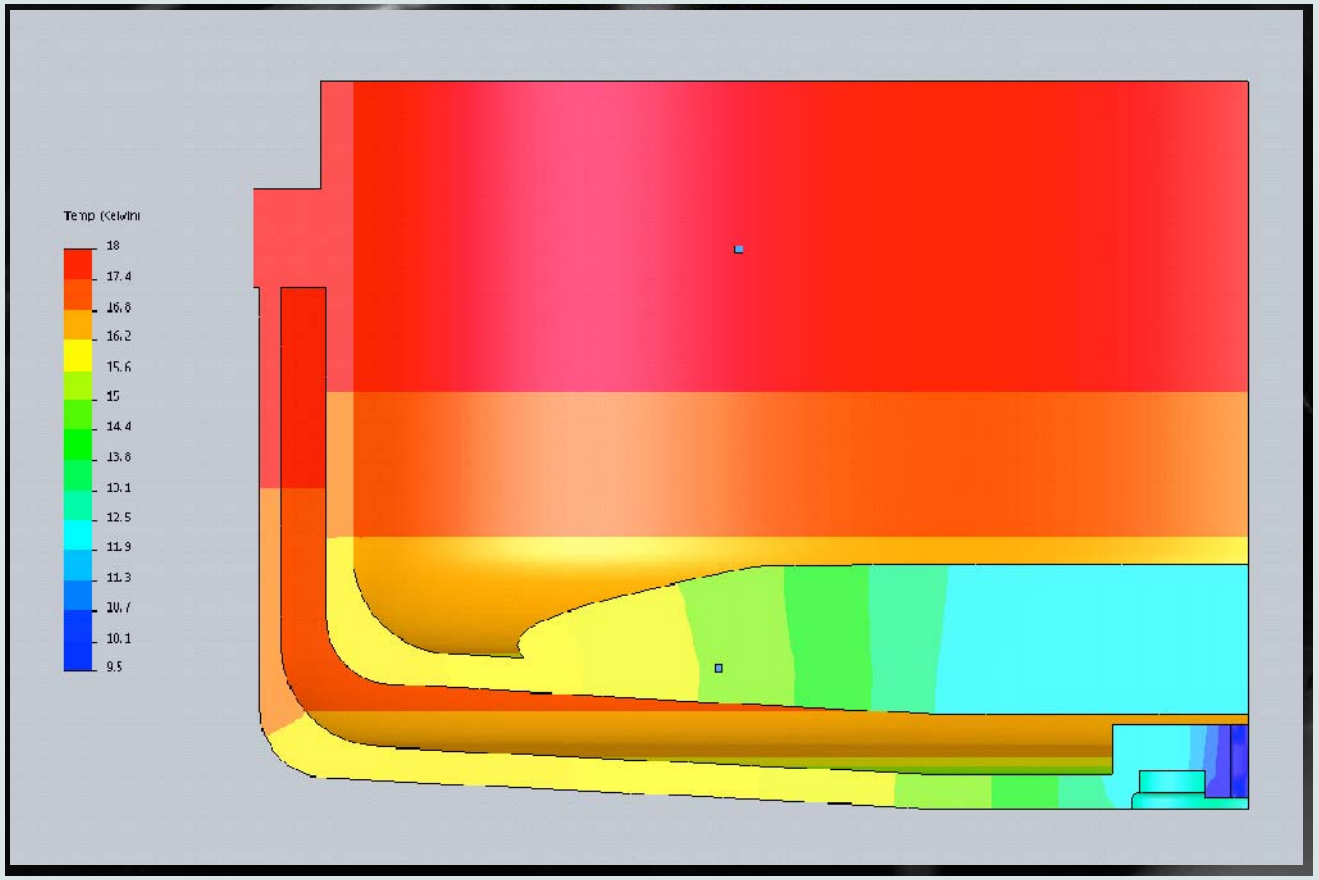

# Overview of 2016 results

**Summary/conclusions from 2016**

- There is a significant difference in crystal quality vs D2 flow, depending on cryostat temperature:
  - flow > 0.8 l/m & cryostat at 6K - result is snowflakes;
  - cryostat above 10K - good shiny crystal
- Quality of crystal depends critically on the growth temperature:
  - growing at T =6K results in a disconnected polycrystalline structure
  - growing or annealing crystal at T =9.5K results in a one solid while very grainy structure
  - for good crystal the coldest spot should be at T > 12K
- We observed extremely high mobility of SD2 even at 11.5K (couple of mm per hour):
  - large temperature gradients result in deformed crystal shapes
  - better to avoid use of heaters

# Growing perfect sD2 from vapor above the UCN source operational temperature following 2016 conclusions in 2018

# May condensation

- this run was done in one step, with one continuously decreasing flow of D2
- initial Ts: **8K/ 18K/ 18K;** no heater on during condensation; Ts controlled by cold He-flow tuning.
- final Ts: **7K/ 15K/ 15K,** D2 probes **at 14K -** gradient only **1K**

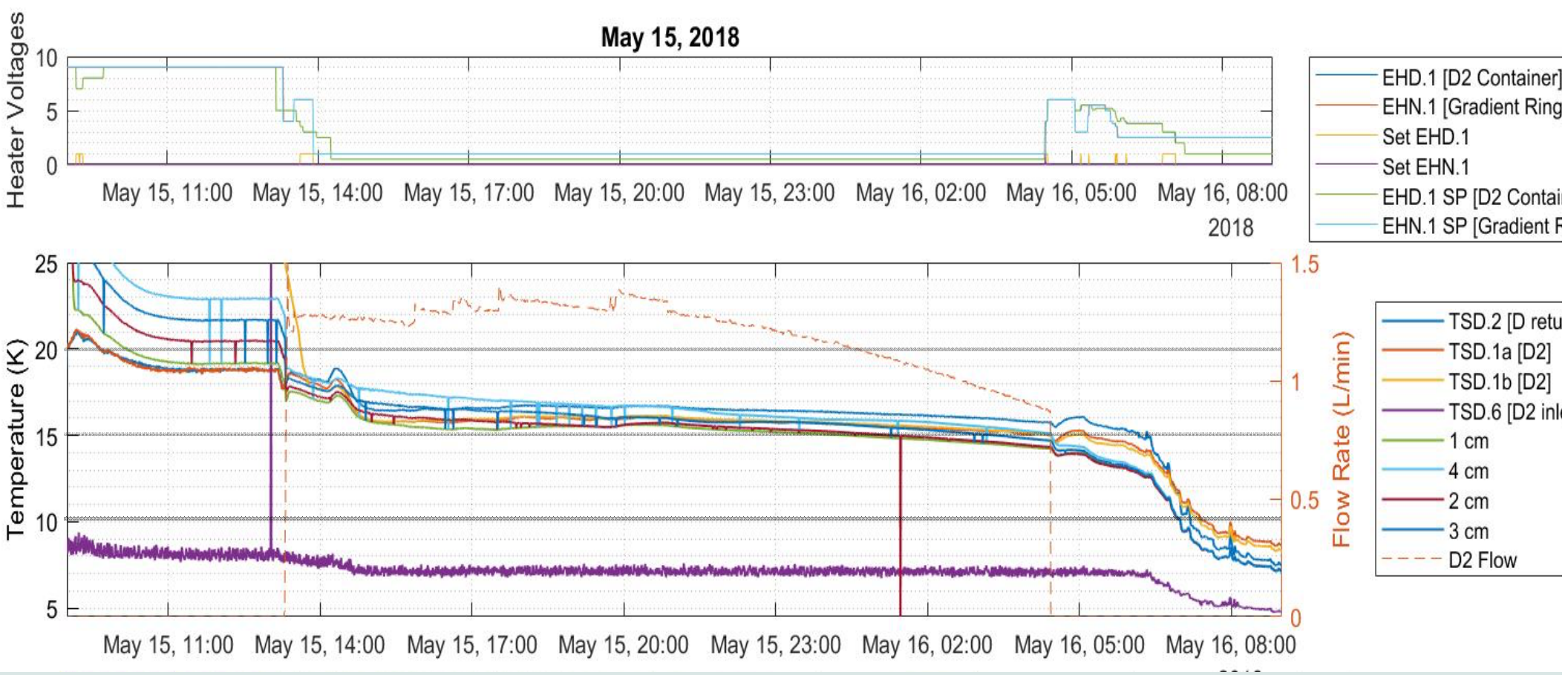

# May condensation

- this run was done in one step, with one continuously decreasing flow of D2
- initial Ts: **8K/ 18K/ 18K;** no heater on during condensation; Ts controlled by cold He-flow tuning.
- final Ts: **7K/ 15K/ 15K,** D2 probes **at 14K -** gradient only **1K**

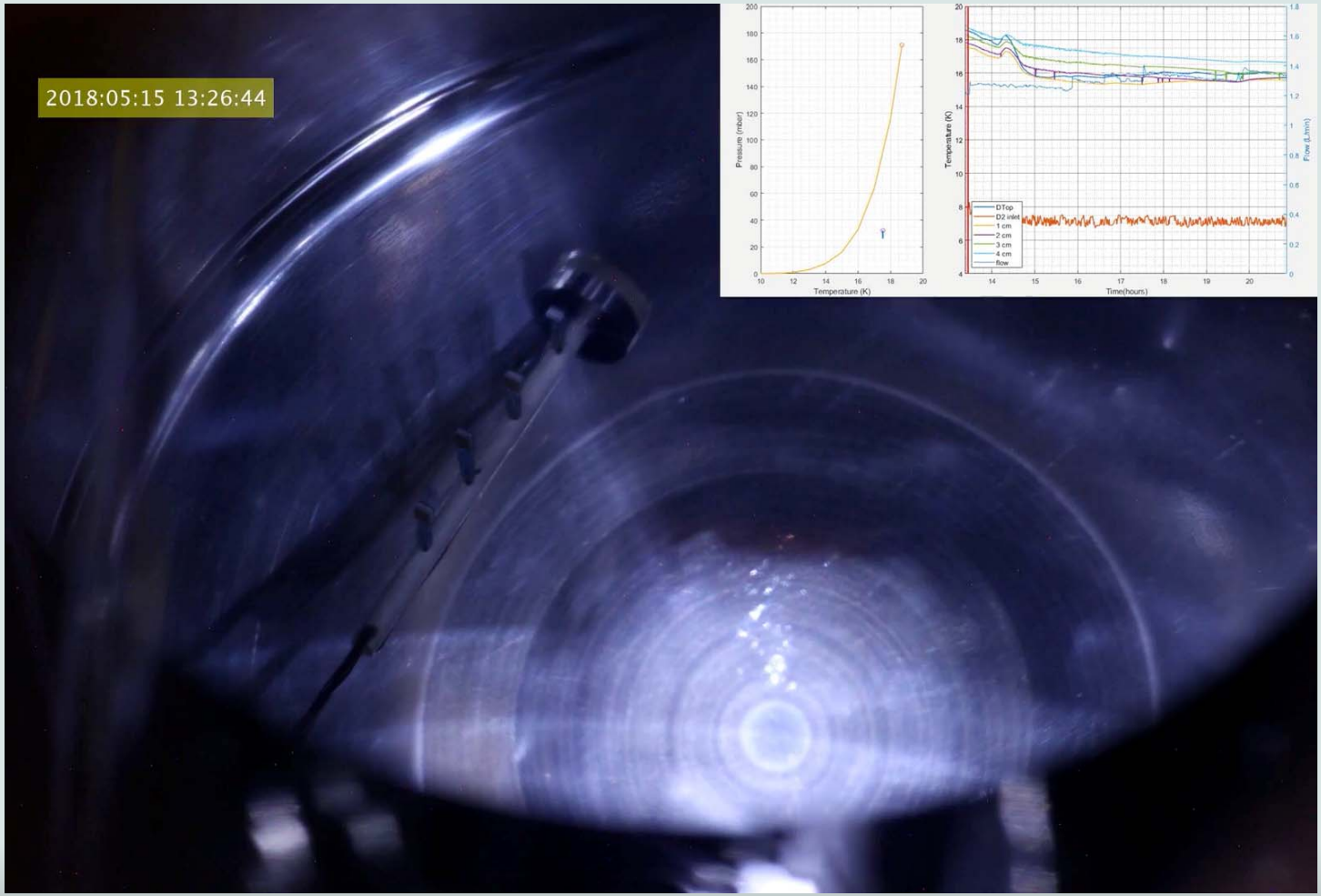

# May condensation: cooling

- 
- 
- 

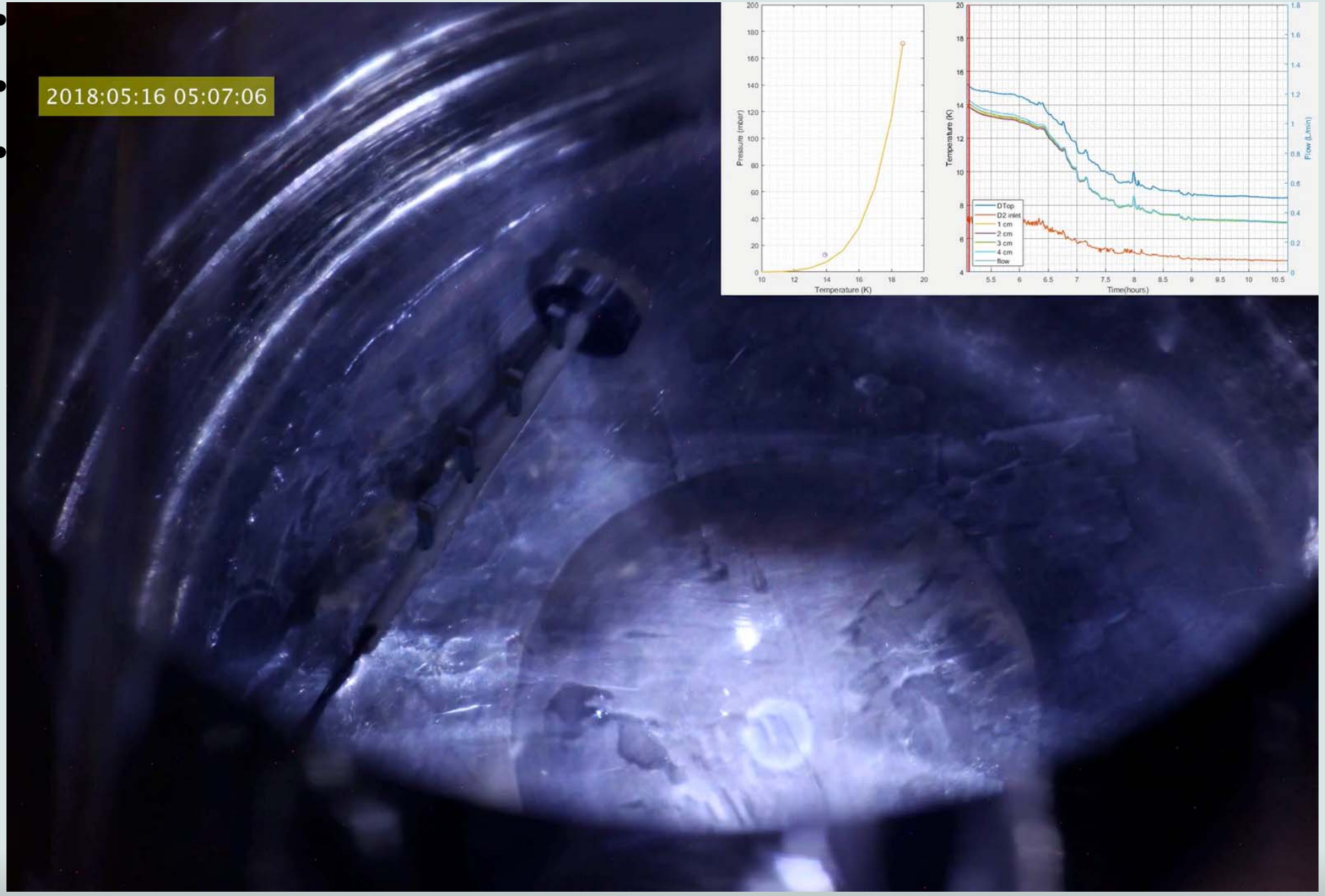

# May condensation: accidental annealing

- I set up heat shooting, as result at one point there was a bible in LHe line and the crystal was annealed to 14K without significant increase of pressure
- All surface facets were gone after such annealing

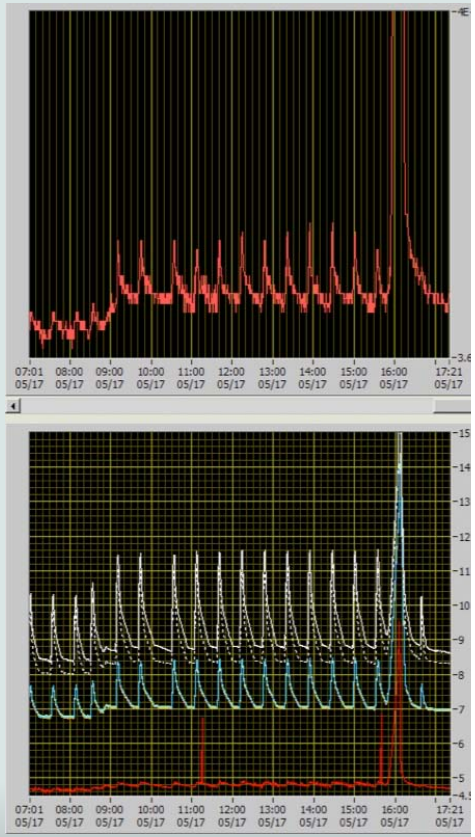

# Main Conclusion

quality and shape of the crystal can be predicted if we know the Temperature distribution of the cry-container walls

# Backup slides

# Growing from liquid phase ( melting and re-freezing)

# SD2 growing test 2016: melting

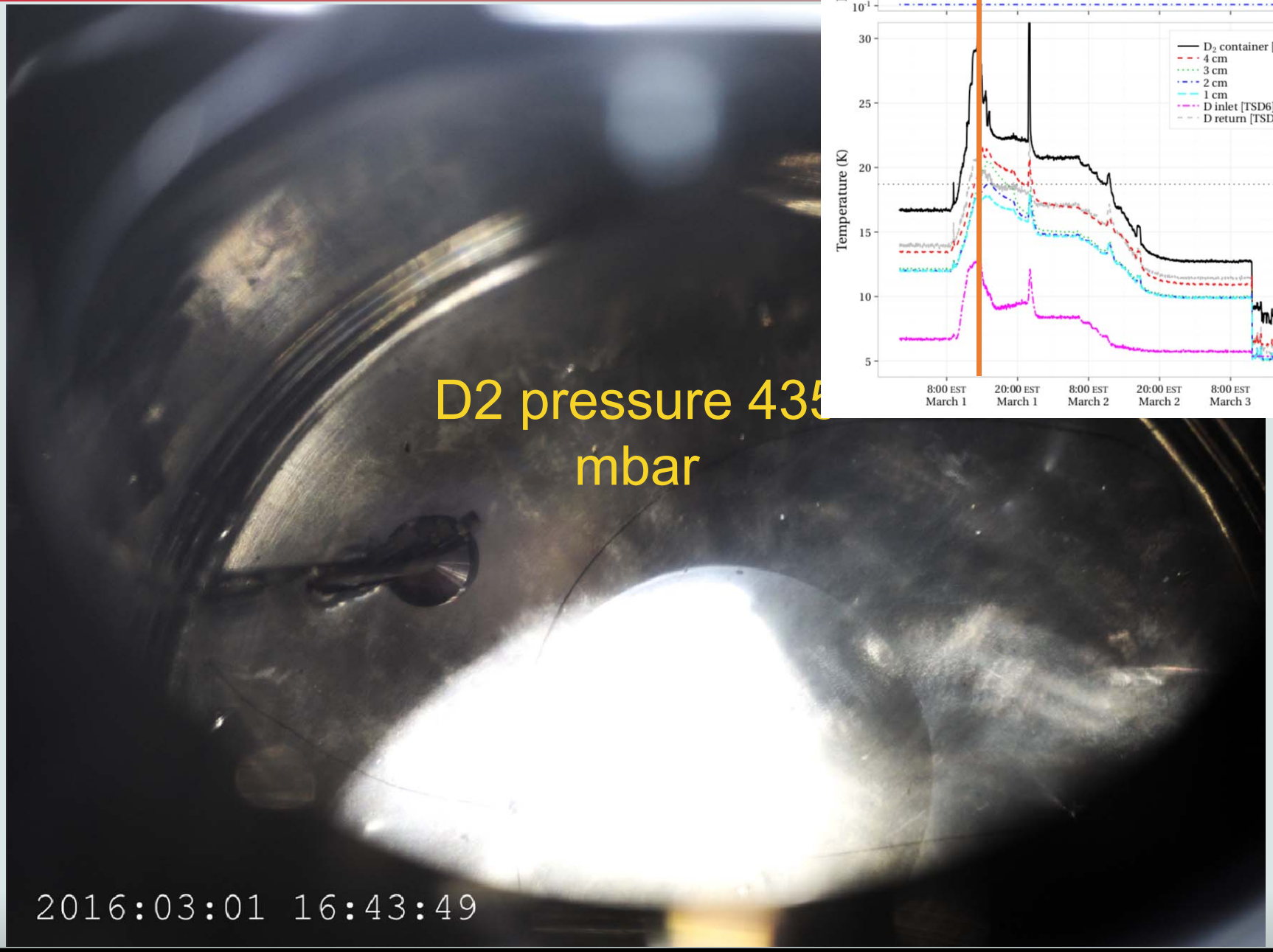

# SD2 growing test 1: start of freezing

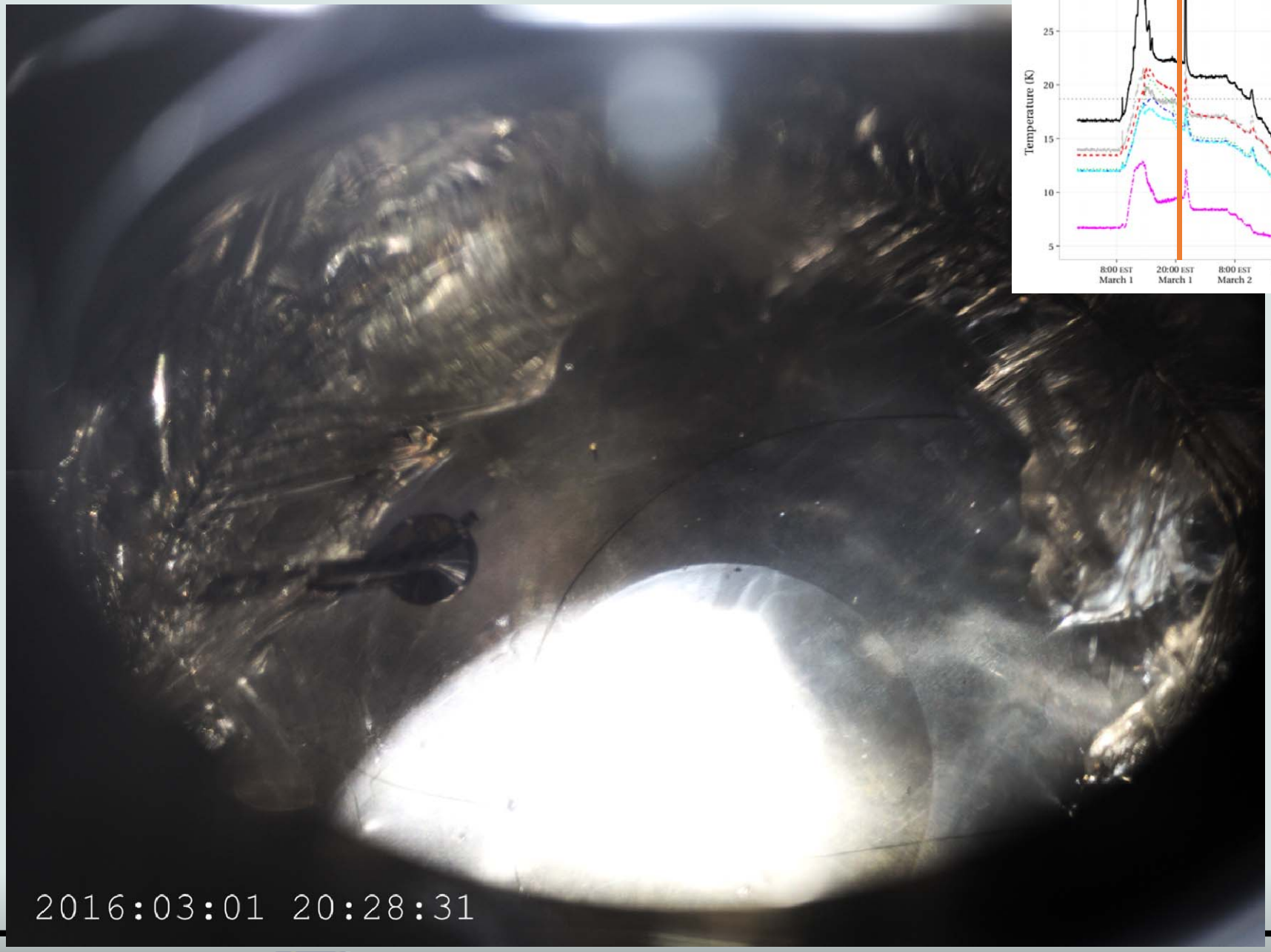


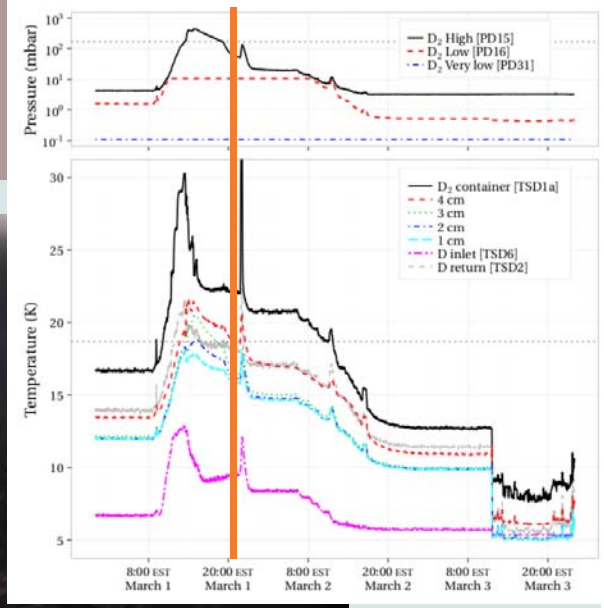

# SD2 SD2 freezing after melting

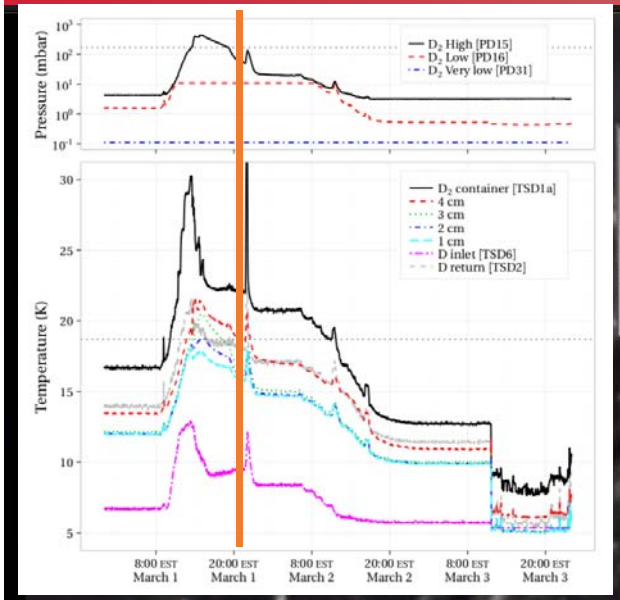

# SD2 freezing after melting, accidental warm up

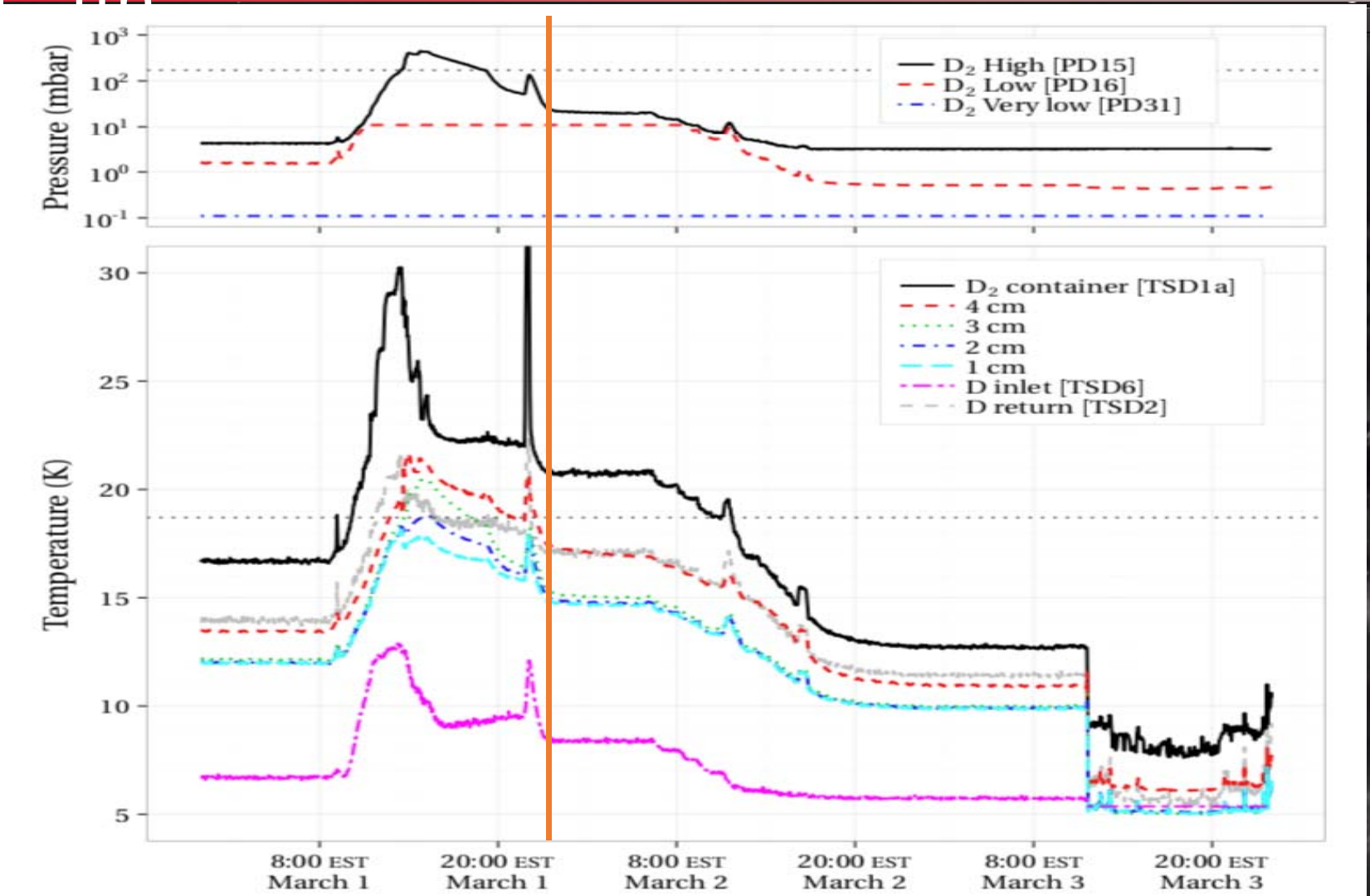

# SD2 after annealing overnight at 16K


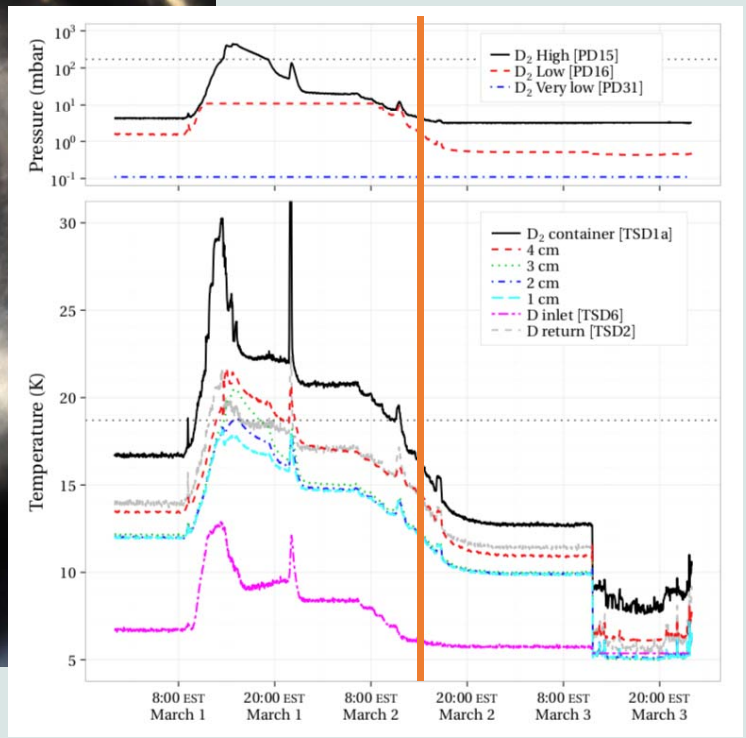

# SD2 after cooling down to 5K


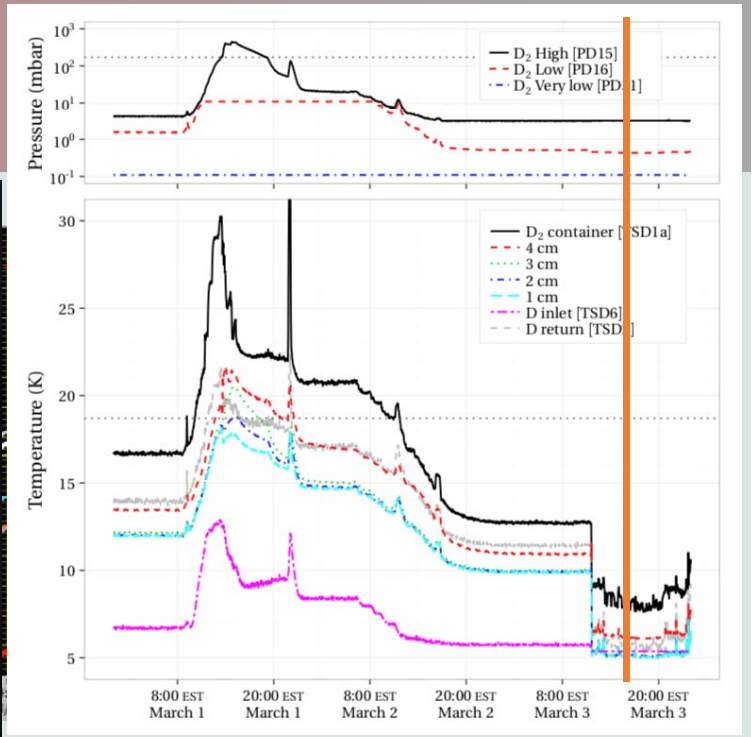


- It seems that because of annealing we were able to avoid contraction strain and obtain crystal of the quite good quality
- during annealing crystal was re-shaping and moving from the walls

CREMLIN PLUS
Connecting Russian and European Measures
for Large-scale Research Infrastructures

# On simulation of VCN sources

L. Zanini on behalf of

Zs. Kókai, J.I. Márquez Damián, V. Santoro, L. Zanini

This project has received funding from the European Union's Horizon 2020 research and innovation programme under grant agreement No. 871072.

CREMLIN PLUS

# Goals

- **Determine yields of VCN from candidate converter materials, including the effects of ND reflectors**
- **Determine best converter material for prototype experiment to be performed at PF1B/ILL**
- NOTE: ILL PF1B cold spectrum used, some calculations done with generic ILL cold spectrum
- Results are in progress and preliminary

| | Material | Temperature | Density (g/cm$^3$) |
|---|---|---|---|
| converter | Solid deuterium | 5 K | 0.2059 |
| converter | Liquid parahydrogen | 14 K | 0.071 |
| converter | Liquid orthohydrogen | 14 K | 0.071 |
| reflector | Solid methane | 22 K | 0.5 |
| reflector | Magnesium-hydride | 20 K | 0.5 (bulk density) |
| reflector | Nanodiamond | 296 K | 0.6 (bulk density) |

This project has received funding from the European Union's Horizon 2020 research and innovation programme under grant agreement No. 871072.



CREMLIN PLUS

# MCNP geometry to compare different converters

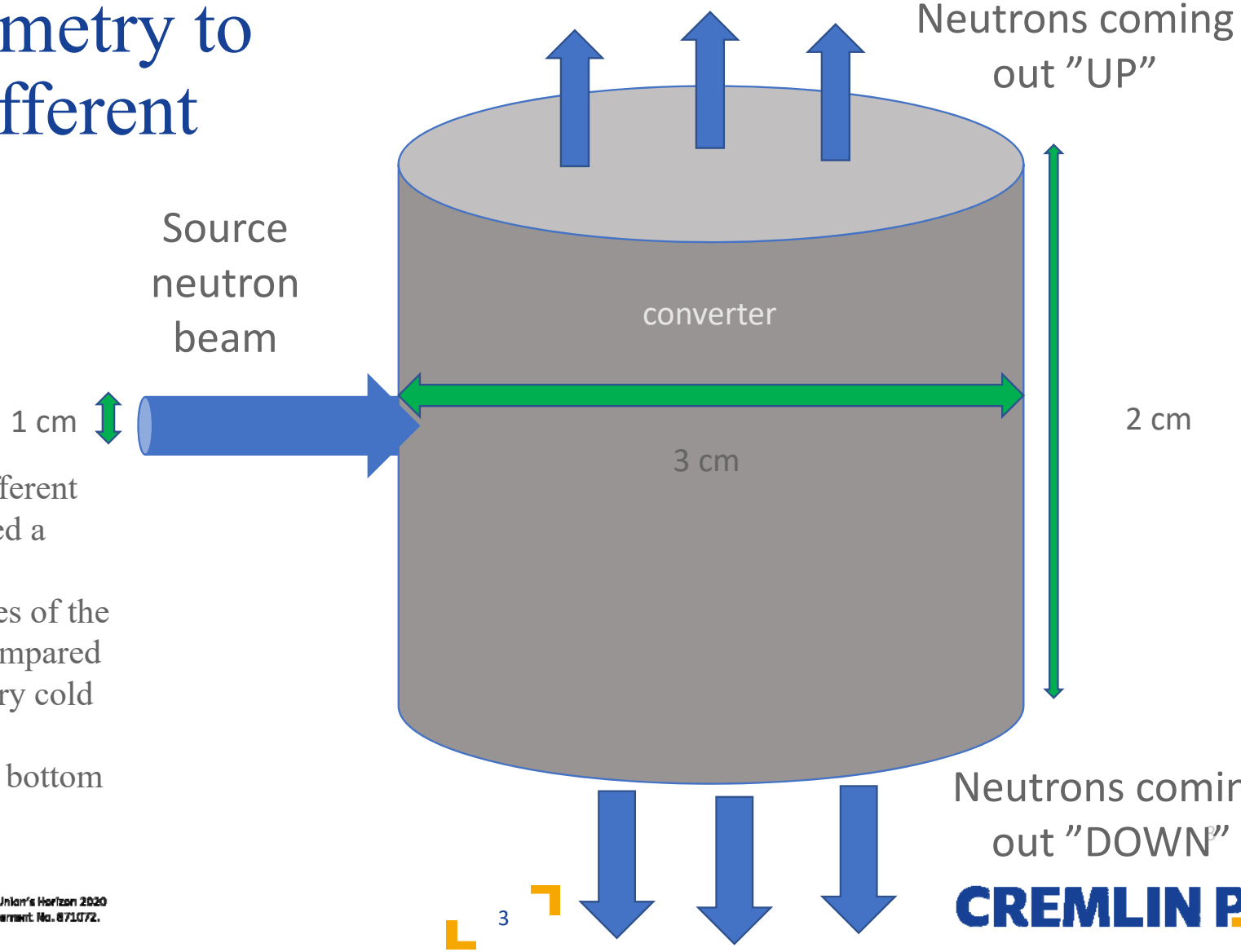


In order to compare the different converter materials, we used a cylindrical bare converter geometry. The performances of the various converters were compared based on the outcoming very cold neutron intensity (F1 tally) integrated over the top and bottom surface of the converter.

This project has received funding from the European Union's Horizon 2020 research and innovation programme under grant agreement No. 871072.



CREMLIN PLUS

# MCNP geometry with ND reflector

We measured neutron intensity through this surface

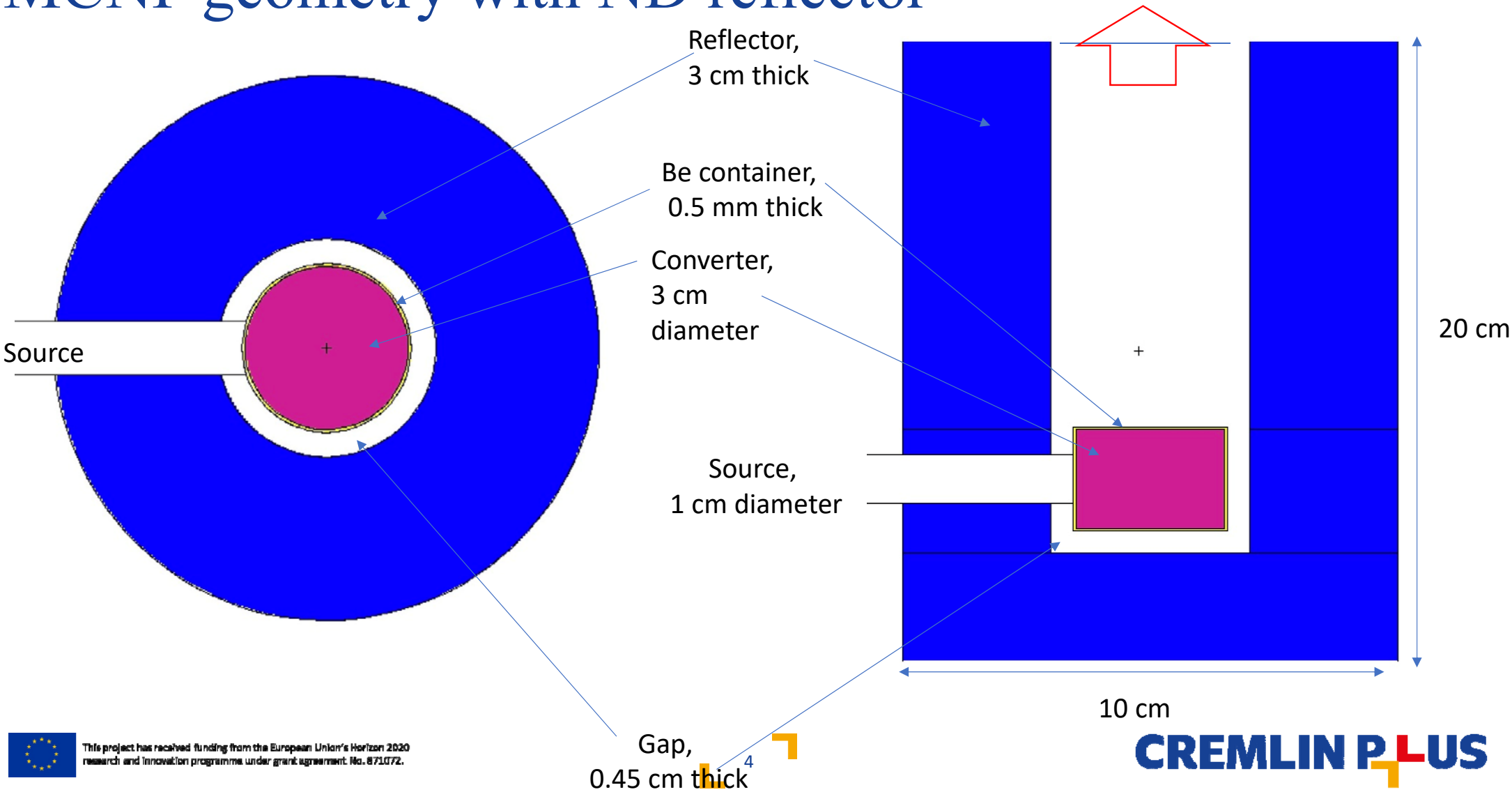


This project has received funding from the European Union's Horizon 2020 research and innovation programme under grant agreement No. 871072.



CREMLIN PLUS

# Solid deuterium cross section

- The SD2 ACE library used in MCNP contains artifacts in energy distribution due to use of (old format) discrete angular and secondary energy distributions.
- Together with the need of better knowledge of SD2 cross section, this motivates the work for improved SD2 cross section (See R. Granada talk).
- At present we are using free gas SD2 cross sections at 5.4 K.

Spectrum inside ”infinite” sphere with neutrons generated at the center

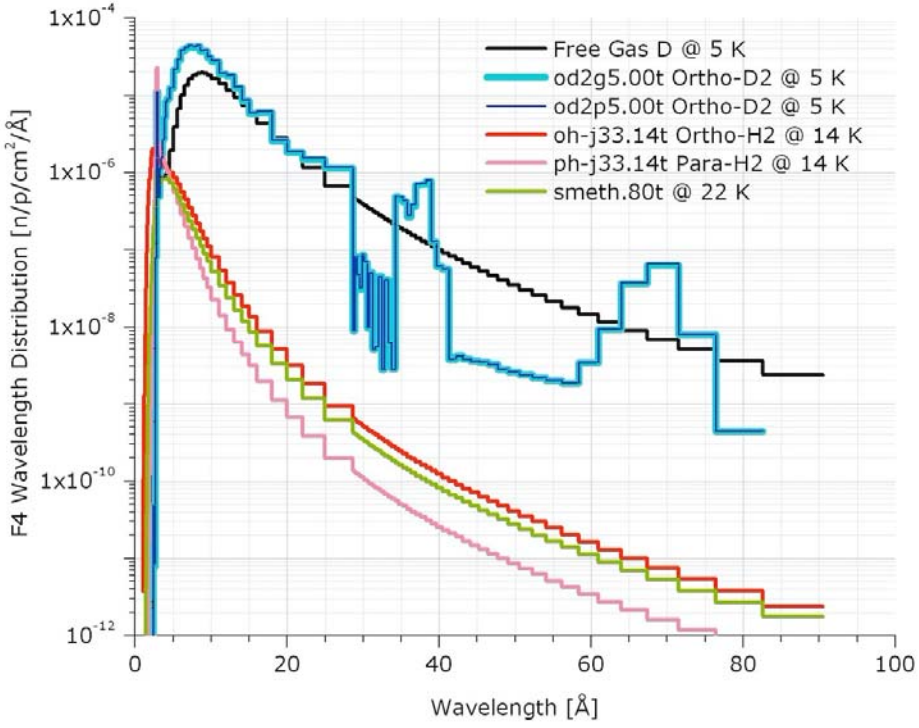


This project has received funding from the European Union's Horizon 2020 research and innovation programme under grant agreement No. 871072.



CREMLIN PLUS

# spectra from bare converter

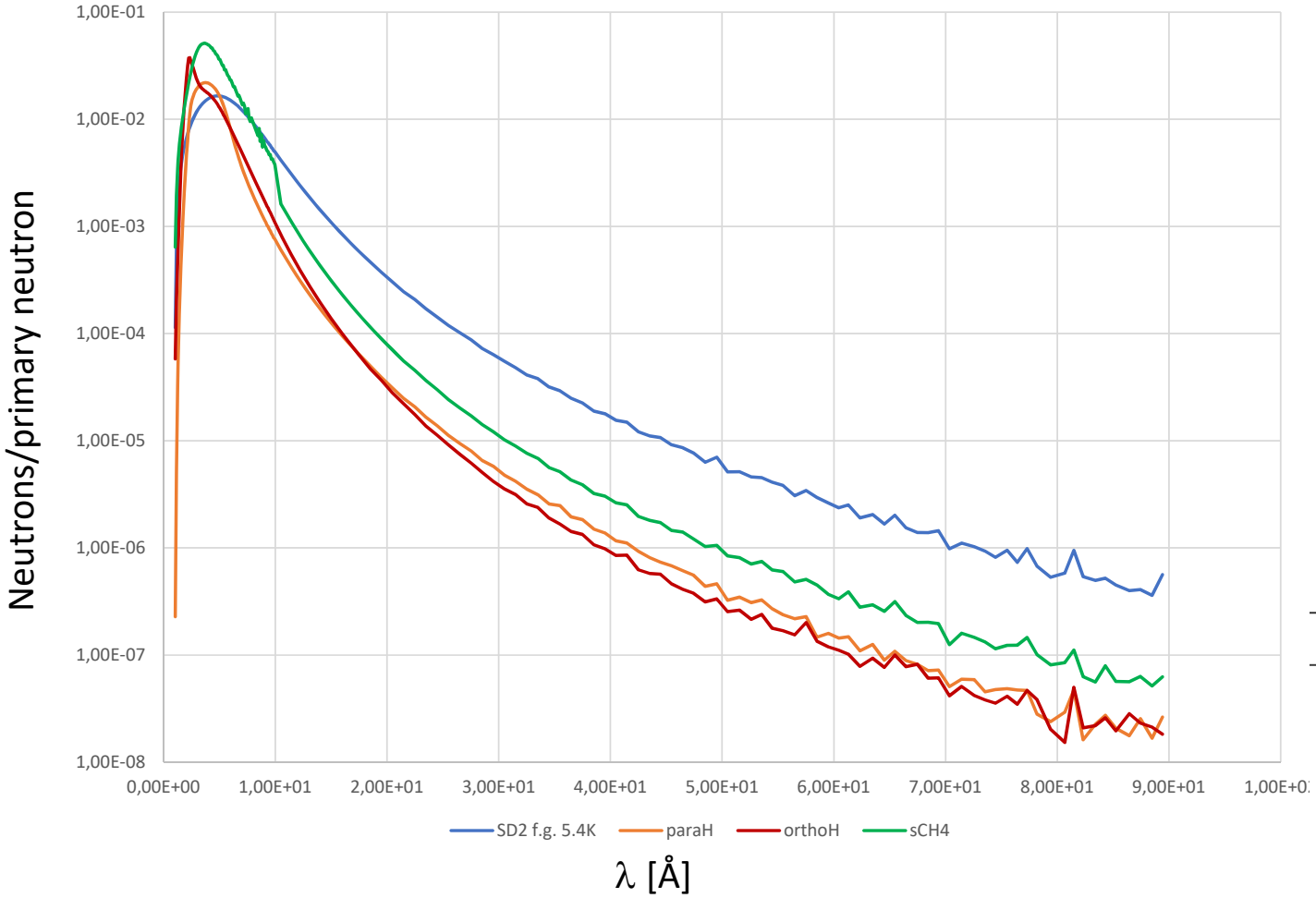


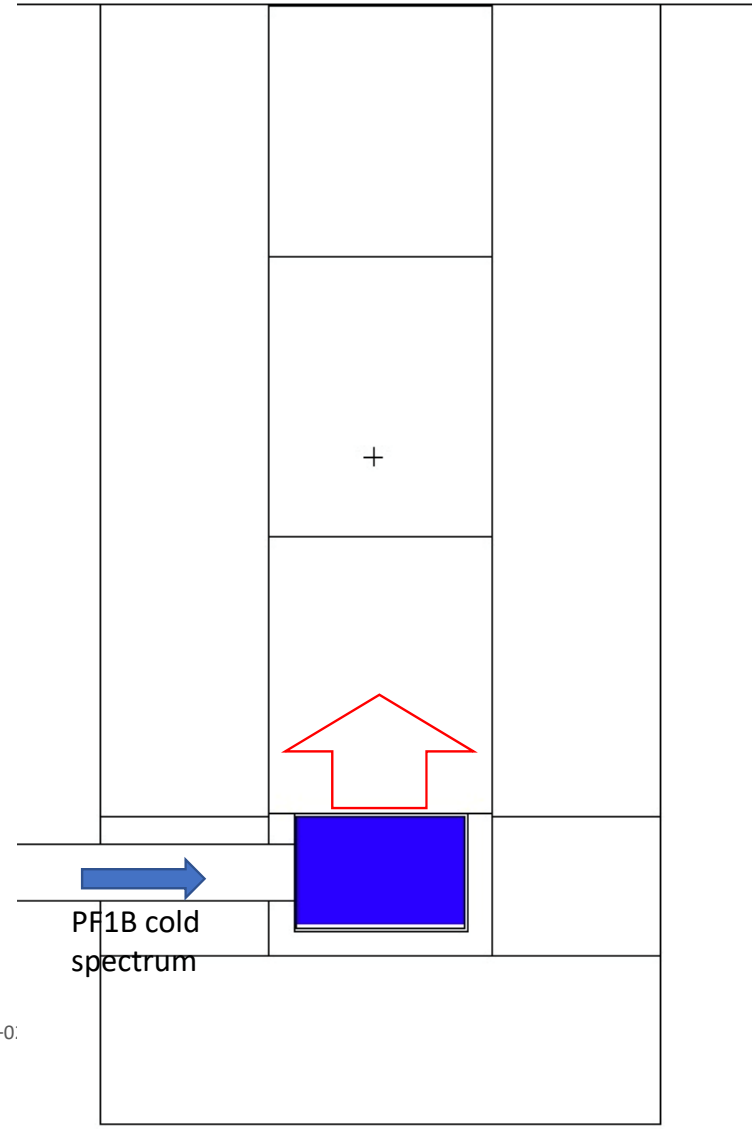


This project has received funding from the European Union's Horizon 2020 research and innovation programme under grant agreement No. 871072.



CREMLIN PLUS

# MCNP geometry of different reflector concepts

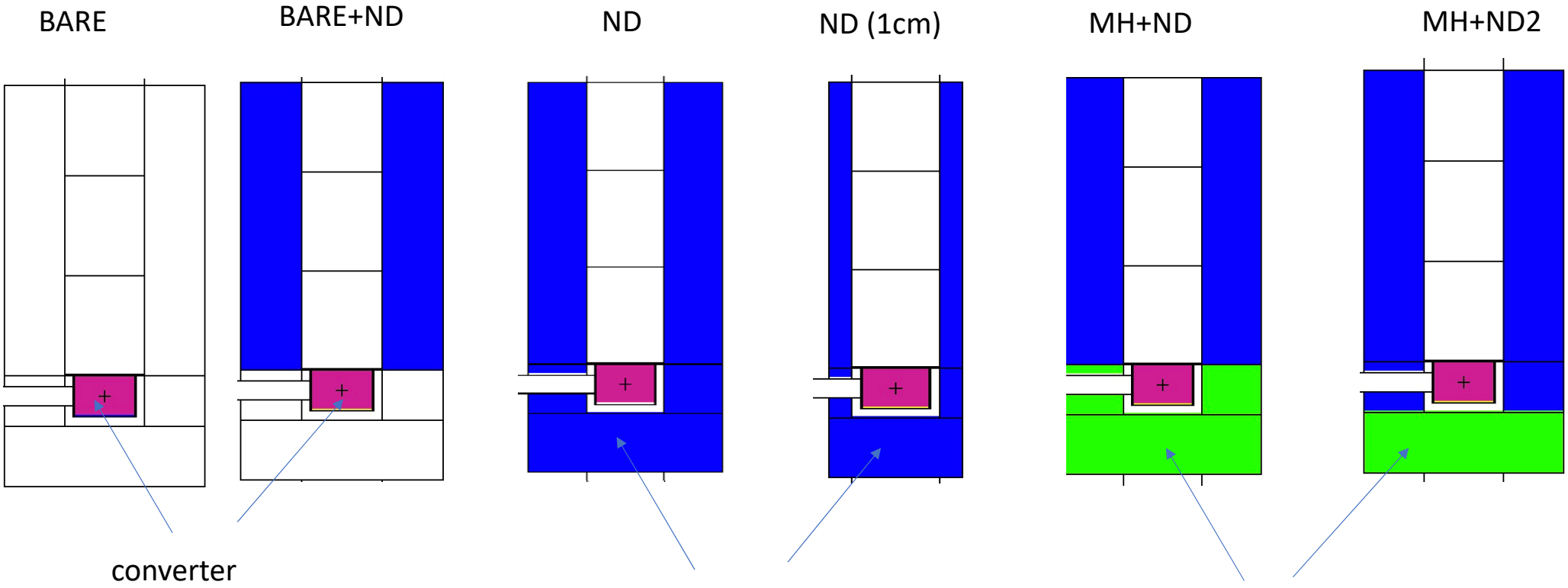


This project has received funding from the European Union's Horizon 2020 research and innovation programme under grant agreement No. 871072.



CREMLIN PLUS

# Modeling of nanodiamonds in MCNP

- A simple model for SANS as described by Granada [Granada, J. Rolando, J. Ignacio Márquez Damián, and Christian Helman. ”Studies on reflector materials for cold neutrons.” EPJ Web of Conferences, 231, 04002 (2020)]:
  - Bragg scattering and inelastic scattering are modeled using an ACE file produced with NJOY-Ncrystal
  - SANS is modeled with a piecewise power function that approximates the S(Q) measured by Teshigawara [Teshigawara, M., Y. et al. ”Measurement of neutron scattering cross section of nano-diamond with particle diameter of approximately 5 nm in energy range of 0.2 meV to 100 meV.” Nucl. Instr. and Meth. A, 929, 113 (2019)]

- The parameters for this function are stored in the ACE file, and a modified version of the Monte Carlo code reads these parameters and sample the outgoing direction.

- The modification was implemented in MCNP 6.2, PHITS 3.21 and OpenMC.

***[J. I. Márquez Damián et al., Nuclear Data Development at the ESS, UCANS-web 2020]***

This project has received funding from the European Union's Horizon 2020 research and innovation programme under grant agreement No. 871072.

# Effect of ND reflector on flux increase

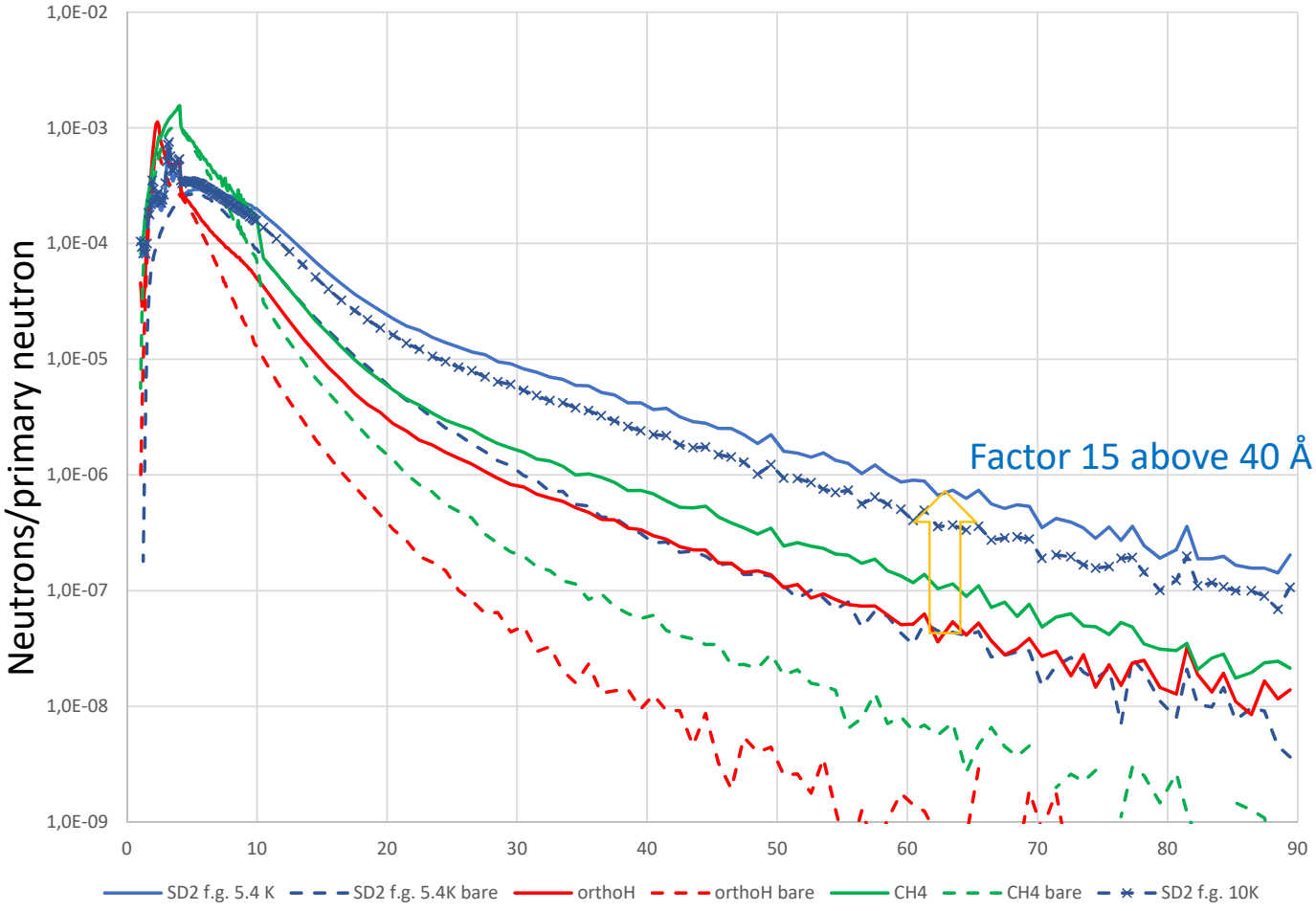


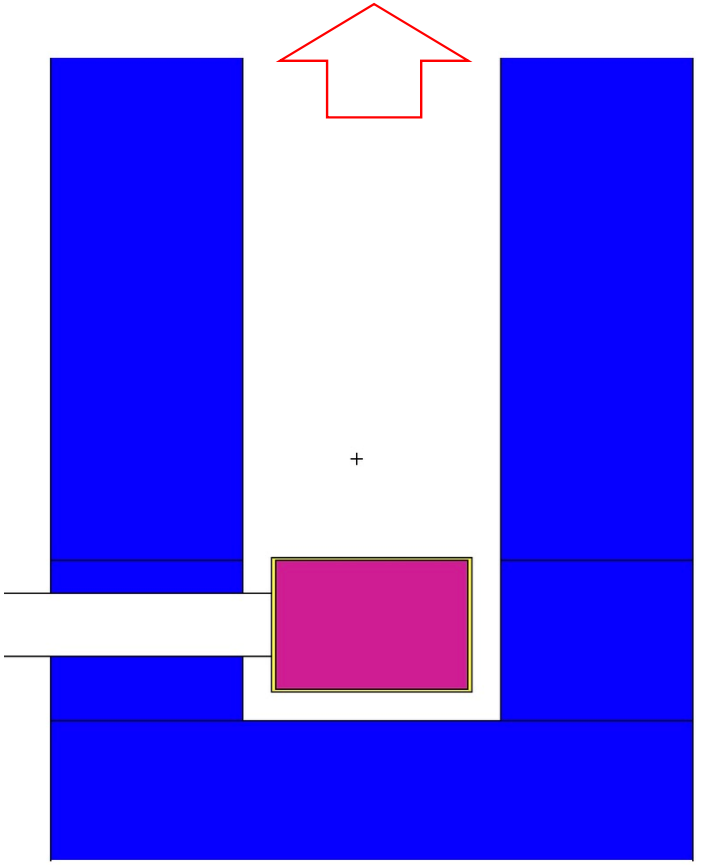

This project has received funding from the European Union's Horizon 2020 research and innovation programme under grant agreement No. 871072.



CREMLIN PLUS

# Relative intensity through the tube, solid deuterium converter

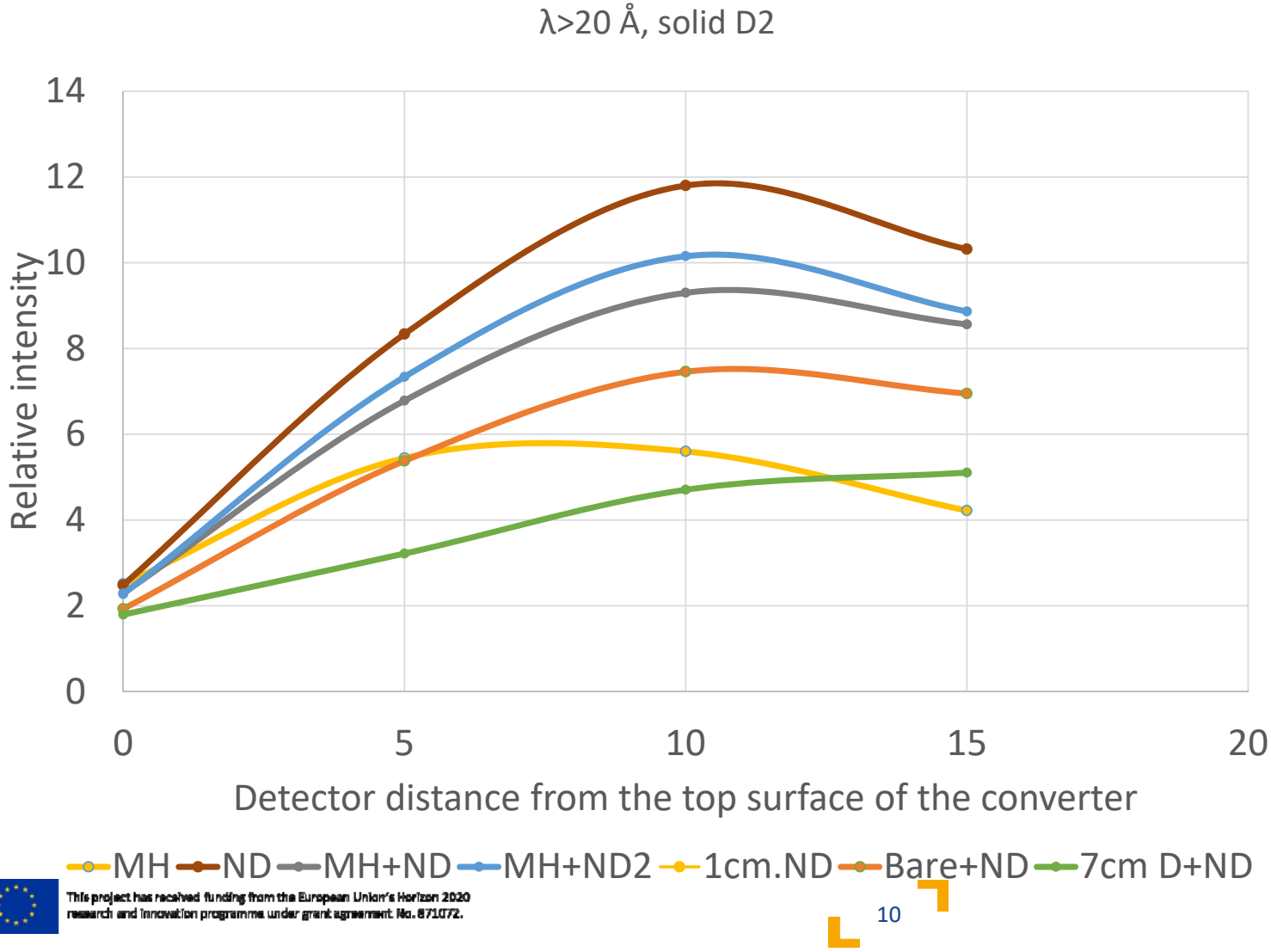


Existing SD2 cross section used

- With nanodiamond around the converter and nanodiamond tube, we can reach 10 times increase in intensity comparing with the bare case.
- The effect is less for a larger converter (green curve)

This project has received funding from the European Union's Horizon 2020 research and innovation programme under grant agreement No. 871072.



CREMLIN PLUS

# Angular histogram (orthodeuterium converter and nanodiamond reflector)

Simulation with existing SD2 cross section used and generic ILL cold spectrum

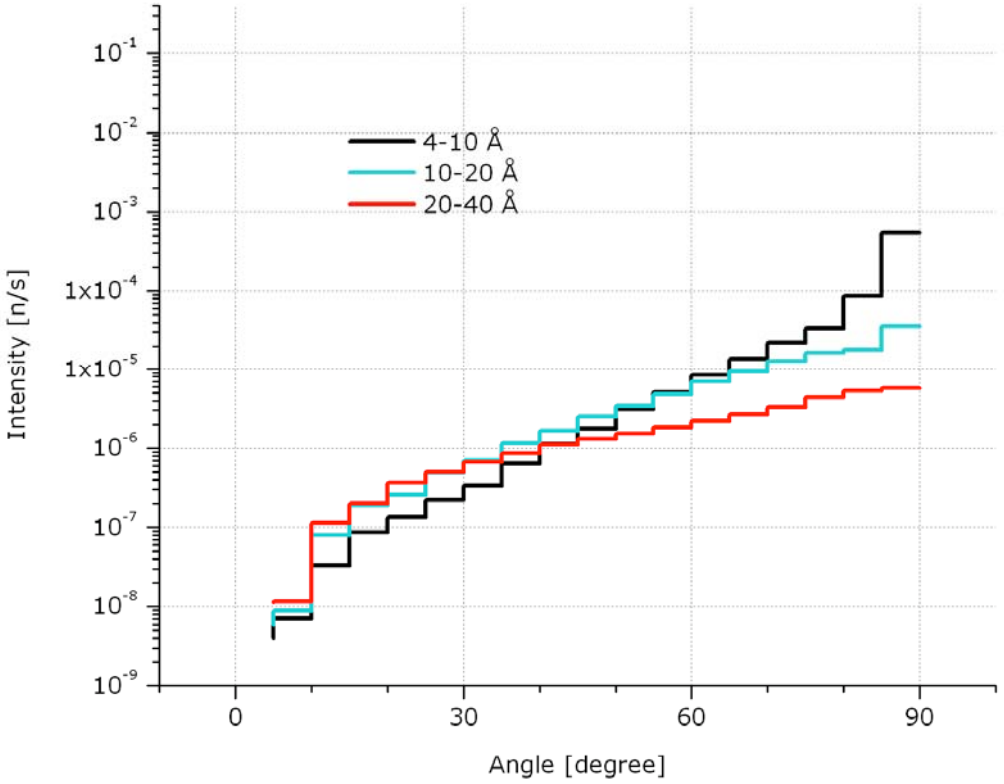


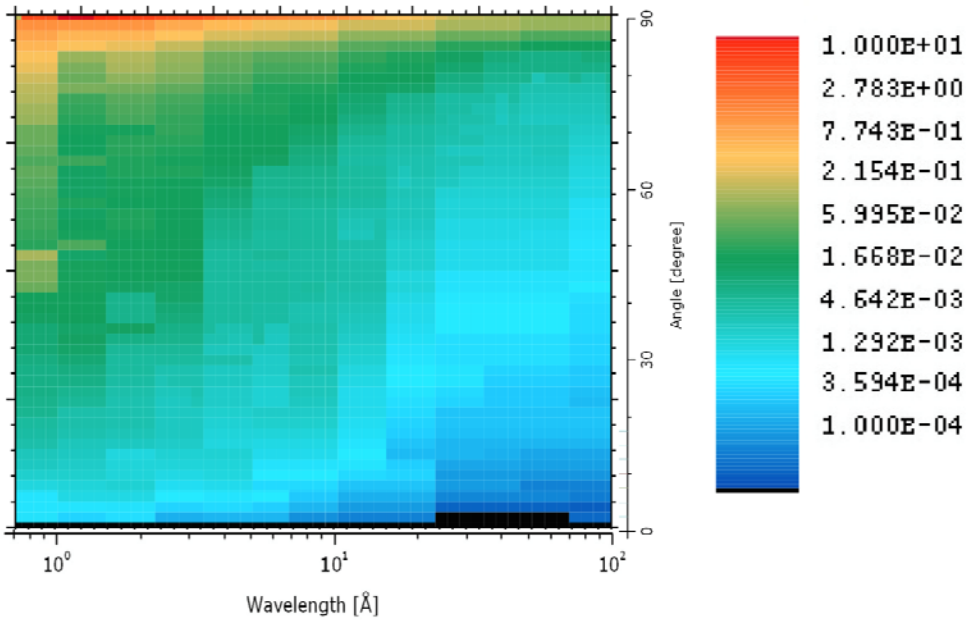


The colder neutrons are less collimated as expected

This project has received funding from the European Union's Horizon 2020 research and innovation programme under grant agreement No. 871072.



CREMLIN PLUS

# For the prototype experiment we need the intensity at different distances from source, λ> 40 Å

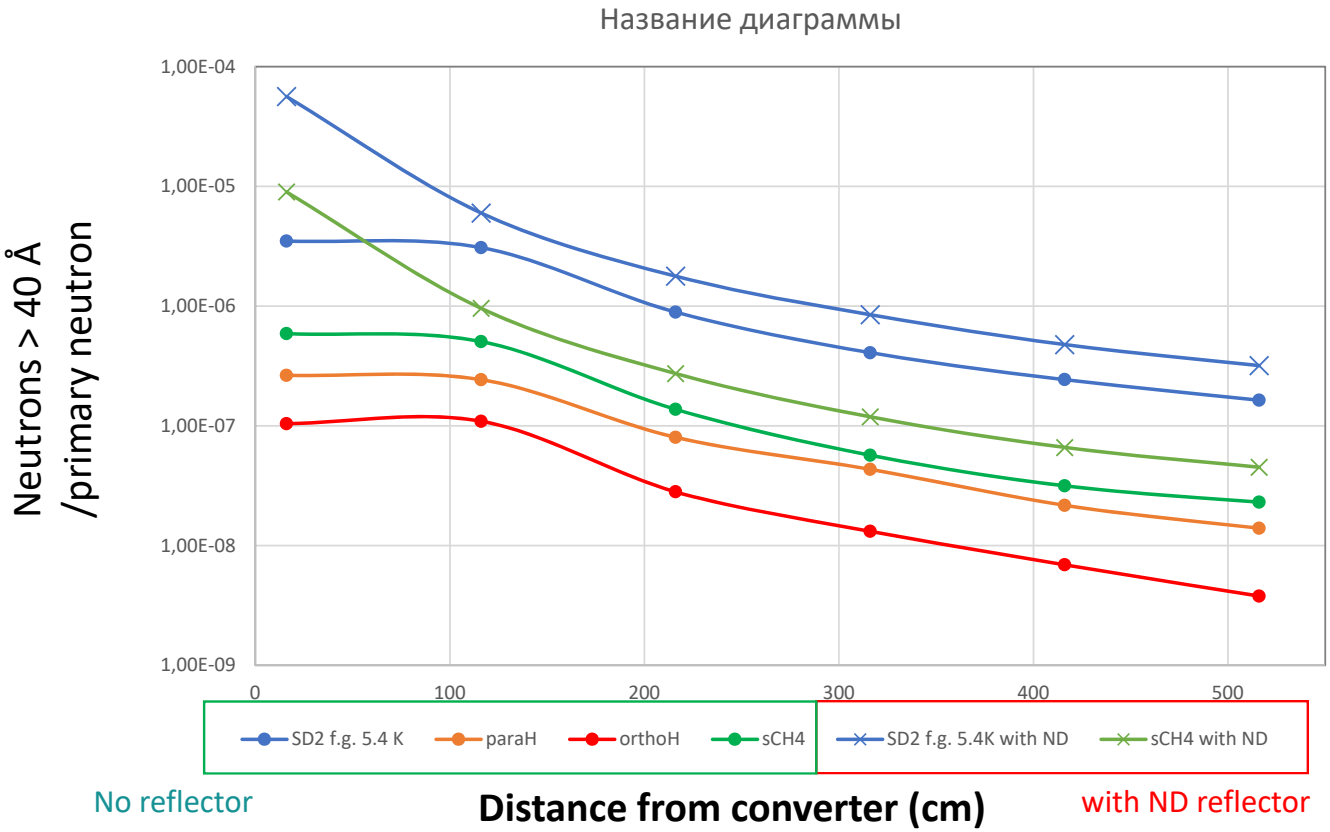


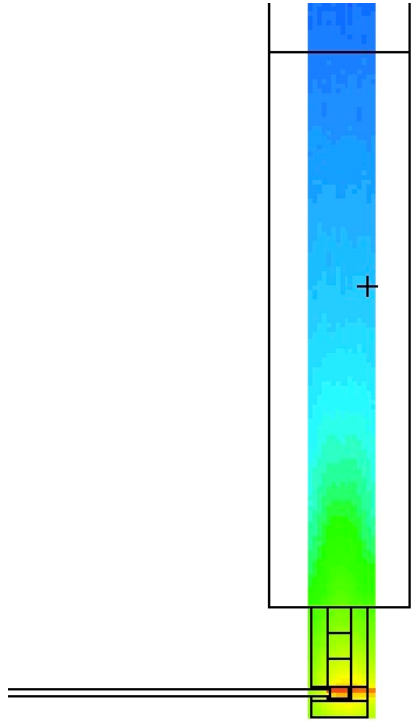

This project has received funding from the European Union's Horizon 2020 research and innovation programme under grant agreement No. 871072.



CREMLIN PLUS

# Conclusions

- With nanodiamond around the converter and nanodiamond tube, we can reach >10 times increase in intensity comparing with the bare case
- The effect is larger for smaller converters (about 3 cm diameter), even though larger converters deliver more VCNs

**NEXT STEPS**

- For more reliable results, especially above 40 Å, we have identified the need for improved solid deuterium cross sections
- Simulations with different ND types will be added in the course of the project
- Neutron spectra and count rates of the prototype experiment will be calculated

This project has received funding from the European Union's Horizon 2020 research and innovation programme under grant agreement No. 871072.

CREMLIN PLUS

Connecting Russian and European Measures for Large-scale Research Infrastructures

**Second meeting of the Subcommittee on Fundamental Physics of WP3**

# *On the fluorination of nano-diamonds*

***Marc DUBOIS***

UNIVERSITÉ Clermont Auvergne

cnrs

sigma CLERMONT

Institut de Chimie de Clermont-Ferrand

Réseau Français du Fluor - CNRS

## How to remove $sp^2$ shell and hydrogen?

## Fluorination

## Flurorination of $sp^2$ carbons : 3 effects (crystallinity, SSA, curvature)

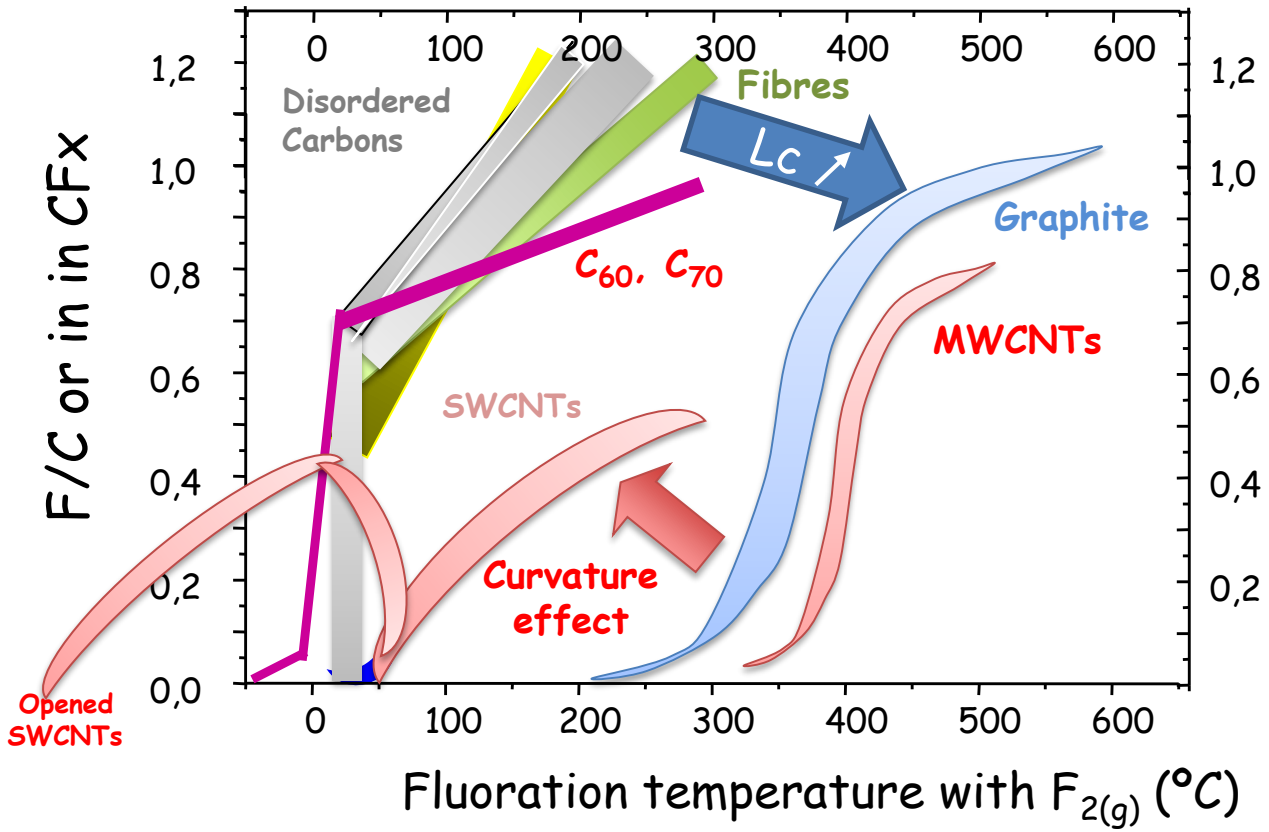


$C(s) + x/2\ F_2(g) \rightarrow CF_x(s)$

$0<x<1$ Fluorination

$1<x<1.2$ Extra-Fluorination

$2<x<4$ Decomposition

$C(s) + xF_2(g) \rightarrow CF_4(g) + C_2F_6(g)$



Institut de Chimie de Clermont-Ferrand

## How to remove $sp^2$ shell and hydrogen?

## Fluorination

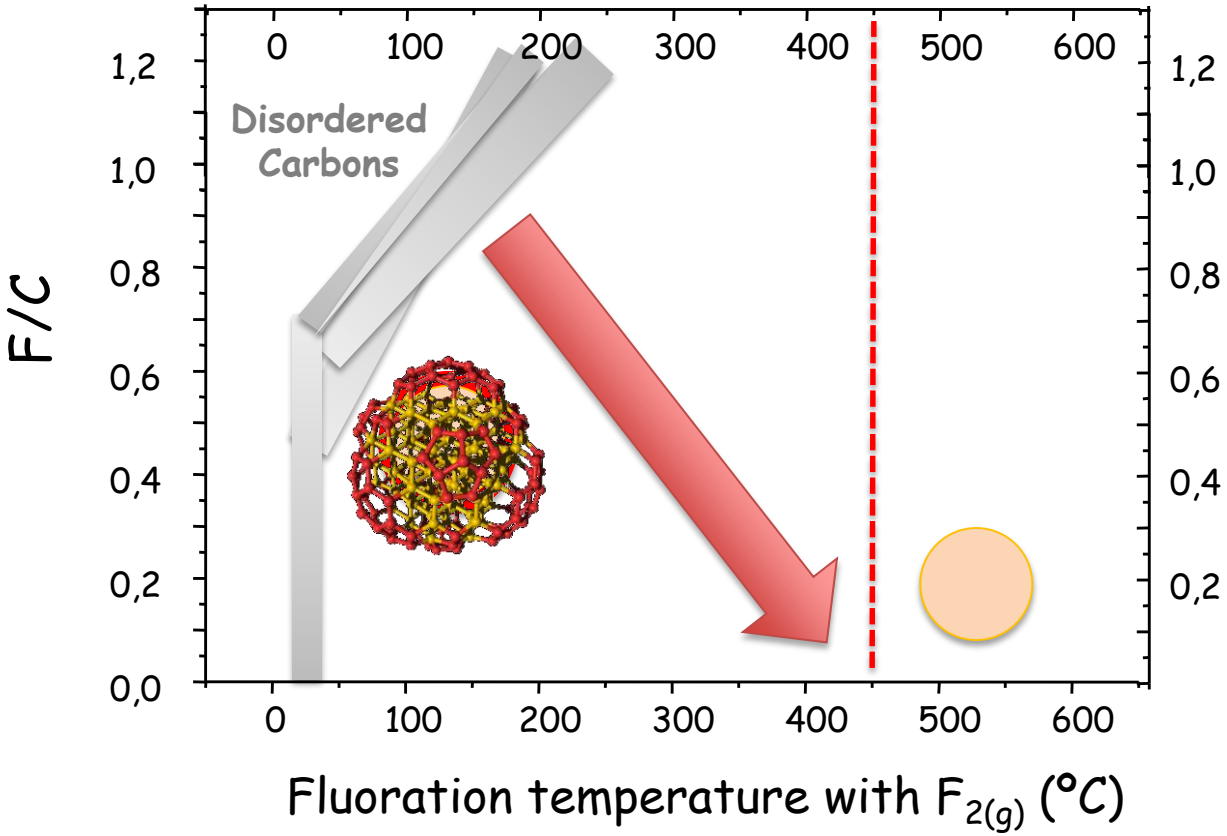


$C(s) + x/2\ F_2(g) \rightarrow CF_x(s)$

$0<x<1$ Fluorination

$1<x<1.2$ Extra-Fluorination

$2<x<4$ Decomposition

$C(s) + xF_2(g) \rightarrow CF_4(g) + C_2F_6(g)$



Institut de Chimie de Clermont-Ferrand

✓ 1 kg fluorinated nano-diamonds

✓ 2cvcle fluorination (99.9 % $F_2$ gas, 1 bar, at 450 $^oC$ for 12 hours.)

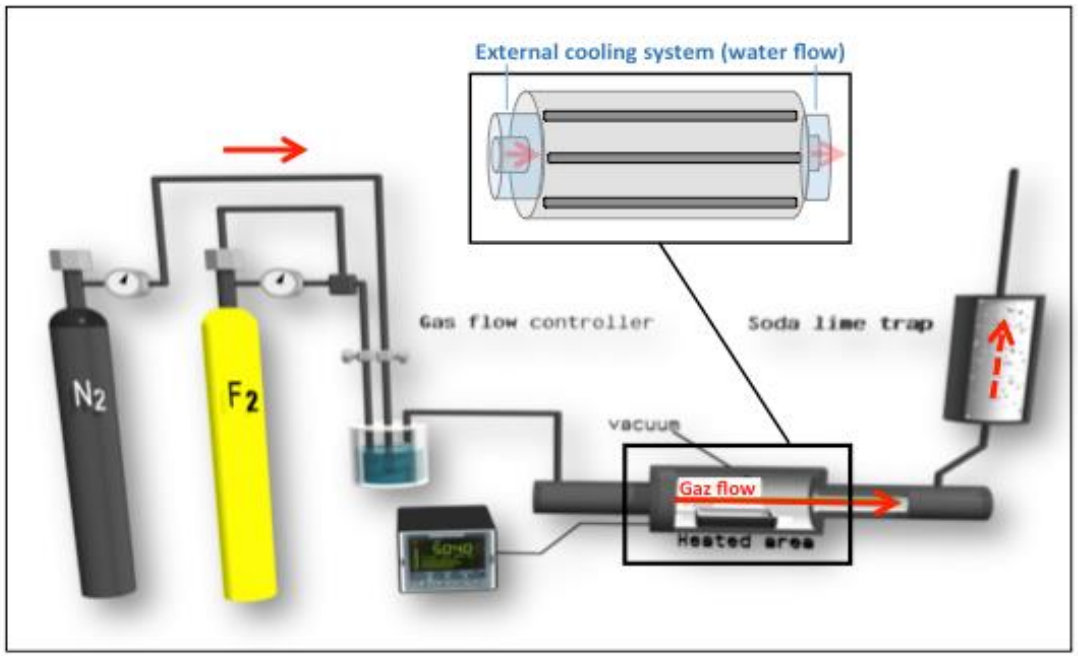




Institut de Chimie de Clermont-Ferrand

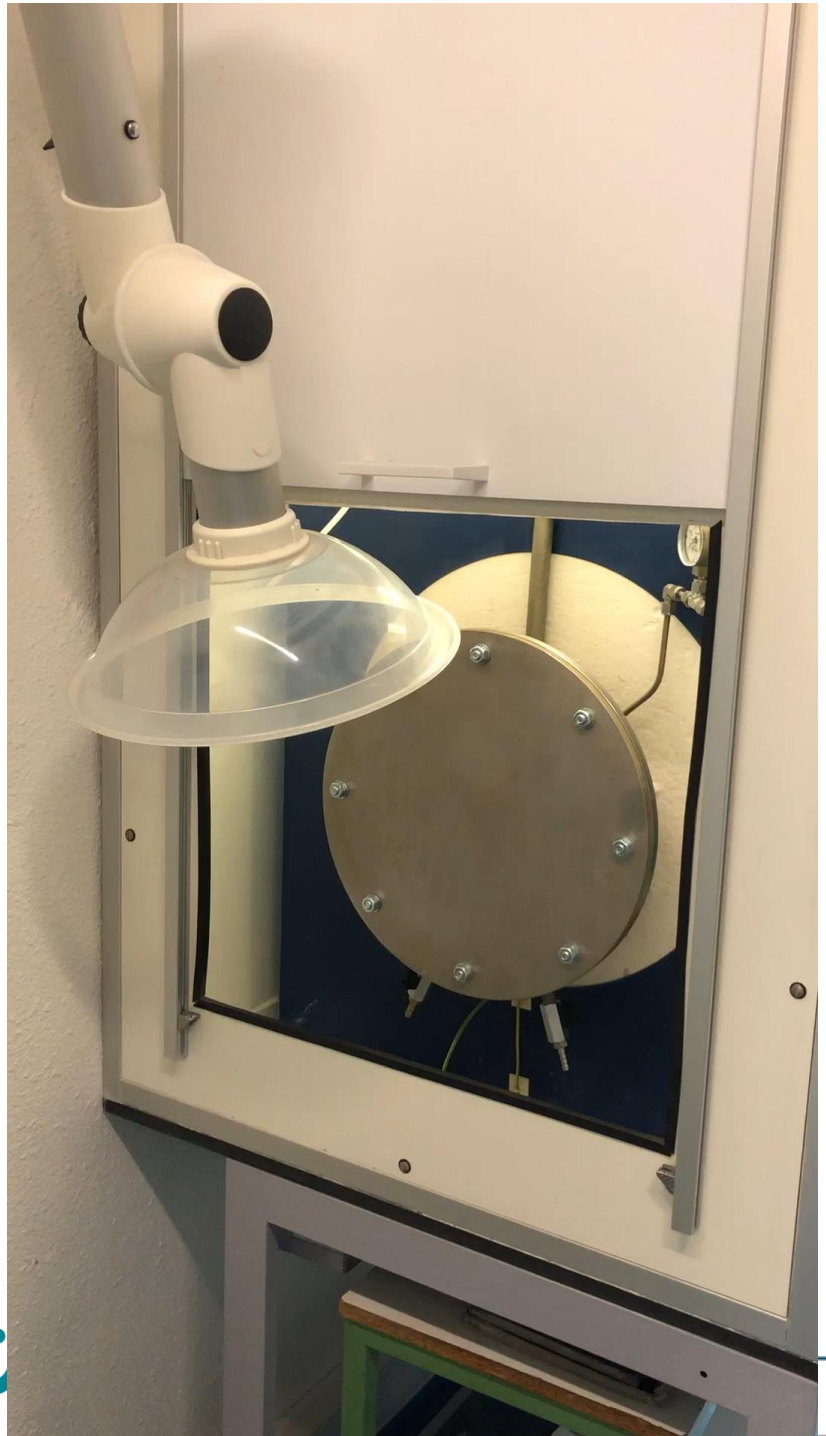

Chimie de
Clermont-Ferrand

## ✓ Solid state NMR (MAS $^{19}F$ and $^{13}C$, CP)

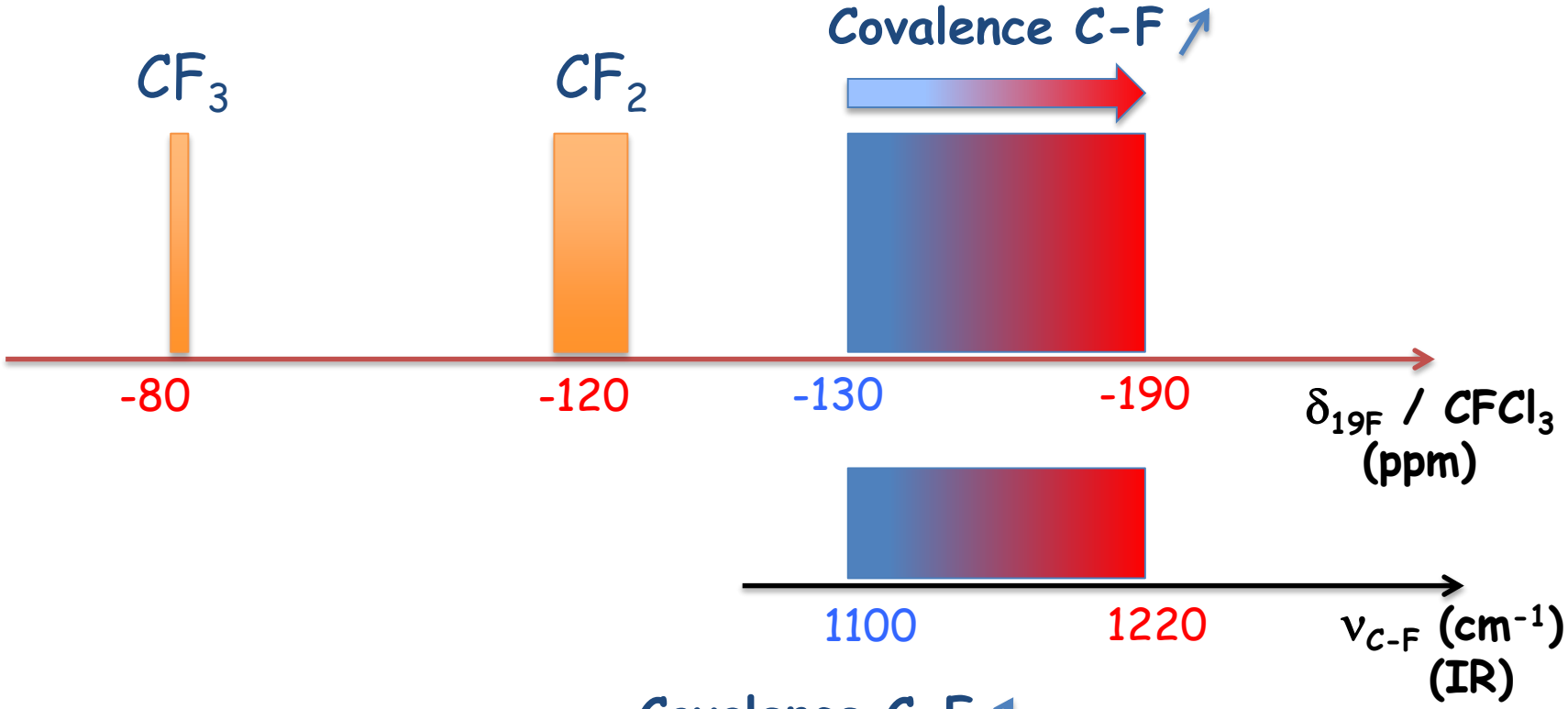


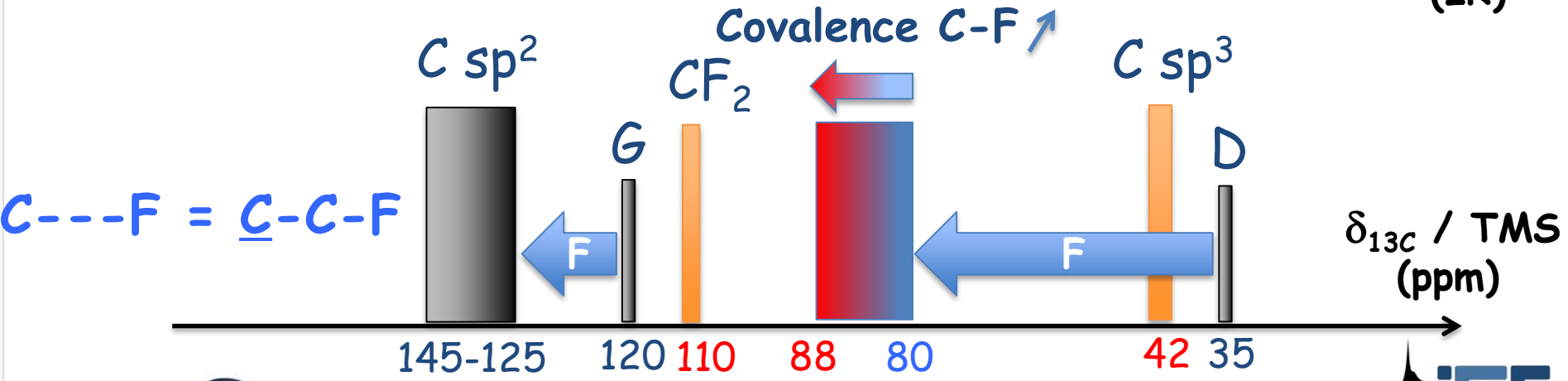




Institut de Chimie de Clermont-Ferrand

# IR spectroscopy

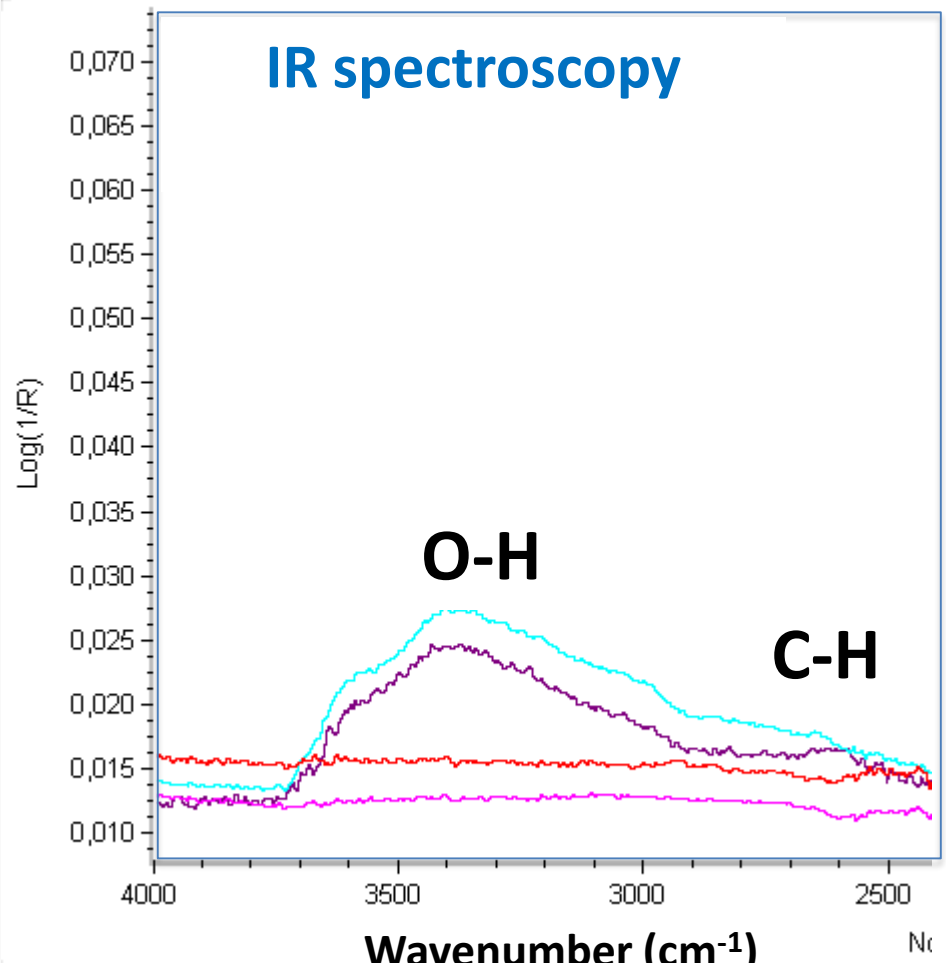


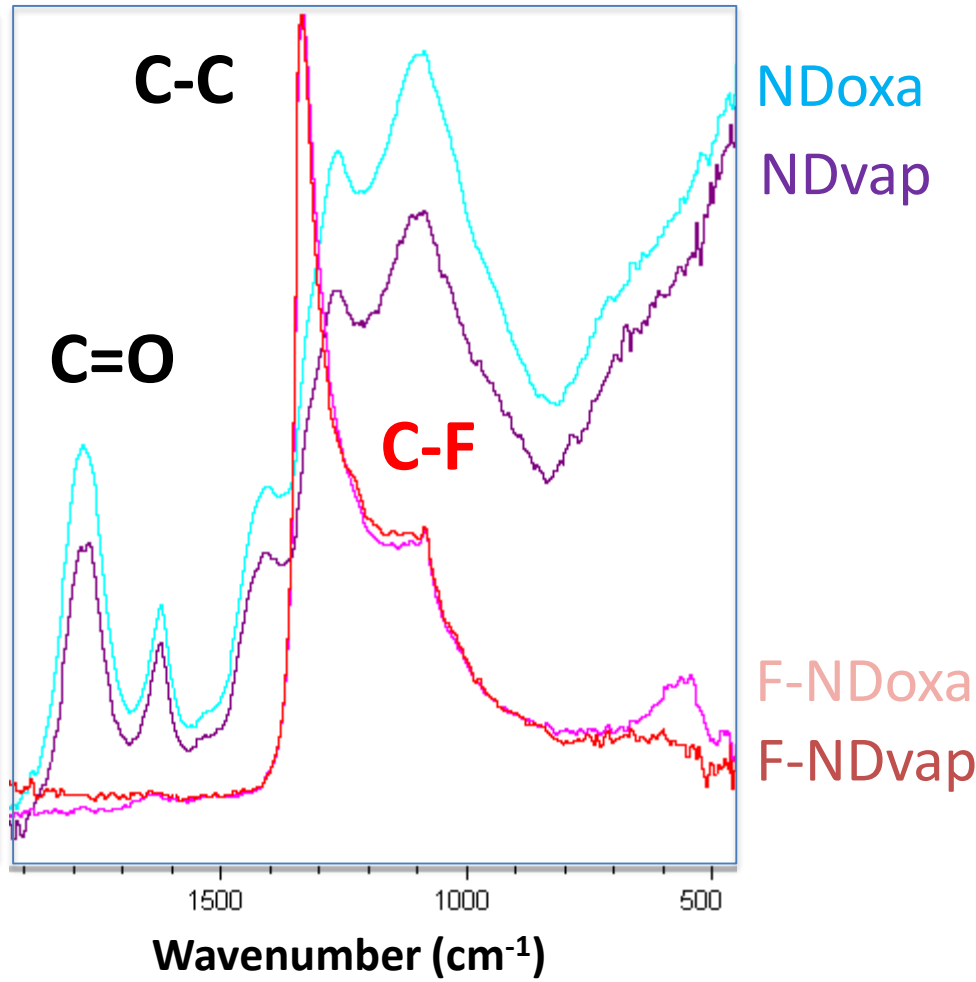


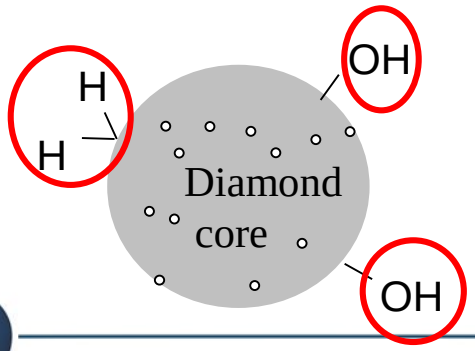


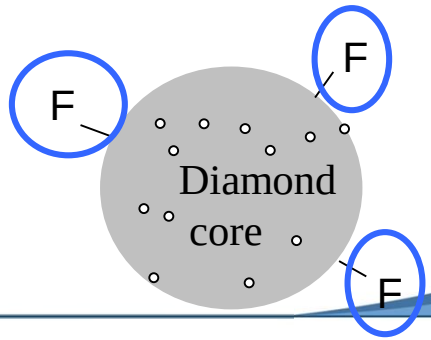




Institut de Chimie de Clermont-Ferrand

# $^{1}$H MAS NMR (14 kHz)

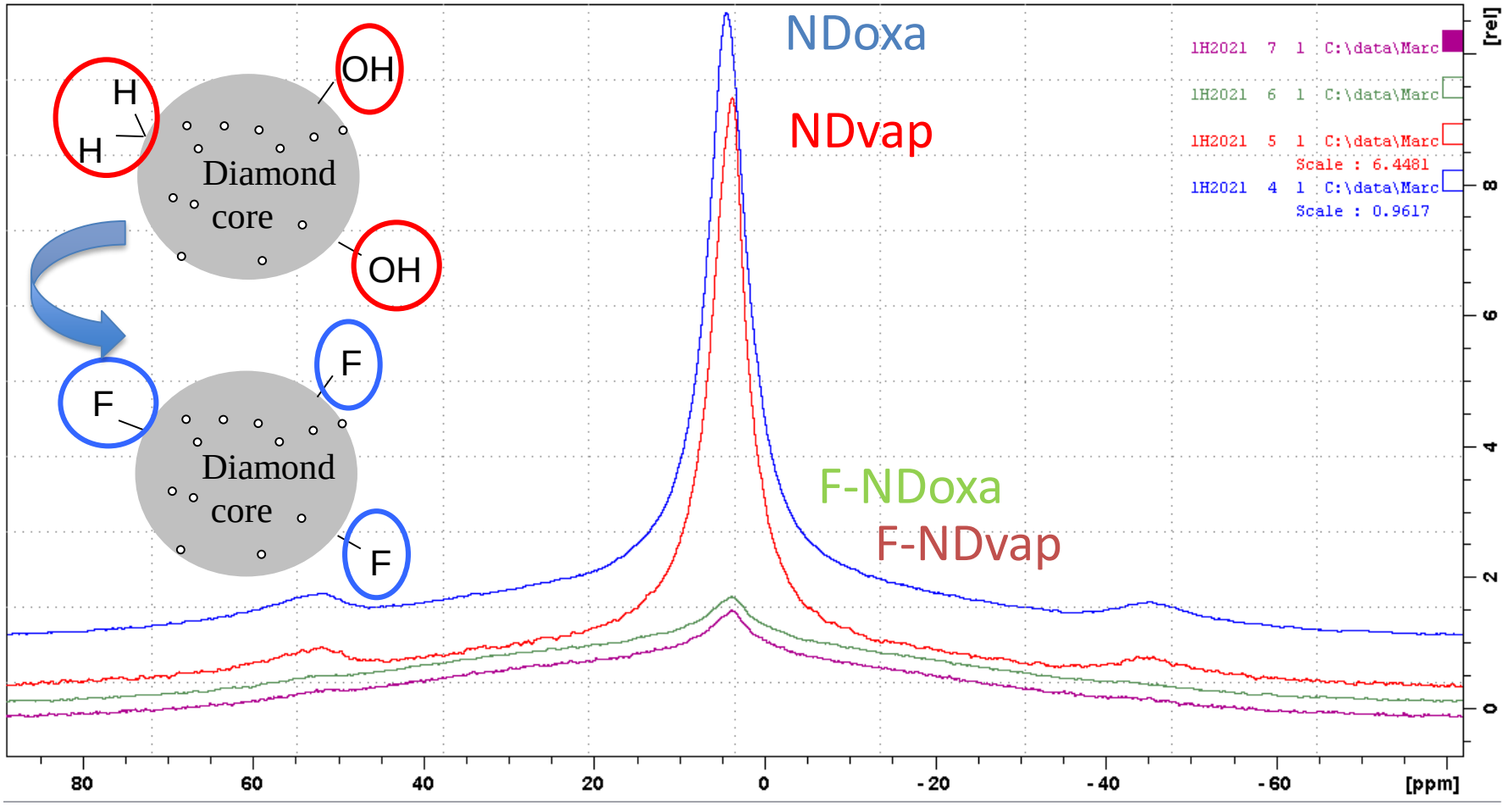


**$^{1}$H chemical shift (ppm) vs TMS**



Institut de Chimie de Clermont-Ferrand

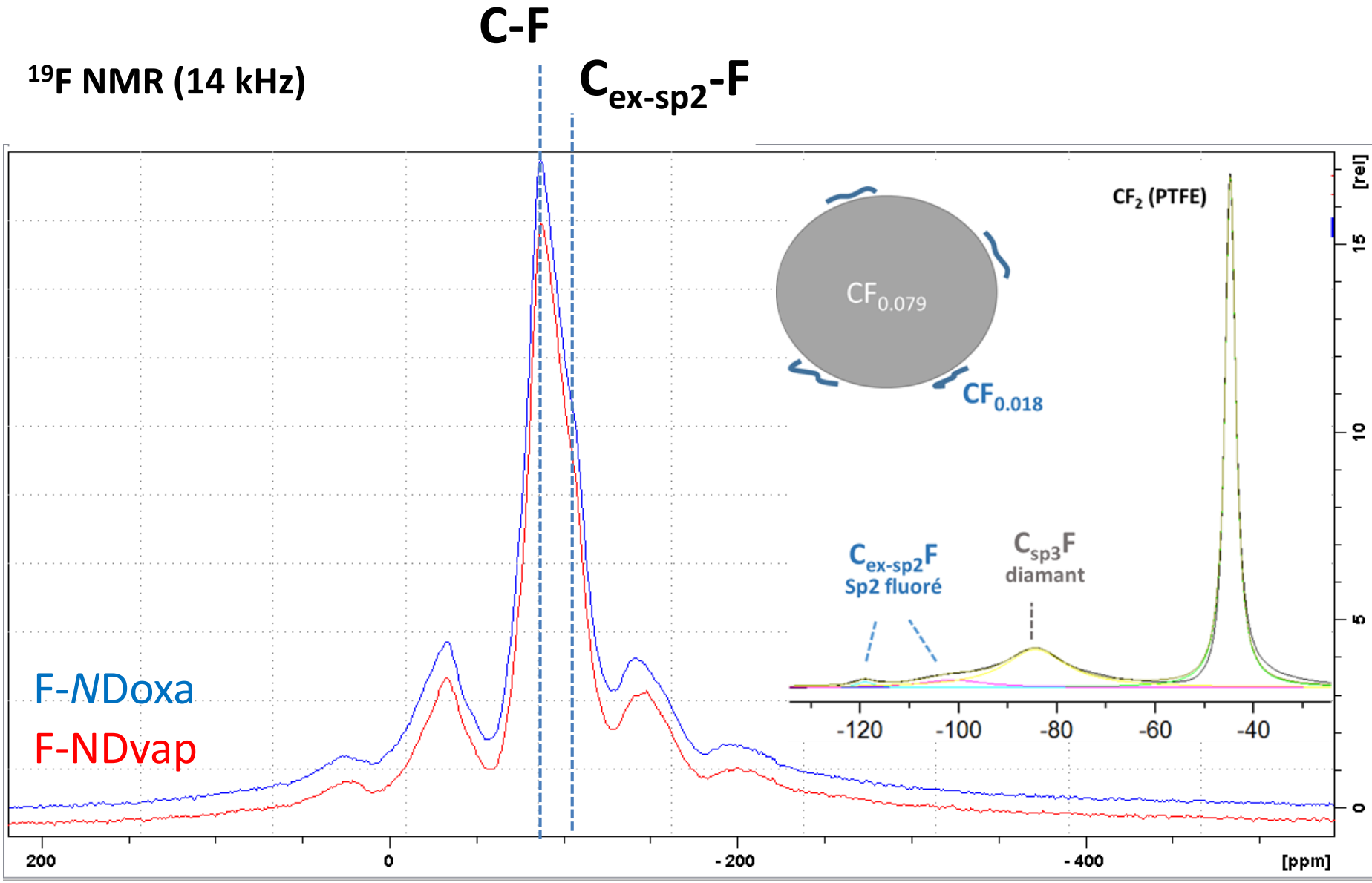


$^{19}$F chemical shift (ppm) vs $CF_3COOH$



Institut de Chimie de Clermont-Ferrand

# $^{13}$C NMR (10 kHz)

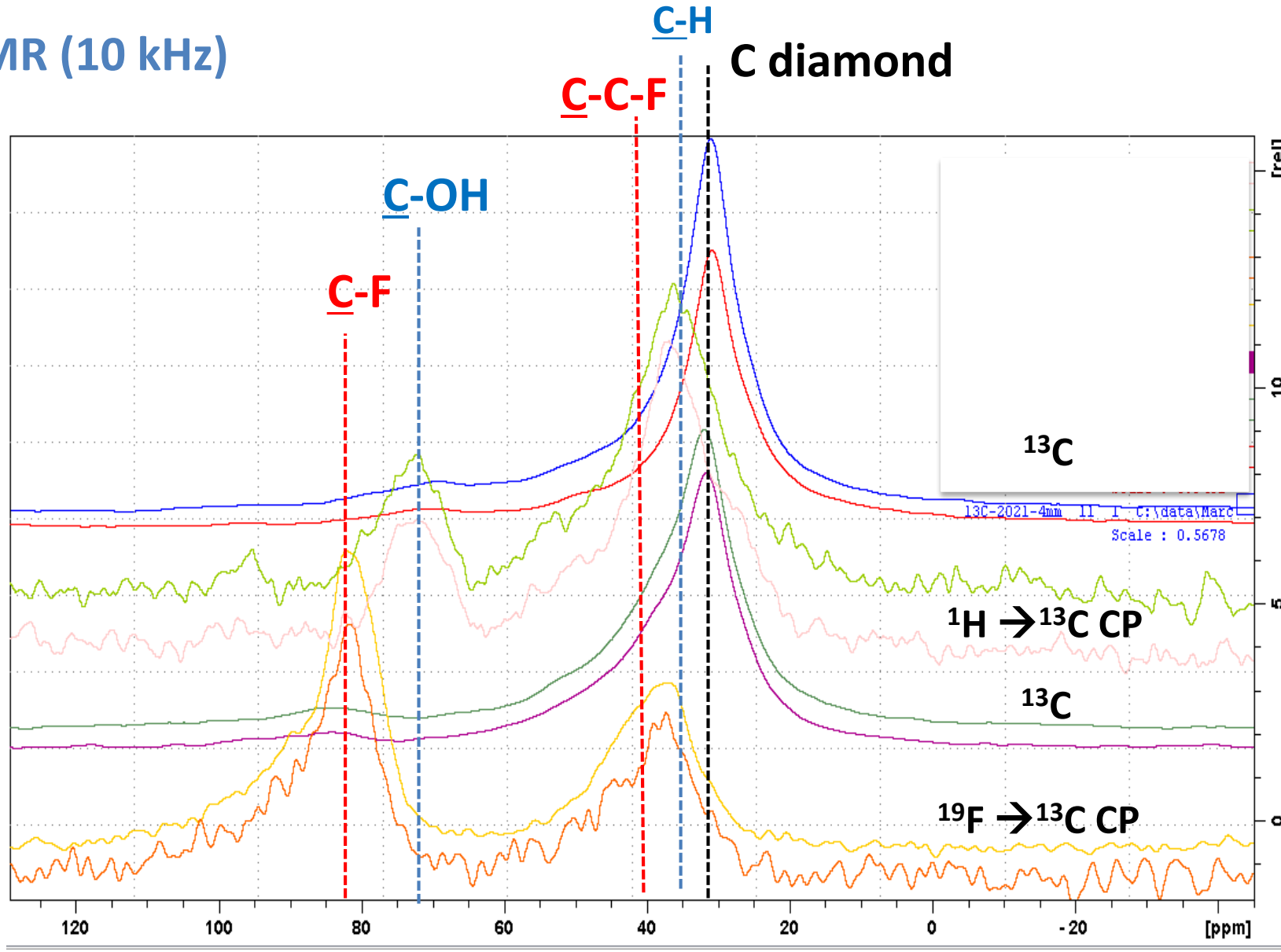


$^{13}$C chemical shift (ppm) vs TMS



Institut de Chimie de Clermont-Ferrand

# $^{13}C$ NMR (10 kHz)

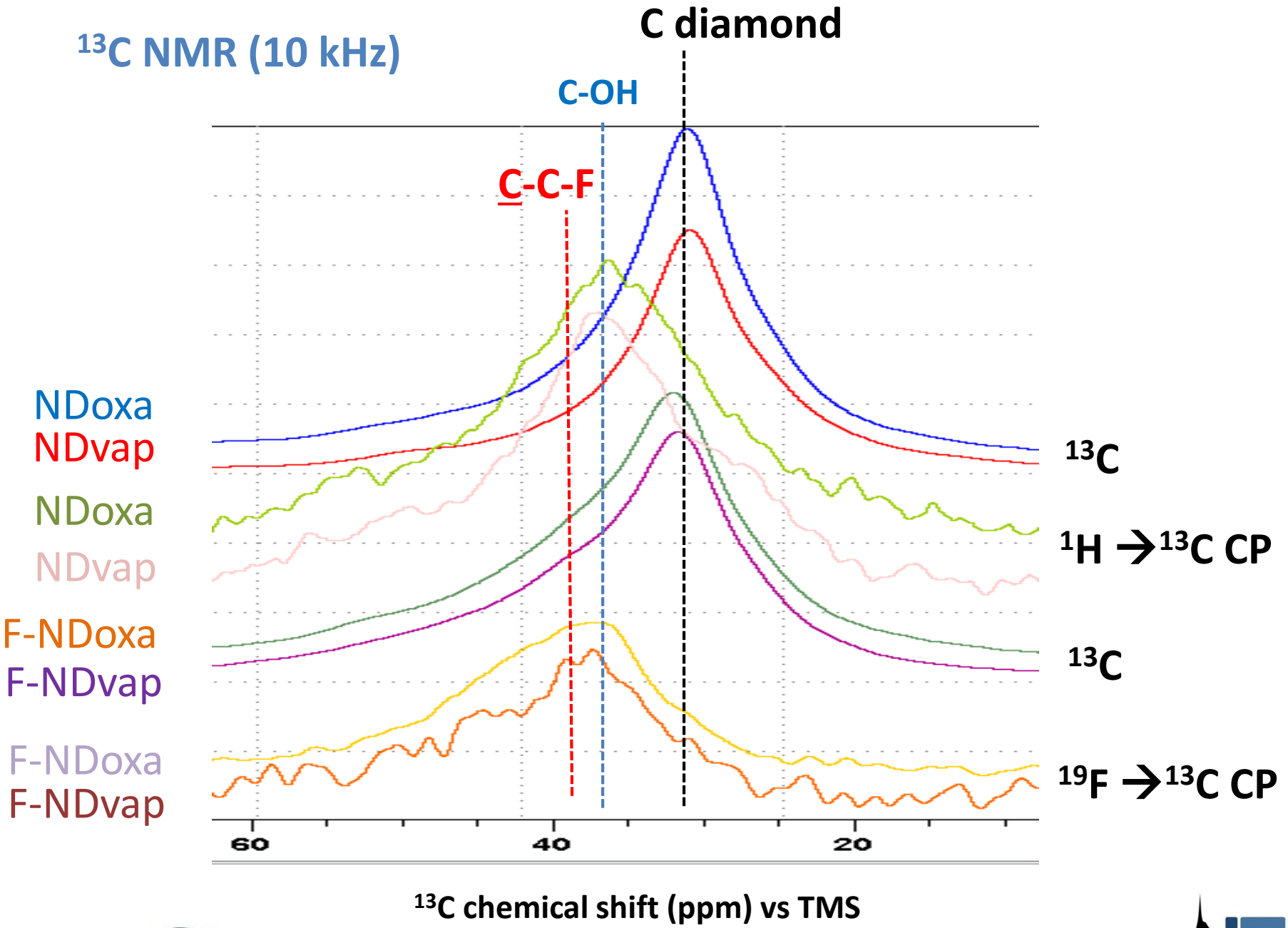




Institut de Chimie de Clermont-Ferrand

# Fluorination removes the $sp^2$ C shell…

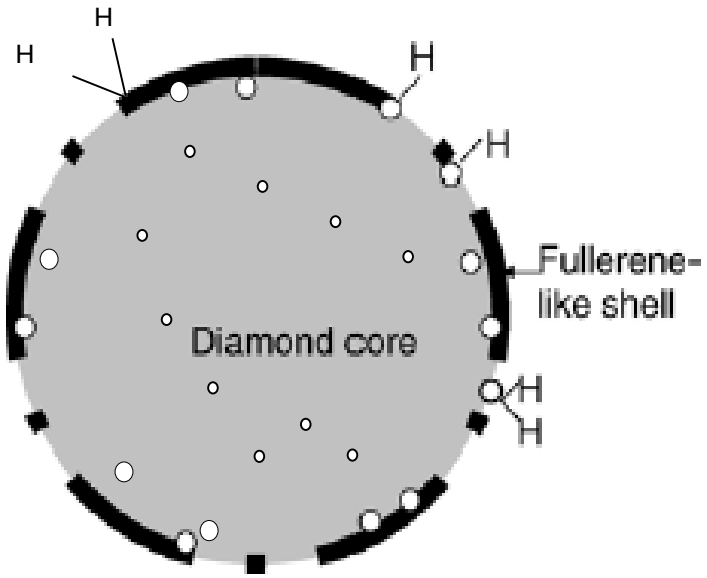


Fluorination

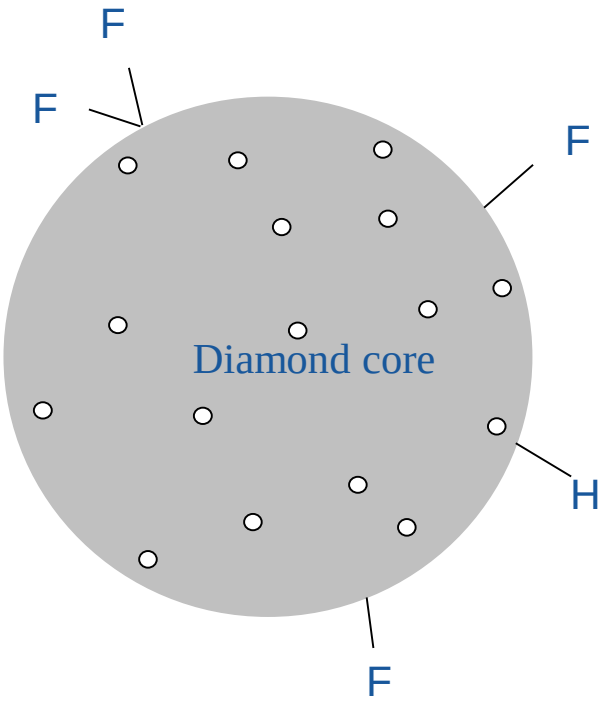


- Paramagnetic Centers


Zagrebina et al, J. Phys. Chem. C, 119 (1) (2015) 835–844.
Dubois et al, Solid State Nuclear Magnetic Resonance, 40(4) (2011) 144-154.
Dubois et al, J. Phys. Chem. C, 113 (24) (2009) 10371–10378

# Thanks you for your kind attention

Fluorinated nanodiamonds as unique neutron reflector
V. Nesvizhevsky, U. Köster, M. Dubois, N. Batisse, L. Frezet, A.Bosak, L. Gines, O. Williams
Carbon, 130 (2018) 799-805

Effect of nanodiamond fluorination on the efficiency of quasispecular reflection of cold neutrons
V. V. Nesvizhevsky, M. Dubois, Ph. Gutfreund, E. V. Lychagin, A. Yu. Nezvanov, and K. N. Zhernenkov
Phys. Rev. A 97 (2018) 023629

Institut de Chimie de Clermont-Ferrand

Réseau Français du Fluor - CNRS

CREMLIN PLUS
Connecting Russian and European Measures for Large-scale Research Infrastructures

Second meeting of the Subcommittee on Fundamental Physics of WP3
8 July 2021

# TOWARDS A NEW SCATTERING KERNEL FOR SOLID DEUTERIUM

Rolando Granada

CENTRO ATOMICO BARILOCHE - ARGENTINA

epl A Letters Journal Exploring the Frontiers of Physics

June 2009

EPL, **86** (2009) 66007
doi: 10.1209/0295-5075/86/66007

www.epljournal.org

# Neutron scattering kernel for solid deuterium

J. R. Granada[(a)]

*Centro Atómico Bariloche and Instituto Balseiro, Comisión Nacional de Energía Atómica 8400 S.C. de Bariloche (RN), Argentina*

The Van Hove scattering function $S(\mathbf{Q},\omega)$ is directly related to the double-differential cross section:

$$\frac{d^2\sigma}{d\Omega d\omega} = \frac{k}{k_0} S(\mathbf{Q},\omega)$$

$\mathbf{k}$ , $\mathbf{k_0}$ are the scattered and initial neutron wave vectors,
$\hbar\omega$ is the neutron energy loss, and
$\hbar\mathbf{Q} = \hbar(\mathbf{k_0} - \mathbf{k})$ is the momentum transferred to the system

The scattering law of a molecular system is

$$S(\mathbf{Q},\omega) = \frac{1}{2\pi\hbar}\int_{-\infty}^{\infty} dt e^{-i\omega t} \left\langle \sum_{l,l'}\sum_{\nu,\nu'} \overline{a^{*}_{l\nu} a_{l'\nu'}} \exp\{-i\mathbf{Q}.\mathbf{R}_{l\nu}(0)\} \exp\{i\mathbf{Q}.\mathbf{R}_{l'\nu'}(t)\} \right\rangle$$

where $\mathbf{R}_{l\nu}(t)$ denotes the position of the atom $\nu$ within the molecule $l$ ,

$$\mathbf{R}_{l\nu}(t) = \mathbf{a}_l + \mathbf{b}_\nu(t) + \mathbf{u}_\nu(t)$$

and can be written as the sum of inter ($l \neq l'$)- and intra ($l = l'$)- molecular contributions (also referred to as the *outer* and *inner* terms, respectively).

The outer and inner terms, for the intermediate scattering function are

$$\chi(\mathbf{Q},t) = \left\langle \sum_{l\neq l'}\sum_{v,v'} \overline{a^{*}_{lv}a_{l'v'}} \exp\{-i\mathbf{Q}.\mathbf{R}_{lv}(0)\}\exp\{i\mathbf{Q}.\mathbf{R}_{l'v'}(t)\} \right\rangle + \quad \text{“Outer”}$$

$$\left\langle \sum_{l}\sum_{v,v'} \overline{a^{*}_{lv}a_{lv'}} \exp\{-i\mathbf{Q}.\mathbf{R}_{lv}(0)\}\exp\{i\mathbf{Q}.\mathbf{R}_{lv'}(t)\} \right\rangle \quad \text{“Inner”}$$

Here the brackets denote the average of the time-dependent operators over an equilibrium-distribution function in the full phase space of the scattering system.

In terms of the usual coherent, $b_c^{\nu}$ , and incoherent, $b_i^{\nu}$ , scattering lengths for nuclei $\nu$,

$$a_v = b_c^v + 2b_i^v (\mathbf{S}_v.\mathbf{s})\left[S_v(S_v+1)\right]^{-1/2}$$

Leaving aside for the moment the consideration of vibrational modes:

$$\chi^{out}(\mathbf{Q},t) = \sum_{l \neq l'} \left\langle \exp\{-i\mathbf{Q}.\mathbf{a}_l(0)\} \exp\{i\mathbf{Q}.\mathbf{a}_{l'}(t)\} \right\rangle . \sum_{v,v'} \left\langle \overline{b^*_{lv}} \exp\{-i\mathbf{Q}.\mathbf{b}_{lv}(0)\} \overline{b_{l'v'}} \exp\{i\mathbf{Q}.\mathbf{b}_{l'v'}(t)\} \right\rangle$$

$I_d$ (**Q**,t) u (**Q**,t)

There is no correlation between atoms belonging to different molecules, and then

$$u(\mathbf{Q}) = |\Sigma_v \langle b_{lv} \exp\{i\mathbf{Q}.\mathbf{b}_v(0)\}\rangle|^2 = 4\,(b_c)^2\, j_0^2\,(Qd/2)$$

$$\therefore\ \chi^{out}(\mathbf{Q},t) = 4\,(b_c)^2\, j_0^2\,(Qd/2)\ .\ I_d(\mathbf{Q},t)$$

$$\chi^{inner}(\mathbf{Q},t) = \sum_{l} \left\langle \exp\{-i\mathbf{Q}.\mathbf{a}_l(0)\} \exp\{i\mathbf{Q}.\mathbf{a}_l(t)\} \right\rangle . \sum_{JJ'} \sum_{\pi\pi'} A_{\pi\pi'}(J)\, f_{\pi\pi'}(Q;J,J')\, e^{-i(\omega_J - \omega_{J'})t}$$

$I_s$ (**Q**,t) v (**Q**,t)

$A_{ee}(J) = c \{ 4\, b_c^2 + 5/2\, b_i^2 \} P_e(J)$

$A_{oo}(J) = (1\text{-}c) \{ 4\, b_c^2 + b_i^2 \} P_o(J)$

$A_{eo}(J) = c\ 3/2\, b_i^2\ P_e(J)$

$A_{oe}(J) = (1\text{-}c)\ 3\, b_i^2\ P_o(J)$

c: o-$D_2$ concentration

$f_{\pi=\pi}(Q;J,J') = (2J+1)\ \Sigma_{l\ even}\ (2l+1)\ C^2(JlJ';000)\ j_l^2(Qd/2)$

$f_{\pi\neq\pi}(Q;J,J') = (2J+1)\ \Sigma_{l\ odd}\ (2l+1)\ C^2(JlJ';000)\ j_l^2(Qd/2)$

$\therefore\ \chi^{inner}(\mathbf{Q},t) = v(\mathbf{Q},t)\ .\ I_s(\mathbf{Q},t)$

$$I_d(\mathbf{Q},t) = \sum_{l \neq l'} \left\langle \exp\{-i\mathbf{Q}.\mathbf{a}_l(0)\} \exp\{i\mathbf{Q}.\mathbf{a}_{l'}(t)\} \right\rangle .$$

$$= \sum_{l,l'} \left\langle \exp\{-i\mathbf{Q}.\mathbf{a}_l(0)\} \exp\{i\mathbf{Q}.\mathbf{a}_{l'}(t)\} \right\rangle - \sum_{l} \left\langle \exp\{-i\mathbf{Q}.\mathbf{a}_l(0)\} \exp\{i\mathbf{Q}.\mathbf{a}_l(t)\} \right\rangle$$

$\therefore$ $I_d(\mathbf{Q},t) =$ $I(\mathbf{Q},t)$ - $I_s(\mathbf{Q},t)$

$$\chi(\mathbf{Q},t) = \chi^{out}(\mathbf{Q},t) + \chi^{inner}(\mathbf{Q},t)$$

$$\chi(\mathbf{Q},t) = 4\, b_c^2\, j_0^2\,(Qr/2)\,\{I(\mathbf{Q},t) - I_s(\mathbf{Q},t)\} + v(\mathbf{Q},t)\,.\, I_s(\mathbf{Q},t)$$

$$\chi(\mathbf{Q},t) = 4\, b_c^2\, j_0^2\,(Qr/2)\,\{I\,(\mathbf{Q},t) - I_s\,(\mathbf{Q},t)\} + v(\mathbf{Q},t)\,.\,I_s\,(\mathbf{Q},t)$$

Now, (must multiply everything by $\chi^{vib}(\mathbf{Q},t)$ !)

$$\chi(\mathbf{Q},t) = \chi(\mathbf{Q},0) + \chi(\mathbf{Q},t\neq 0)$$

(elast) (inelast)

but because

$$I_s\,(\mathbf{Q},0) = 1 \quad , \quad I(\mathbf{Q},0) = |F(\mathbf{Q},0)|^2$$

$$\chi^{el}(\mathbf{Q},0) = 4\, b_c^2\, j_0^2\,(Qr/2)\,|F(\mathbf{Q})|^2 + v(\mathbf{Q},0) - u(\mathbf{Q})$$

within the Incoherent Approximation: $I(\mathbf{Q},t\neq 0) \cong I_s(\mathbf{Q},t\neq 0)$

$$\chi^{inel}(\mathbf{Q},t) = v(\mathbf{Q},t)\,.\,I_s\,(\mathbf{Q},t)$$

The old calculations were performed according to:

$$\chi^{el}(\mathbf{Q},0) = 4\, b_c^2\, j_0^2\,(Qr/2)\,|F(\mathbf{Q})|^2\;\chi^{vib}(\mathbf{Q},0) \qquad \text{Convent.El.Coh}$$

$$+\ 2\,(1+\alpha)\, b_i^2\,\chi^{vib}(\mathbf{Q},0) \qquad \text{Total El.Incoh}$$

($\alpha$ = ¼ for o-D2, - ½ for p-D2, 0 for n-D2)

$$\chi^{inel}(\mathbf{Q},t) = v(\mathbf{Q},t)\,.\,I_s\,(\mathbf{Q},t)\,.\,\chi^{vib}(\mathbf{Q},t) \qquad \text{Total Inelast.}$$

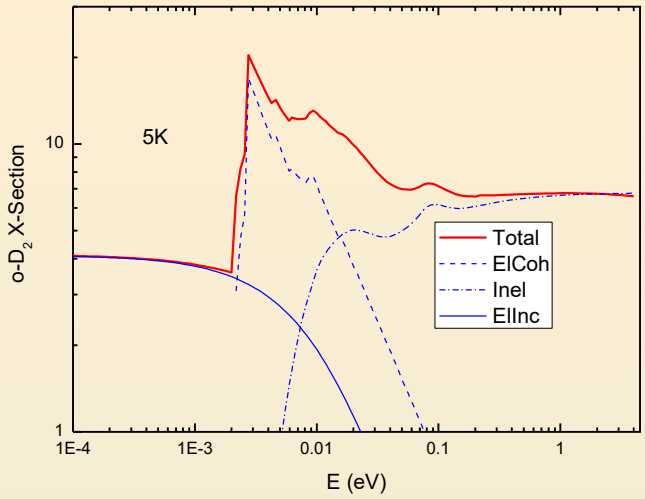
5K
o-D2 X-Section
E (eV)
Total
ElCoh
Inel
ElInc

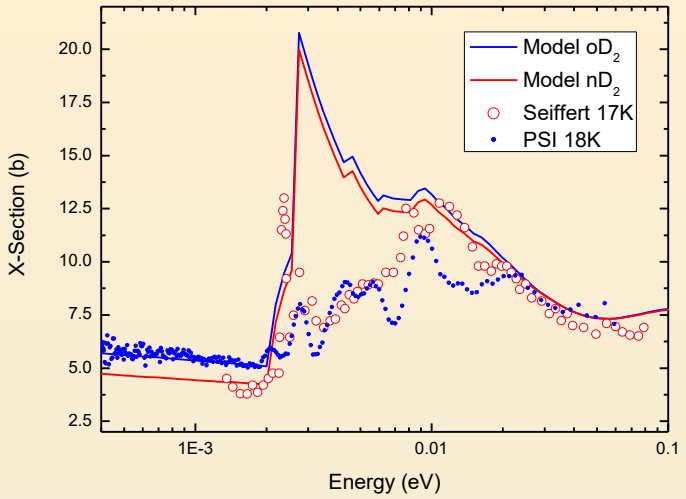
Model oD2
Model nD2
Seiffert 17K
PSI 18K
X-Section (b)
Energy (eV)

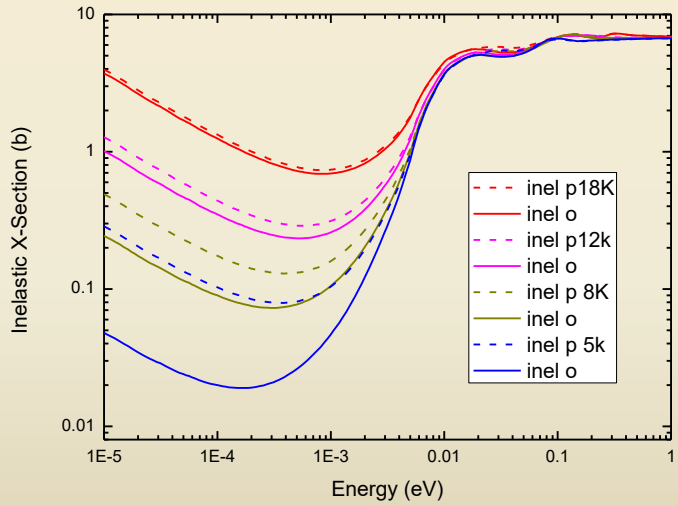
Inelastic X-Section (b)
Energy (eV)
inel p18K
inel o
inel p12k
inel o
inel p 8K
inel o
inel p 5k
inel o

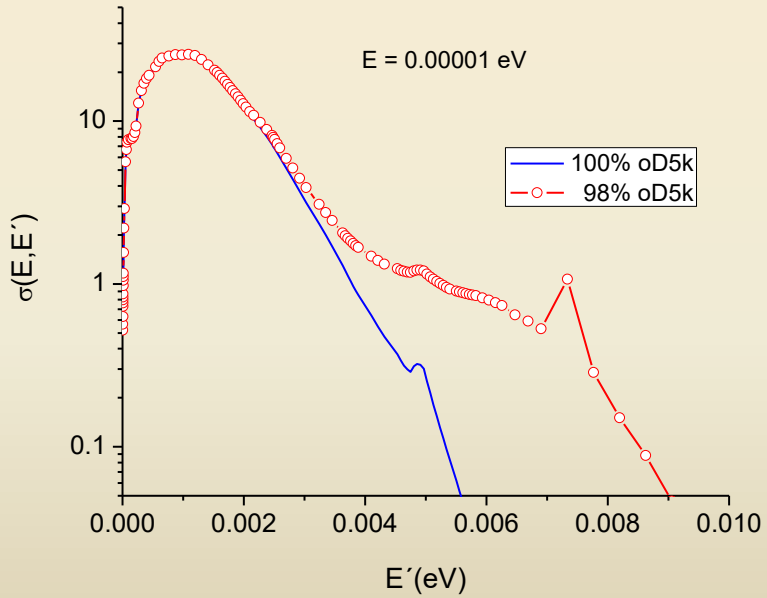
E = 0.00001 eV
σ(E,E´)
E´(eV)
100% oD5k
98% oD5k

Whereas the complete elastic components are,

$$\chi^{el}(\mathbf{Q},0) = 4\, b_c^2\, j_0^2\,(Qr/2)\,|F(\mathbf{Q})|^2\;\chi^{vib}(\mathbf{Q},0) \quad \text{Convent.El.Coh}$$

$$+ 2\, b_i^2\,\chi^{vib}(\mathbf{Q},0) \quad \text{Convent.El.Incoh}$$

$$+ 2\, b_i^2\;\alpha\, j_0\,(Qd)\,\chi^{vib}(\mathbf{Q},0) \quad \text{Spin Correlation}$$

$$+ 2\, b_c^2\,\{1+ j_0\,(Qd) - 2\, j_0^2\,(Qd/2)\}\,\chi^{vib}(\mathbf{Q},0) \quad \Delta \text{ structure}$$

($\alpha$ = ¼ for o-D2, - ½ for p-D2)

However, a better description of the lattice inelastic component can be attained by preserving the correct expressions for the one-phonon coherent and incoherent terms in the phonon expansion of $I(\mathbf{Q},t \neq 0)$ and $I_s(\mathbf{Q},t \neq 0)$ respectively, and applying the incoherent approximation only for the higher phonon terms ($\geq 2$).

$$\chi^{inel}(\mathbf{Q}, t \neq 0) = [4\, b_c^2\, j_0^2\, (Qr/2)\, \{I^{1ph}(\mathbf{Q},t) - I_s{}^{1ph}(\mathbf{Q},t)\} + v(\mathbf{Q},t)\, .\, I_s(\mathbf{Q},t)\,]\, \chi^{vib}(\mathbf{Q},t)$$

This is the one-phonon correction to the Incoherent Approximation.

## Phonon Dispersion Relations (o-D2)

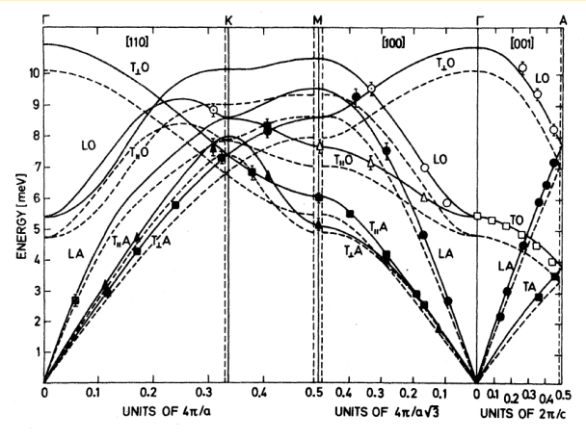


## Phonon Density of states

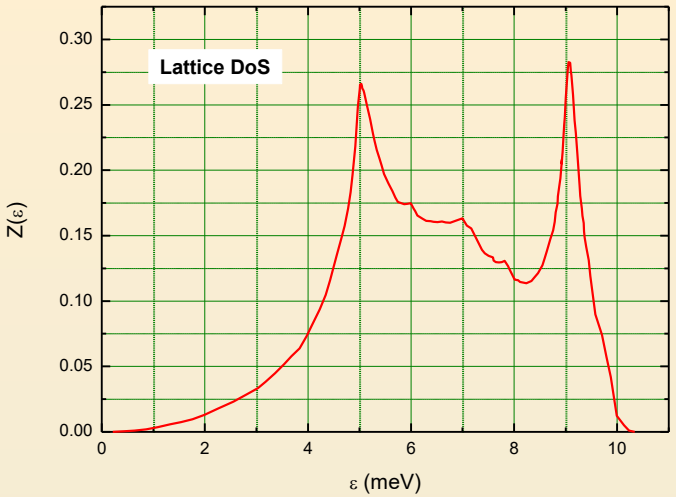


## Angular dependence Elas.Incoh.

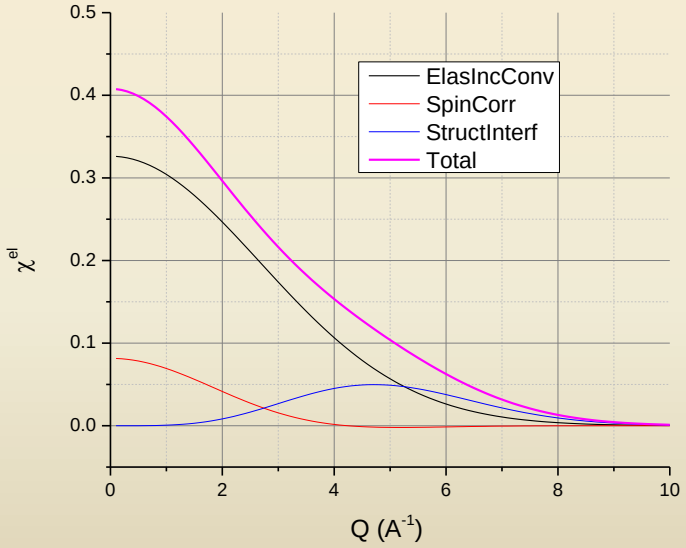


## Structural characteristics

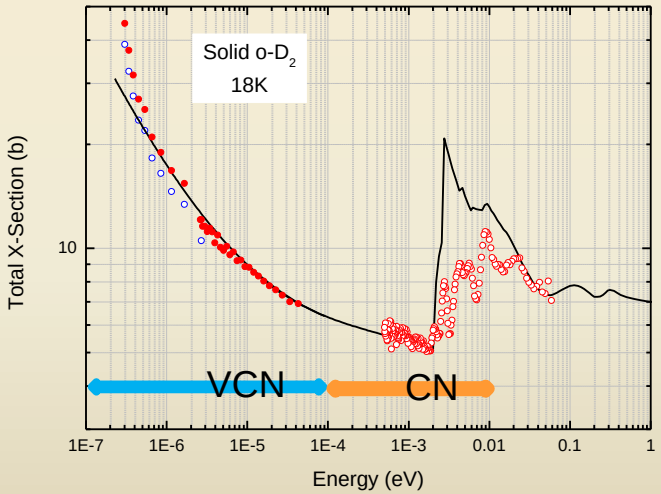

# CONCLUSIONS

- A new scattering kernel to describe the interaction of slow neutrons with solid Deuterium is being developed.
- The main characteristics of this molecular solid are contained in the formalism, including dynamical aspects related to:
  - the lattice's density of states,
  - the Young-Koppel quantum treatment of the rotational motion,
  - the exact treatment of the one-phonon IA in the inelastic term,
  - the internal molecular vibration.
- The elastic processes involving coherent and incoherent contributions are also fully described, as well as the spin-correlation effects caused by the coupling of intrinsic and rotational angular momenta.

# CONCLUSIONS

► The validation of a new scattering kernel and its generated cross section data demands the comparison with experimental data.

► Total cross section measurements are an appropriate set of data to check the theoretical predictions.

► The preparation of solid o-Deuterium samples with good repetitive characteristics has to be well understood.

THANKS FOR YOUR ATTENTION!

NRC "Kurchatov institute"-PNPI

CREMLIN PLUS
Connecting Russian and European Measures for Large-scale Research Infrastructures

# Reactor PIK and VCN Source

*Vladimir Voronin,*
*NRC "Kurchatov institute"-PNPI*

# Reactor PIK parameters

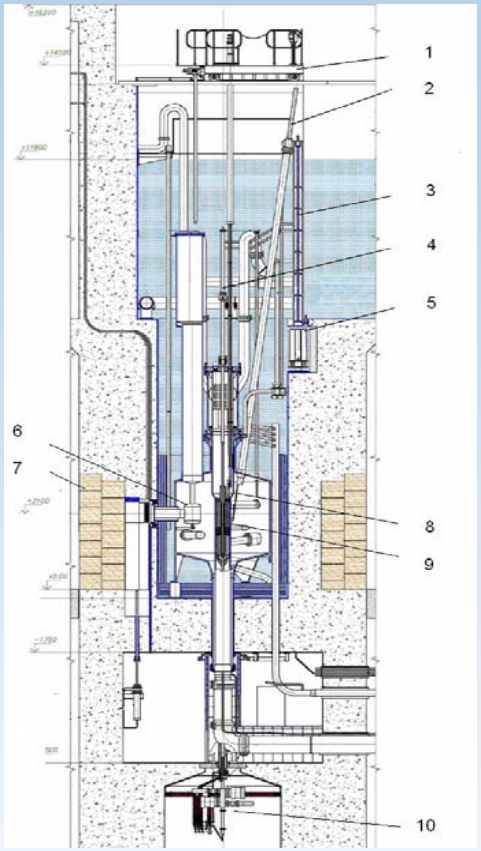


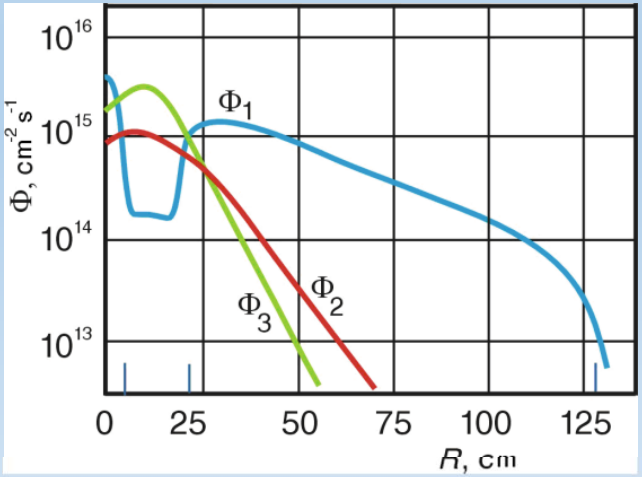


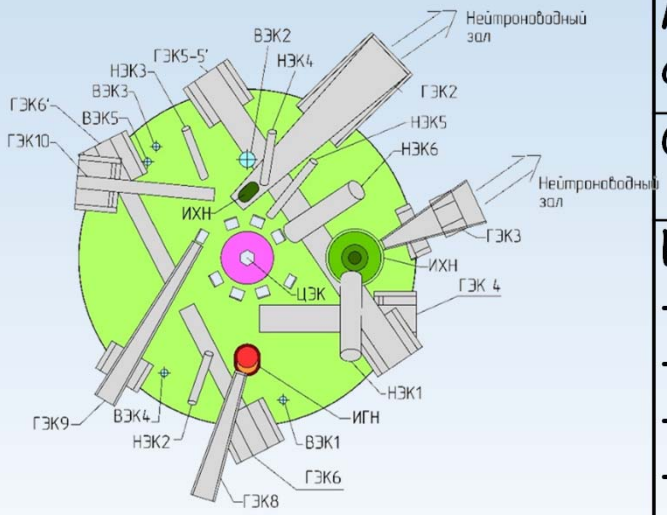


| | Value |
|---|---|
| Power | 100 MW |
| Reactor core volume | 50 l |
| Core height | 500 mm |
| Coolant | $H_2O$ |
| Reflector | $D_2O$ |
| Maximal thermal neutron flux in moderator | **$1.3 \times 10^{15}$ n/cm$^2$c** |
| Maximal neutron flux in central trap | **$5 \times 10^{15}$ n/cm$^2$c** |
| Operation cycle | ~30 day (25+5) (200 days per year) |
| Experimental channels<br>- Horizontal (HEC)<br>- Vertical (VEC)<br>- Inclined (IEC)<br>- Central (CEC) | <br>10 (2+8)<br>6<br>6<br>1 |

# Reactor PIK status and plans (optimistic)

- We have permission (Dec. 2020) for 10 MW power from State Regulator (Rostehnadzor).
- Individual systems for reaching 10 MW are launching with a check of their operability now.
- This year we plan to reach power 10MW.
- Shut down until the end of 2022 to switch to another type of fuel elements, change experimental channels….
- End of 2022 – to the permission for 100 MW and the start full power program
- 2024 – to start user program

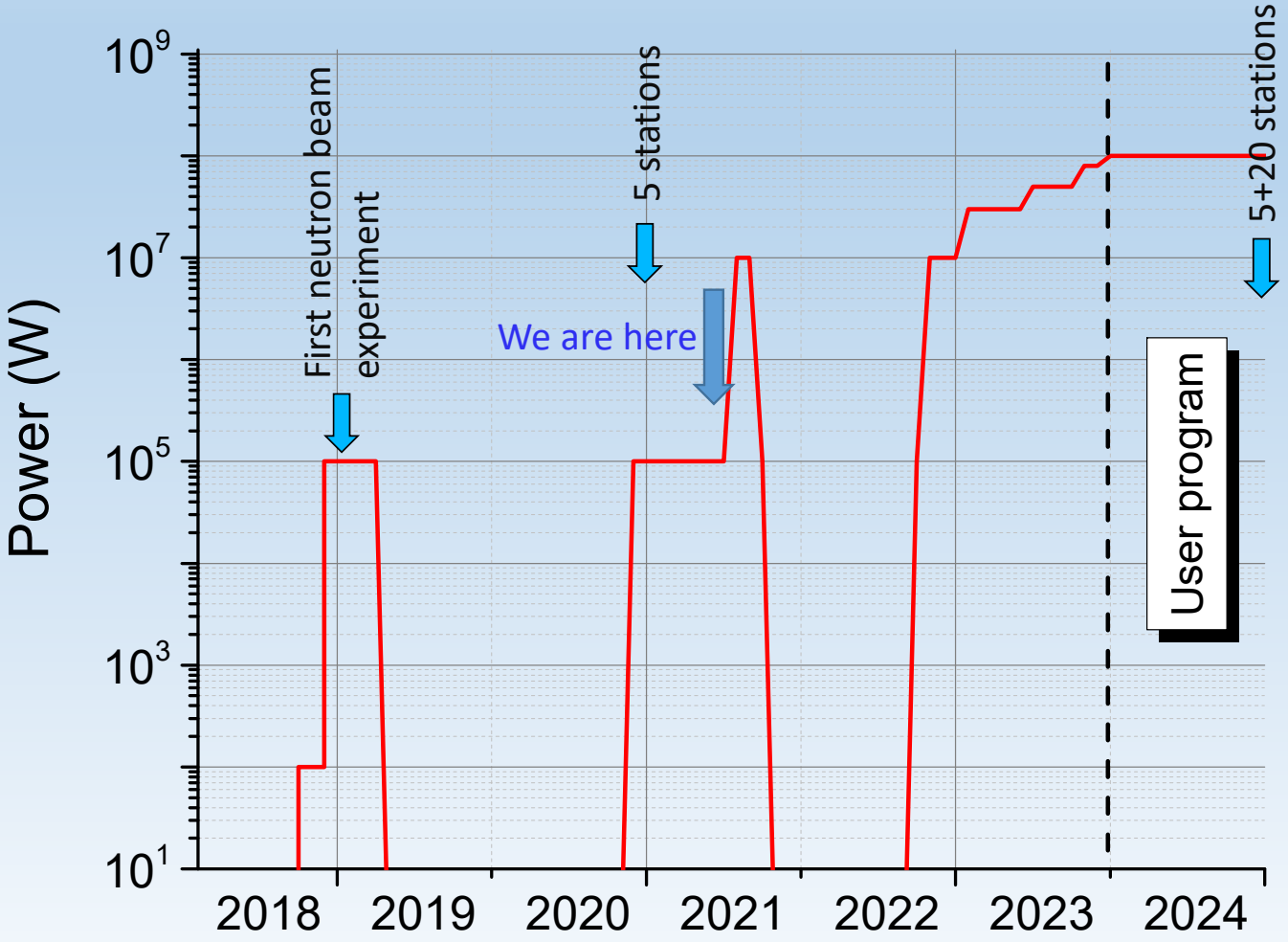

# 5 "first day" stations

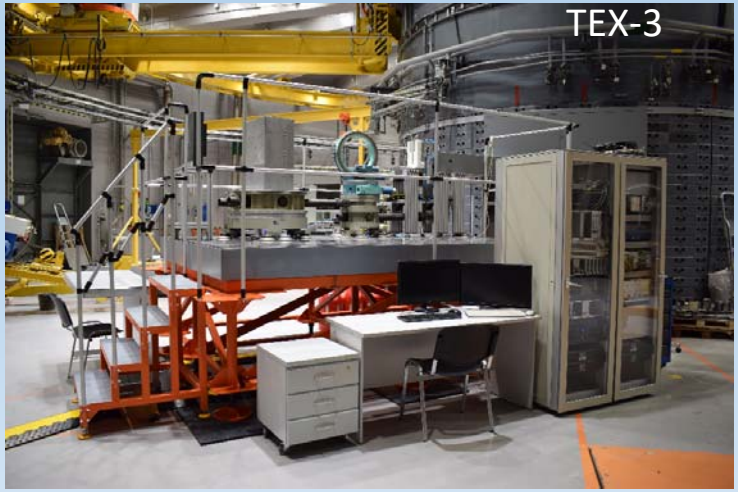


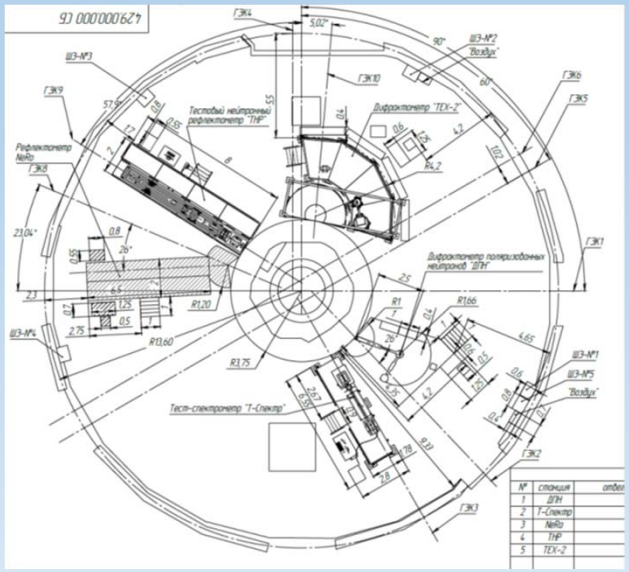


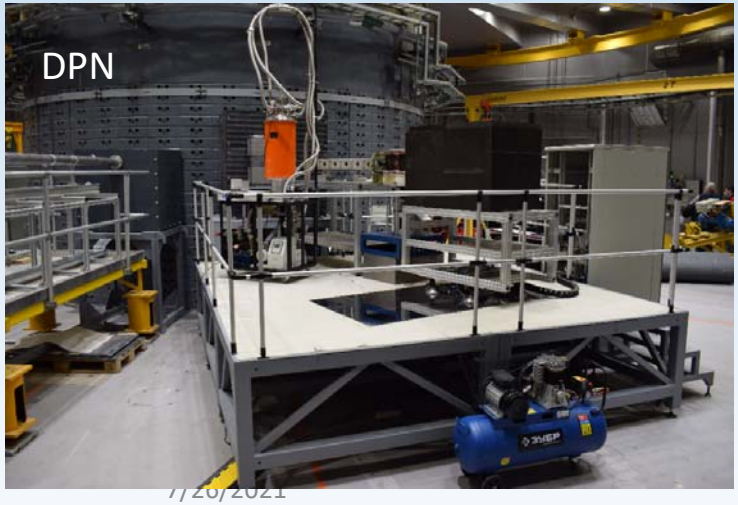



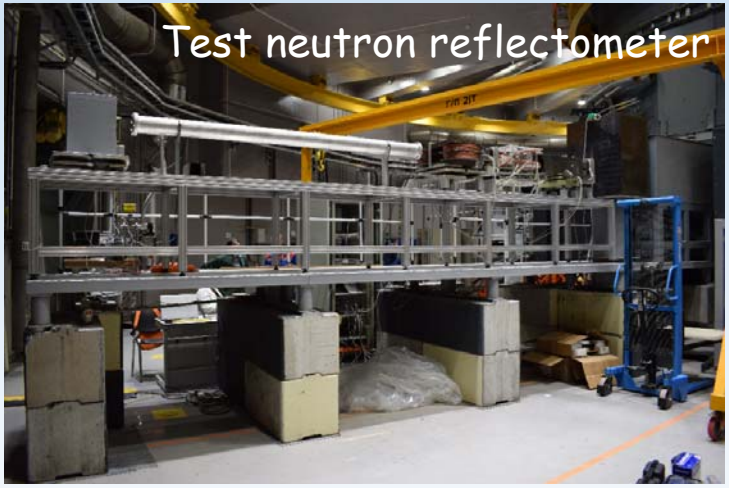

# Status of the "first day" stations

1. TNR test neutron reflectometer
2. NERO Polarized Neutron Reflectometer (GKSS)
3. DPN polarized neutron diffractometer
4. Texture Diffractometer TEX-2 (GKSS)
5. Test neutron spectrometer

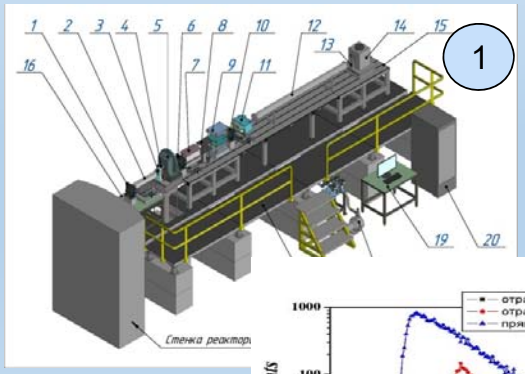


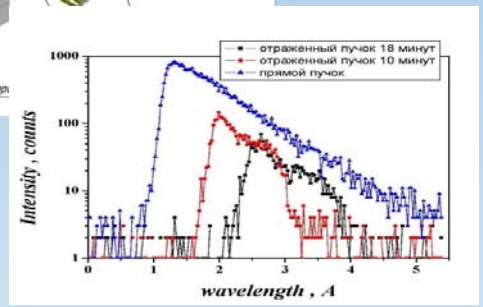


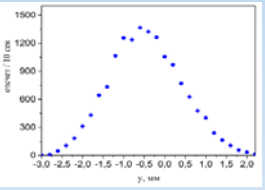

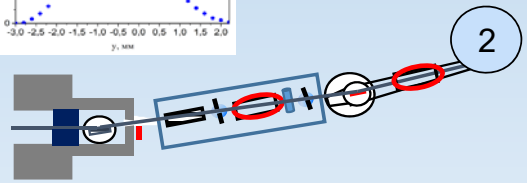


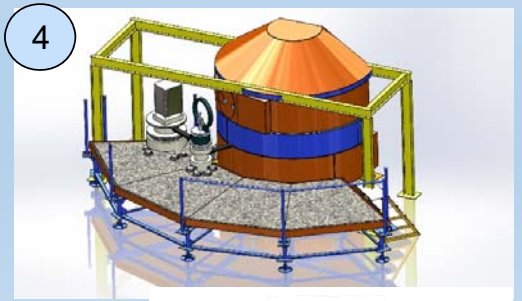


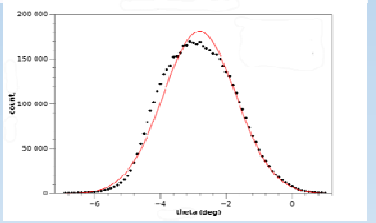

- Commissioned at the December 2020
- First "demonstration" experiments at 100kW power were carried out
- All results coincide with the theoretical predictions
- Program for updates of these stations to the power of 100 MW is developed

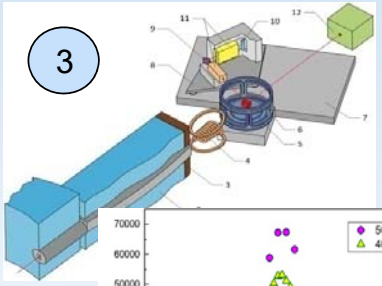


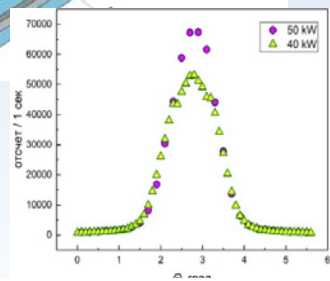


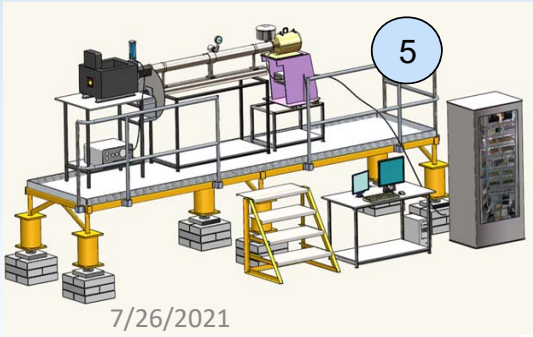


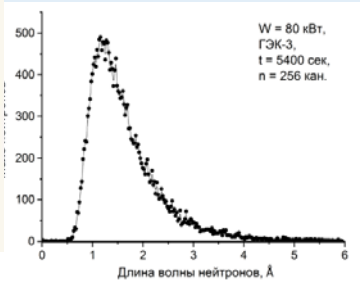

# Status of the instrumentation program

- Funding confirmed and started **last year (2020)**
- The **design of the project** get the positive state expertise decision in **September 2020**
- Construction of the **first phase** instruments started in **December 2020**
- **Second phase** instruments construction started **June 2021**
- The **third phase** will be started in the **beginning of 2022**

# Road map of the national instrumentation program

| # | | | 2019 | | 2020 | | | | 2021 | | | | 2022 | | | | 2023 | | | | 2024 | | | |
|---|---|---|---|---|---|---|---|---|---|---|---|---|---|---|---|---|---|---|---|---|---|---|---|---|
| | | | III | IV | I | II | III | IV | I | II | III | IV | I | II | III | IV | I | II | III | IV | I | II | III | IV |
| 0 | | **Reactor PIK commissioning** | **100 kW** | | | | | | **10MW** | | | | | | | | **10-100MW** | | | | **~100MW** | | | |
| 1 | | **Project of instruments** | | | | | | | | | | | | | | | | | | | | | | |
| 2 | | **Experimental channel** | | | | | | | | | | | | | | | | | | | | | | |
| 3 | | **HNC HEC-8** | | | | | | | | | | | | | | | | | | | | | | |
| 4 | | **UCNS HEC-4** | | | | | | | | | | | | | | | | | | | | | | |
| 5 | | **CNS HEC-2** | | | | | | | | | | | | | | | | | | | | | | |
| 6 | | **CNS HEC-3** | | | | | | | | | | | | | | | | | | | | | | |
| 7 | | **Neutronguide system** | | | | | | | | | | | | | | | | | | | | | | |
| | | **Neutron stations** | | | | | | | | | | | | | | | | | | | | | | |
| 1 | | SESANS | | | | | | | | | | | | | | | | | | | | | | |
| 2 | | INAA | | | | | | | | **Phase 1** (4 instruments) | | | | | | | | | | | | | | |
| 3 | | «Нейтрино» (Neutrino) | | | | | | | | | | | | | | | | | | | | | | |
| 4 | | D1 | | | | | | | | | | | | | | | | | | | | | | |
| 5 | | DC-1 | | | | | | | | | | | | | | | | | | | | | | |
| 6 | | D3 | | | | | | | | | | | | | | | | | | | | | | |
| 7 | | IN-1 | | | | | | | | | | | | | | | | | | | | | | |
| 8 | | IN-2 | | | | | | | | | | | **Phase 2** (7 instruments) | | | | | | | | | | | |
| 9 | | ИРИНА (IRINA) | | | | | | | | | | | | | | | | | | | | | | |
| 10 | | DEDM | | | | | | | | | | | | | | | | | | | | | | |
| 11 | | FISCO | | | | | | | | | | | | | | | | | | | | | | |
| 12 | | Tenzor | | | | | | | | | | | | | | | | | | | | | | |
| 13 | | Мембрана – 2 (Membrane – 2) | | | | | | | | | | | | | | | | | | | | | | |
| 14 | | IN-3 | | | | | | | | | | | | | | | | | | | | | | |
| 15 | | IN-4 | | | | | | | | | | | | | | | | | | | | | | |
| 16 | | SONATA | | | | | | | | | | | | | | | | | | | | | | |
| 17 | | SEM | | | | | | | | | | | | | | | **Phase 3** (9 instruments) | | | | | | | |
| 18 | | Harmony | | | | | | | | | | | | | | | | | | | | | | |
| 19 | | PROGRAS | | | | | | | | | | | | | | | | | | | | | | |
| 20 | | «Бета-распад нейтрона» (neutron beta decay) | | | | | | | | | | | | | | | | | | | | | | |

*Nuclear physics and particle physics*
*Large scale*
*Structure*
*Spectroscopy*

**Commissioning**

# Layout of neutron instruments

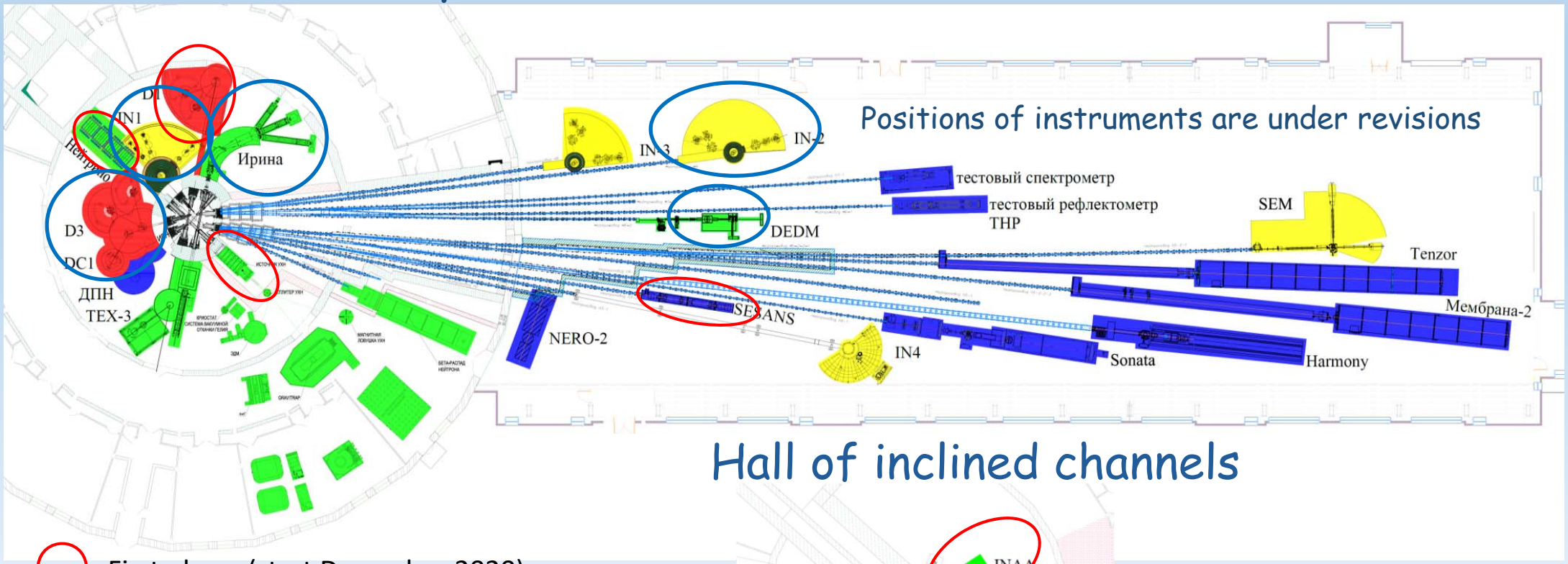


# Hall of inclined channels

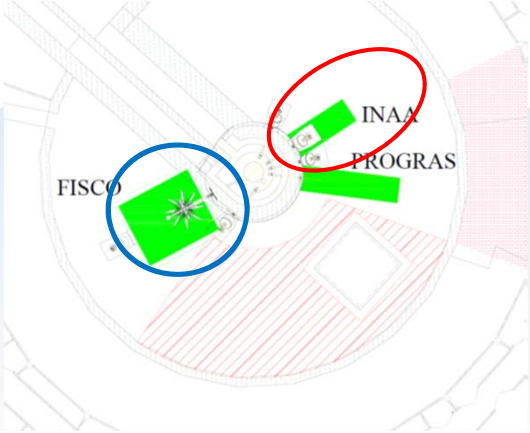


First phase (start December 2020)

Second phase (start June 2021)

Third phase (start March 2022)

Spectroscopy
Diffraction
SANS and reflectometers
Fundamental physics

# Hall of experimental channels

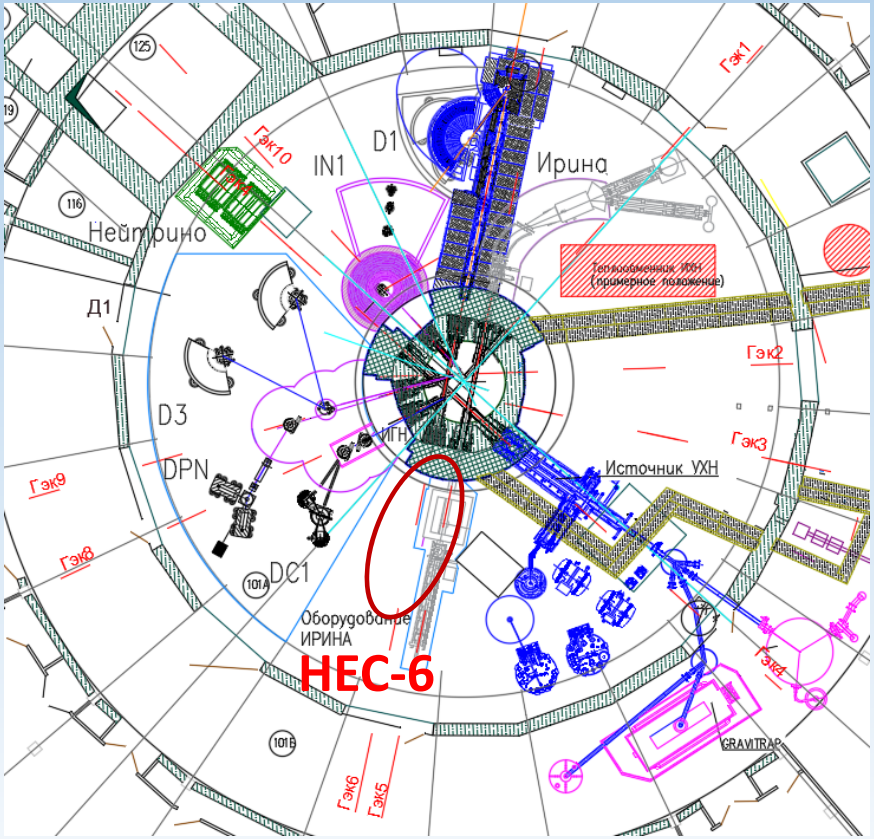


| № | Beam position | Instrument |
|---|---|---|
| 1 | HEC-2 | CNS |
| 2 | HEC-3 | CNS |
| 3 | HEC-4 | ИУХН (UCN source) |
| 4 | HEC-5-5’ | ИРИНА (IRINA) |
| 5 | HEC-6 | |
| 6 | HEC-6’ | D1 |
| 7 | HEC-8 (HNS) | DC1 |
| 8 | HEC-9-1 | D3 |
| 9 | HEC-9-2 | ДПН (PolDi) |
| 10 | HEC-10 | IN-1 |
| 11 | | NEUTRINO |

All channels are occupied by the instruments and CN sources from National instrumentational program with the commissioning in 2024-2025. **Only HEC-6 is empty.**

# Problems and questions

Is it a prototype or full scale installation with beam positions and infrastructure?

1. We need a conceptual design of the VCN project with the calculation of radiation shield, weight, sizes, infrastructure requirements (electric power, air, helium,….). What neutron do you need? What flux?

**Technical**

1. Insufficient space for equipment

**Administrative**

1. National instrumental program is almost fixed. The changes are extremely difficult

# Conclusion

Feasibility of VCN source at PIK reactor depends on answer the question:

- What type of source we want to build - prototype or **full scale installation** with beam positions and infrastructure?

To involve PNPI to VCN source project is very easy. Give us:

- A conceptual design of the VCN project and experimental stations which will use the VCN
- Scientific background

# Thank You for attention